WIND ENERGY, ELECTRIC VEHICLES AND DEMAND AGGREGATORS IN POWER MARKETS AND SYSTEMS

A Dissertation

Presented to the Faculty of the Graduate School

of Cornell University

In Partial Fulfillment of the Requirements for the Degree of

Doctor of Philosophy

by

KEENAN FU VALENTINE

JANUARY 2015

WIND ENERGY, ELECTRIC VEHICLES AND DEMAND AGGREGATORS IN POWER MARKETS AND SYSTEMS

Keenan Fu Valentine, Ph. D.

Cornell University 2015

Volatile wind generation and demand resources are entering the electric power sector and projected to penetrate in significant quantities in the next decades. It becomes critical to better understand their economic and dispatch interactions with each other and with the grid for economic efficiency and operational reliability.

The four chapters tackle this challenge. Each chapter builds upon the previous chapters, other scholarly works and industry reports to deliver a central message: *wind power, electric vehicles (EVs) and aggregator-facilitated demand response are system-level resources with complex interactions with each other and with the power system*. Under various conditions, they synergistically aid the grid; under other conditions, they are competitive substitutes for each other. The characterization and integration of these resources require detailed and comprehensive studies that do not yield to simple "rule of thumb" conjectures.

With the first chapter as introduction, the second chapter investigates the system's response to exogenously unregulated and regulated charging of plug-in electric vehicles (PEVs) using optimal power flows, generator dispatches and resultant

emissions. Results show regulated charging is preferred over unregulated charging economically, from a system reliability perspective and from an emissions standpoint. The second chapter focuses on PEV charging as an aggregated system-level demand resource in the New York Independent System Operator's (NYISO) two-settlement energy market. The study finds EV charging mostly overnight and sometimes during double load peaks to lower the combination of steady-state and ramping system costs. The third study answers questions regarding the interactions between wind generation and PEV charging not as directly-paired supply and demand resources, but rather as system-level resources while ensuring lowest wholesale energy costs and realistic dispatch patterns. In particular, the chapter finds: (1) the existence of time-series correlation between PEV charging and wind dispatch, and (2) PEVs are adversely coupled to curtailable wind, and decoupled with must-take wind. Lastly, the fourth chapter offers a framework: (1) to understand the probabilistic nature of demand response (DR), (2) to describe the role of utility-scale storage in DR, (3) to improve DR compliance rates using load aggregation and storage dispatch, and (4) to calculate an aggregator's payoff in DR and energy arbitrage.

BIOGRAPHICAL SKETCH

Keenan Valentine was born in Shanghai, China in 1987 and immigrated to the United States in 1999. Under the loving care and judicious nurture of his family, Keenan experienced NASA as a wind tunnel engineer and graduated Summa Cum Laude from Arizona State University with a Bachelor's degree in Mechanical Engineering, specializing in thermal sciences. Under the mentorship of his professors at Cornell University, he strived to advance the goal of a more efficient and responsive electric power industry. As a life-long learner, Keenan aspires to build a career underpinned by his passion for energy and the environment.

ACKNOWLEDGMENTS

The impracticality of listing all of the people that influenced me and the beginning of my career in energy shows how fortunate I am to have them as mentors, family and friends. Particularly at Cornell University, I thank Professors Max Zhang, Bob Thomas, Tim Mount and Brandon Hencey for guiding my research and industry exposure. Max gave me the freedom to learn from thinkers and practitioners while mentoring me toward the light at the end of the tunnel. Bob led the electricity research across a consortium of universities and learning from him grounded my research in practicality. Tim is the veteran energy economist that taught me to never be satisfied with a legacy system. Classes and conversations with Brandon brought me back to my roots as a mechanical engineer. I am forever grateful to these four professors for guiding me through the Ph.D. chapter of my life.

Like most Ph.D. students, my family was hundreds to thousands of miles away from school. For me, their love is independent of the space and time separation. I can never make it even to them. There is one new family member that now accompanies me—my wife, Olivia. Thank you.

Last, but not least, I thank my dearest friends who helped me during endless Ithacan blizzards, climbed walls for me, taught me wisdom and shared experiences that will last a lifetime. Joy summons partners and misery likes company—Hao, Victor, Peng, Chavez and Max. Another group of friends came by happenstance—Deans

Sheri Notaro and Patricia Nguyen. Through their generosity, I have gained a hands-on appreciation for a diverse society and hope I have meaningfully served the broader student community at Cornell.

TABLE OF CONTENTS

CHAPTER 1

INTRODUCTION

1.1 Electric Vehicles

Electric vehicle (EV) is a general term for a type of ground vehicle with electric motors as the primary or only source of locomotion. There are two main varieties of EVs: (1) electric-only or battery vehicle (BV) and (2) hybrid electric and internal combustion engine(s) vehicle (HEV). An EV has an onboard battery that stores electricity. Battery capacity is a main driver in the distance range of an EV. This type of vehicle recharges via a charging station equipped with various levels of charge rate. A Level 1 charger (via SAE standards) provides the slowest charge rate of 3.44 kW per hour. A step above is a Level 2 charger capable of a 7.68 kW per hour or higher charge rate. Level 3 and above chargers are either available in limited locations or in R&D phase.

HEVs generally have a smaller battery where electric motors are supported by internal combustion engines (ICEs). The configuration of such propulsion system can be in series, in parallel or in substitution. A series-configured HEV uses ICEs to generate electricity for storage in the battery or battery-like device (e.g. capacitor). The electric motors then withdraw power from the battery to propel the HEV. A parallel-configured HEV uses both ICEs and motors to propel the vehicle. A substitution-

configured HEV uses either electric motors or ICE to propel vehicle for some distance range and then switches to the other power source to travel additional distances. Usually, electric motors are engaged first. A HEV's batteries can also be directly charged via charging stations.

A hybrid vehicle (HV) on the other hand usually denotes a ground vehicle that uses a much-smaller installation of batteries and motors for propulsion. But, ICE is the only primary energy source without battery charging capabilities. A HV is not considered an EV.

On the consumer market, several coastal states in the U.S., e.g. California and New York, have a relatively larger quantities of EVs than inland states. However, for the country on the whole, current penetration of EVs is minimal, percentage-wise. Nevertheless, the future belongs to EV technology as integration of the electric power and transportation industries is inevitable. The usefulness of EVs as a resource in the electric power industry is a topic of this dissertation. This is fueled by the realization that EVs remain parked for as much as 95% of the time. Therefore, tapping the battery as an asset to the grid during these idle hours holds the promise for increased EV value. Moreover, spent batteries from EVs can create a secondary market for stationary usage.

Aside from the operational and economic aspects of EV and grid integration, there are strong motivations for the technology itself: (1) to decrease transportation sector's

dependence on low-efficiency fossil fuel combustion technology, and (2) to decrease mobile emissions.

1.2 Wind Power

Wind power in the U.S. and around the world has grown significantly over the last decades. As a renewable energy resource, it has environmental advantages and enjoys economic and regulatory favoritism over traditional thermal generators. In most projections, the power industry expects to have more wind power for the foreseeable future.

However, the hard-to-dispatch nature of wind power poses operational and economic challenges to the existing structure of the power grid and markets. While most thermal units have low outage or unavailability rates (<20%) and are considered reliable, wind power has considerably higher unavailability rates and is much less reliable, particularly during peak loads. The volatile nature of wind power places additional requirements on the existing electric power structure in terms of increased load following and operational reserve capabilities. These are necessary to balance the effects of wind forecast errors and variability on net load in order to balance the grid.

There are additional challenges to wind power beyond the scope of this thesis—issues with wind not adding to long-term resource adequacy and challenges with generation

deliverability, i.e. need for transmission builds and improvements.

1.3 Energy Markets

Power markets are the platform to settle supply and demand bids, derive locational marginal prices (LMPs), dispatch assets economically, value grid assets, and be influenced by market rules and regulatory policies. Dominant U.S. power markets are categorized into three interdependent markets: (1) energy market, (2) capacity market and (3) ancillary service market. There are also markets without a capacity market, e.g. ERCOT. The energy markets are usually two-settlement markets, where the day-ahead market schedules generator commitment and dispatch schedules and the real-time markets makes incremental changes to these schedules in near real-time. The total cost of the wholesale energy market is the sum of day-ahead market costs and real-time adjustment costs.

Regional transmission organizations (RTOs) and independent system operators (ISOs) are chartered to administer the economic and operational functions of the power system within their control area. U.S. RTO/ISOs include New York ISO (NYISO), PJM, ISO New England (ISONE), Midcontinent ISO (MISO), California ISO (CAISO) and Electric Reliability Council of Texas (ERCOT). With roots in the government deregulation in the 1980s, RTO/ISOs are generally formed at around the turn of the millennium with PJM being the largest and most established.

1.4 Demand Response and Aggregator

Demand response (DR) aims to bring demand elasticity to the electricity sector. However, current markets are dominated by supply-side flexibility. In nonmarket territories, load-serving entities (LSEs) are obligated to serve demand. In both types of systems, generators of many types, e.g. fossil fuel, nuclear, hydro and renewable, seek to supply a nearly inelastic load. LMPs are volatile due to several factors: (1) demand inelasticity, (2) scarcity of supply at peak loads, (3) lack of electricity storage, and (4) network congestion. Price volatility is often exacerbated by outages of key generators and transmission lines—creating peak LMPs 10 to 50 times the average.

Most residential, many commercial customers do not see these price volatilities. In fact, the majority only see a constant retail price or some form of simple tiered pricing structure that shadows wholesale prices. This disconnect between true cost of electricity and what customers pay at a sufficiently fine time interval creates significant economic inefficiencies called deadweight losses [1]. These losses fundamentally describe the discrepancy between the value of electricity consumed and its cost of production. This leads to adverse consequences of over- and under-consumption and cross-subsidies, e.g. under-consumption at low LMPs subsidizing cost of over-consumption at high LMPs.

Consequently, economic demand elasticity is crucial to lowering price volatility and removing the price disconnect. There are generally two forms of demand elasticity

currently in practice or trial phase, namely (1) DR through an aggregator, e.g. EnerNOC or local utility's DR program, and (2) time-varying rates, e.g. real-time prices (RTP). This study focuses on the currently dominant form of DR. It lowers price peaks by competing with generators for dispatch at sufficiently high LMPs. It helps remove the price disconnect by having demand recognize the true cost of electricity in order to make a deliberate choice between consuming power or foregoing the opportunity.

Being in existence for only a few years, DR programs in wholesale markets have not matured. In particular, DR has an important problem of inconsistent reliability. For example, in PJM administered system, DR programs cost more than $300 million during the first 6 months of 2014, mostly in the form of capacity, while its observed compliance rate is only 28%. In stark contrast, PJM's equivalent availability factor (EAF) for generators is 80% overall, 85% for combustion turbines (CTs) and 82% for combined cycles (CCs)—the types of units that DR competes with—for the same 6 months [2]. However in 2013, DR's observed compliance rate is 82% while the EAF for generators is 84% overall, 90% for CTs and 86% for CCs in PJM [3]. The extreme difference between DR's compliance rates at 28% and 82% is due in part to the voluntary nature of the 2014 DR events while those in 2013 were mandatory. It is tempting to institute all DR events as mandatory. However, such mandates can decrease DR program participation due to customer fatigue and insufficient financial compensation.

Aggregators contract with small to medium size clients to form load classes and may have utility-scale storage assets. On the other hand, RTO/ISOs being responsible for the entire balance area are ill-equipped to administer these demand assets. Aggregators, on behalf of its clients, bid into the capacity and energy markets as part of DR programs. Therefore, the aggregator is ideally positioned to manage demand-side resources in order to improve demand-side flexibility in markets through actions such as improving DR compliance rates.

REFERENCES

[1] Chao, H., 2010. Price-responsive demand management for a smart grid world. The Electricity Journal 23 (1), 7-20.

[2] Monitoring Analytics, LLC, 2014. Quarterly State of the Market Report for PJM: January through June.

[3] Monitoring Analytics, LLC, 2013. State of the Market Report for PJM.

CHAPTER 2

TRANSMISSION NETWORK-BASED ENERGY AND ENVIRONMENTAL ASSESSMENT OF PLUG-IN HYBRID ELECTRIC VEHICLES

2.1 Background

Plug-In Hybrid Electric Vehicles (PHEVs) utilize advanced batteries to obtain between 20 to 60 miles of fully-electric driving and afterwards uses a traditional hybrid electric power train for range extension [1-2]. In the future, PHEVs will likely shift the transportation network's dependence away from petroleum and towards the electric grids, thus inducing a significant transformation within the electric power and transportation sectors [3-5]. Moreover, the pollutant emission changes from mobile sources of vehicles to point sources of power plants as a result of PHEVs will affect air quality, especially at urban centers.

Recently studies have begun to investigate fuel mixtures, emission changes and grid reliability issues associated with PHEV usage [3-9]. The findings from those studies have advanced our understanding on the energy and environmental impacts of PHEVs. Overall, the penetration of PHEVs into the automobile market is expected to reduce tailpipe emissions as well as the total emissions accounting for the increased emissions from coal, natural gas and oil power plants [5-6]. A unit commitment model without transmission constraints was incorporated into an economic dispatch model of the

Electricity Reliability Council of Texas (ERCOT) region to evaluate the change in generator dispatches resulting from PHEV deployment [7]. Researchers also analyzed the potential impacts of PHEVs on electricity demand, supply, generation mixture and emissions in 2020 and 2030 in 13 regions specified by the North American Electric Reliability Corporation (NERC) and the U.S. Department of Energy's Energy Information Administration. Modeled without transmission constraints of the electric power network, the study further assumed a uniform fuel mixture for electricity generation within the region [8]. Using a 10-bus reduced model for the Ontario transmission system, a study in 2010 analyzed the optimality of PHEV's off-peak charging on the reliability of the region's power system [9].

This chapter shows the need to incorporate realistic engineering and operational constraints of the power transmission network into an economic dispatch model when assessing the regional impact of PHEVs on the varying fuel mixture and emissions of power generation. We show that these network constraints noticeably alter the dispatch of generation from that based purely on economics of individual generators. Consequently, an economic dispatch model with network constraints can more realistically model the regional impact of PHEVs.

In this chapter, we present our study on the energy and environmental impacts of PHEV-40 (PHEV with a 40-mile all electric range) with various market penetrations (replacing the corresponding conventional vehicles with PHEVs) in the New York Metropolitan Area (NYMA) using an economic dispatch model subject to realistic

engineering and operational constraints of the reduced NPCC AC power network [10]. Moreover, every generator in our model has an associated fuel type (coal, nuclear, hydro, natural gas and oil), cost function for power generation and emissions characteristics (CO_2, NO_x and SO_x), which we obtained from corresponding Independent System Operators (ISOs). Based on driving patterns of commuters working in New York City (NYC), we aim to evaluate the effects of different PHEV penetrations and charging scenarios on generation fuel mixture and emissions in the Northeast Power Coordinating Council (NPCC) region for the summer and winter seasons.

Methodology

2.2 Transportation System Modeling

This study of the transportation system in NYMA focuses on vehicles commuting in-and-out of NYC. The U.S. Department of Transportation's 2000 Census Transportation Planning Package (CTPP), which contains data specifically designed for transportation planners, reveals that approximately 1,040,000 people within NYMA commute daily to NYC by personal vehicles [11]. These vehicles usually congest the city's main roads and highways, thereby contributing to the high pollution levels near the freeways within and around NYC.

2.2.1 Commuting Patterns

We assume that the NYMA commuters with PHEVs travel to their workplaces in NYC starting with a fully-charged battery and that battery recharge occur immediately after returning home from work. This is known as the "unregulated charging" scenario in this analysis. The increased hourly electricity demand from PHEVs is modeled using the number of commuters, PHEV market penetrations, the times when commuters leave work, the speeds at which they travel, and the daily commuting distance. Unregulated charging of many PHEVs at high demand hours presents significant challenges to the power system such as increased peak demand and decreased grid reliability. Thus, this scenario represents a worst case where PHEV charging is not systematically controlled. Due to the flexibility of charging PHEVs at off-peak hours, a systematically "regulated" charging scenario is introduced in Section 2.4 in order to help alleviate the challenges to the power system from unregulated charging.

Our model of the commuting patterns is based on data from two transportation patterns surveys. The Journey-to-Work data in the 2000 CTPP is used to determine the number of commuters that drive daily to NYC from every county in the NYMA. The Regional Travel Household Interview Survey (RT-HIS) itemizes the time when a random NYMA commuter leaves work for home [12].

A Monte Carlo (MC) method was used to generate a realistic hourly electricity

demand profile in a typical weekday from unregulated charging. From RTHIS and CTPP, a time profile of commuters leaving work, a distance profile of their commuting distances and driving speeds at various commuting segments were derived. Accordingly, the MC method generates a time a random commuter leaves work, the corresponding commute distance, and the driving speeds inside and outside NYC. During rush hours, a traffic congestion factor known as Travel Time Index (TTI) is applied to reduce the speed out of NYC. TTI is estimated to be 1.44 from 6 AM to 9 AM, 1.63 from 3 PM to 6 PM and is 1.00 for other hours [13].

The random commuter's daily energy requirement for PHEV charging is then calculated by assuming a linear relationship between mileage and the electric energy for light-duty gasoline vehicles (LDGVs). This relationship ranges from 0.26 kW h $mile^{-1}$ to 0.46 kW h $mile^{-1}$ within the 40-mile electric-drive range [4]. The charging time of standard PHEV-40 batteries is approximated at 6 hours on a standard 120 V outlet. Repeating this algorithm for a thousand random commuters produces an electricity demand profile for unregulated charging for each hour of the day.

2.2.2 Vehicle emissions

The commuting distances in the transportation modeling and a fuel economy of 17.5 mile gal^{-1} were used to calculate the amount of gasoline that commuters driving LDGVs consume per day [14]. Combined with the emissions rates for VOC, NO_x, CO, $PM_{2.5}$, PM_{10} and CO_2 in g $mile^{-1}$, shown in Table 1, baseline vehicle emissions

were found and compared to reductions from PHEV penetrations [15].

Table 1

Vehicle emission factors in NYMA.

Vehicle Type	VOC (g mi^{-1})	NOx (g mi^{-1})	CO (g mi^{-1})	$PM_{2.5}$ (g mi^{-1})	PM_{10} (g mi^{-1})	CO_2 (g mi^{-1})
LDGV	0.51	0.45	11.19	0.12	0.25	504.0

2.3 Power systems modeling

We model the power system by applying an optimal power flow model (MATPOWER) onto a reduced 36-bus Northeast Power Coordinating Council (NPCC) AC network [16]. MATPOWER simulates power flow while minimizes generation costs, transmission losses and costs for required reserves subject to realistic grid constraints taken from ISOs, such as thermal limits on transmission lines, real and reactive generation capacities, bus voltages and generator voltage settings.

The geographic area of the NPCC region totals approximately one million square miles and includes New York State, the six New England states, Ontario, Québec and the Maritime Provinces. The total population served is approximately 56 million people, and 20% of the Eastern Interconnection load is served within the NPCC region.

The 36 buses are located at geographic points around the Northeast; 19 of which represent the entire state of New York and its corresponding generating facilities. The loads from PHEV activity in NYMA largely affect 13 buses: Farragut, Dunwoodie, Newbridge, Ramapo, Rochestor, Massena, New Scotland, Marcy and Pleasant Valley in New York; Millstone, Norwalk Harbor and Southington in New England; Alburtis in PJM. For this study, we have individually matched the fuel type and emission rates for CO_2, SO_2, and NO_x for 623 generators in the NPCC network according to existing public data in order to simulate the emissions changes due to PHEV penetrations [17].

The baseline load profiles in the NPCC region are taken from the corresponding ISOs: PJM, NYISO, ISONE and Ontario [18-23]. Moreover, to model PHEV's power demands we heterogeneously incorporated different marginal loads to the different buses affected based on PHEV penetration and commuter volume to that bus.

2.4 Scenarios

Five different PHEV market penetrations were used based on the potential market dispersion of these vehicles [24]. The penetrations are 1%, 5%, 10%, 20%, and 50% of the entire Light Duty Vehicle (LDV) fleet, where results for 20% and 50% are reported in detail. Results for 1% to 10% penetrations are briefly discussed. Two seasonal scenarios were analyzed: one in the summer when demand for electricity peaks and another in the winter with low baseline loads. There are significant

differences in the hourly aggregate loads and spatial distribution of these loads between the two seasons. These differences can significantly vary the impact of PHEVs in terms of marginal generation dispatch, fuel mixture, and emissions characteristics. For each season, real-time data from ISOs were taken during a select 24-hour period to represent the base load profile of that season.

Furthermore, beyond the "unregulated charging" described in Section 2.2.1, a "regulated charging" scenario was developed to study the impact of a potential charging regulation. This scenario requires PHEV owners to charge their vehicles at night when base load is low. This scenario creates a uniform power demand from 11 PM to 5 AM, where most vehicles are available for charging while at home [12]. The regulated charging approach can avoid increasing the costly peak loads where generators must ramp up to meet ever larger loads while potentially reducing network reliability. Moreover, regulated charging can avoid additional pollution during peak load by not using the notoriously polluting peaking units.

Results and discussion

2.5 Load profiles

Figure 1 represents the electric demand profiles for the NYMA during a 24-hour period in two different seasons and under various penetration scenarios. The unregulated charging of PHEVs aggravates the late afternoon and early evening peak

electric demand because the additional load coincides with residents turning on their home appliances. In contrast, with regulated charging the additional demand will help to fill the valley of the demand curve in the late night and early morning, particularly in the winter season.

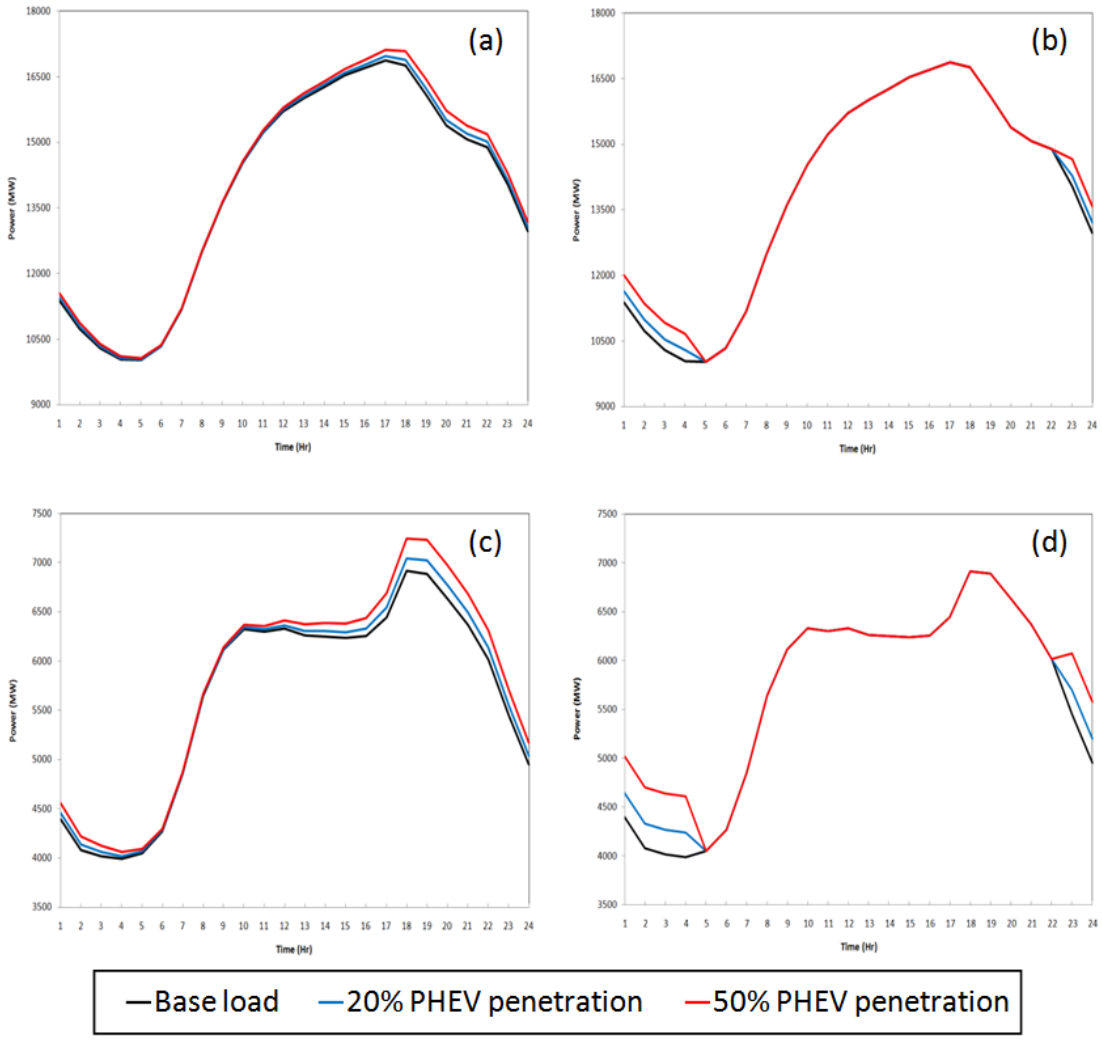

Fig 1. Load profiles in NYMA with 20% and 50% penetrations of PHEVs for the scenarios: (a) unregulated charging in summer, (b) regulated charging in summer, (c) unregulated charging in winter, and (d) regulated charging in winter.

The changes in electric demand will cause the ISOs to re-dispatch the power generators, particularly for the regulated charging case in the winter when significant load from PHEVs is added. This would alter the emission characteristics from the power plants. In real network operations, the sharp increase and decrease of the load profiles at 11 PM and 5 AM in regulated charging would not exist. However, schemes to smooth the profile at 11 PM and 5 AM would not significantly alter the fuel mixture and emission characteristics at the other 22 hours. Consequently, potential schemes to smooth the load profiles for regulated charging are beyond the scope of this study.

2.6 Marginal capacity

In this section, we will investigate how the fuel mix for power generation changes with PHEV penetration. Since the operating costs of electricity generated from hydropower and nuclear power plants are the lowest among different generation types and that these units have slow ramping rates, these power plants typically provide the base-load power. In our model, nuclear and hydro units have zero operating cost per MW produced. These units are already dispatched at their respective full capacities due to base case loads prior to the incorporation of PHEV loads. Therefore, these units are unable to generate additional power when PHEV loads are incorporated. Moreover, nonlinear engineering and operational constraints of the grid modeled were insufficient to reduce the dispatch of nuclear and hydro units when PHEV loads are added. Consequently, the dispatch of nuclear and hydro units does

not change with the additional PHEV loads investigated.

At the current regulatory environment, the electricity generated from coal-fired power plants is still relatively inexpensive compared to natural gas and oil plants and therefore maximized at a lower demand. As a result, remaining coal units not used for base load, natural gas plants, and to a less extend, oil-fired plants will provide the marginal capacity.

Our power systems simulations yield quantitative results on the marginal capacity. We compare the fuel mix in the NPCC region with different PHEV penetrations in the NYMA. Figure 2 illustrates the location specific marginal fuel mix for 20% and 50% PHEV penetration scenarios at peak and valley load hours.

Overall, natural gas plants located in or around the urban centers of NYMA provide the largest portion of the marginal capacity. However, the specific combination of marginal fuel dispatch depends on the season and charging scenario. Despite the differences in the exact marginal dispatch pattern, a few of the buses are affected across multiple PHEV penetrations for most seasonal and charging scenarios, e.g. Long Island and PJM. This is due to the fact that these buses have a compilation of lower cost generators and topological advantage (e.g. lower line flow losses and higher thermal limits) over other buses. Thus for other scenarios these same advantages will likely remain, causing the same buses to be marginal dispatched again.

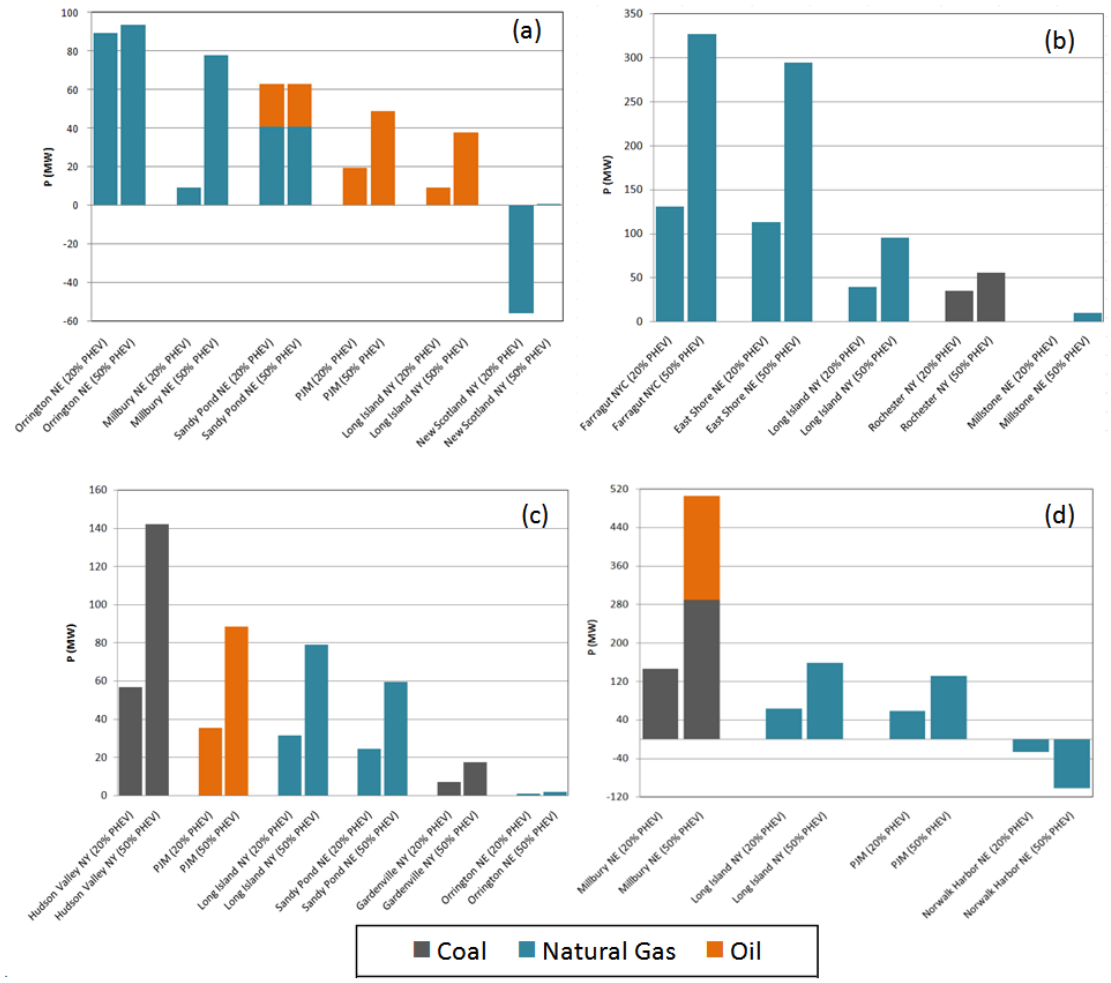

Fig 2. Location-specific marginal fuel mixture at 20% and 50% penetrations of PHEVs for the scenarios: (a) summertime unregulated charging at peak load (5 PM), (b) summertime regulated charging at valley load (4 AM), (c) wintertime unregulated charging at peak load (8 PM), and (d) wintertime regulated charging at valley load (4 AM).

In the summer, natural gas and oil-fired power plants are dispatched to meet the additional load for unregulated charging scenario, because almost all of the coal plants are already fully dispatched for base load. Furthermore, at peak load peaking oil

units in or near NYMA are present in the marginal fuel dispatch due to amount of total load and network constraints. For the regulated charging scenario, natural gas generators provide almost all of the marginal dispatch due to its lower base load at nighttime compared to unregulated charging at daytime peak load. At nighttime, most of the coal units are dispatched for base load, while natural gas is sufficient to provide marginal power without oil units.

In wintertime, coal, natural gas and oil units are all marginally dispatched for both charging scenarios. Coal is used because there is an available coal capacity after serving base load. Natural gas and oil-fired power plants are dispatched to serve the remaining marginal load. Figure 3 shows the fuel mixture in percentage for base load and marginal load from 20% and 50% penetration of PHEV.

Fuel mixture for base load in the NPCC network is dominated by nuclear, natural gas and coal in the summer and by nuclear, coal and hydro in the winter. Marginal fuel mixture is dominated by coal, natural gas and oil, whose specific compilations depend on season and load conditions as shown. More significantly, as base load fuel mixture for the NPCC region uses more clean energy (nuclear and hydro) than the nation currently uses, the NPCC generation mixture can be used as a model representing the future fuel compilation for the national power system [17]. Consequently, the marginal fuel mixture from charging PHEVs in the NPCC region can be representative of the marginal fuel mixture for the nation in aggregate.

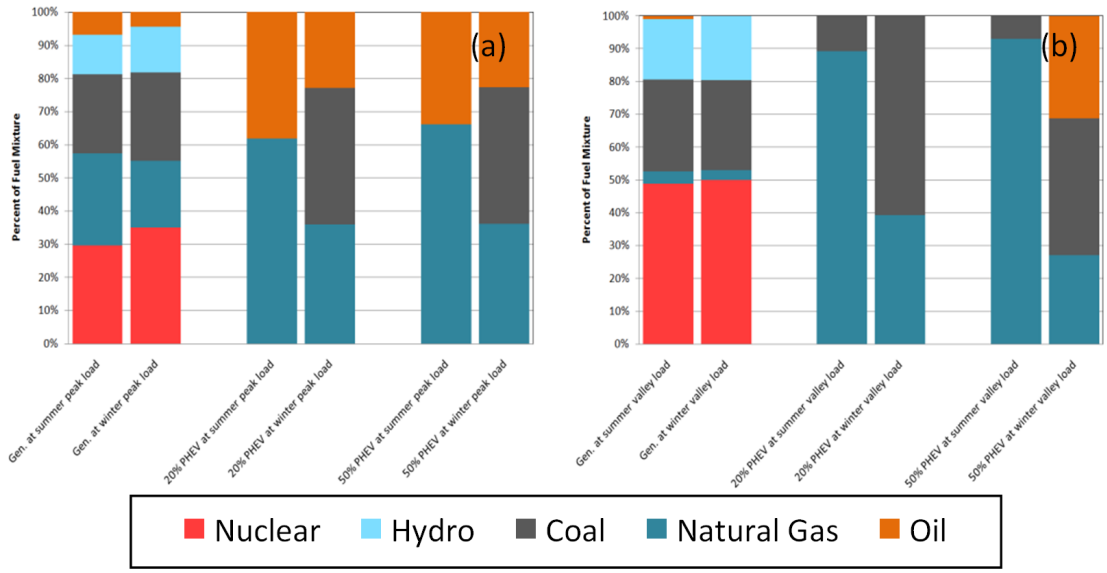

Fig. 3. Percent-wise marginal fuel mixture for 20% and 50% penetrations of PHEV at summer peak and winter valley base loads using: (a) unregulated charging, and (b) regulated charging.

Overall, the non-intuitive negative marginal dispatches at summer peak and winter valley loads, and marginally dispatched oil units in Figures 2 and 3 are caused by power flows deviating significantly from pure economic dispatches without network constraints. Consequently, realistic marginal dispatches are not only subject to generator cost but also transmission constraints. These effects of network constraints are further explained in Section 2.8: Effects of Network Constraints.

2.7 Emissions

2.7.1 Vehicle Emissions

Figure 4 shows significant reductions in CO_2 and NO_x emissions from the transportation sector as a result of PHEV penetration in the NYMA. The hours of 6 AM and 6 PM account for the times when there is significant vehicle traffic and hence when the greatest reductions take place. Spatially, these emissions reductions will occur within the NYMA, particularly in NYC and the immediate surrounding areas. Twenty percent penetration scenarios are enumerated in Table 2. Seasonal variations, heavy-duty vehicles, or transient drivers are not considered in the analysis. At 20% PHEV penetration, daily CO_2 and NO_x emissions in the transportation sector are reduced by nearly 4860 tons and 7 tons, respectively.

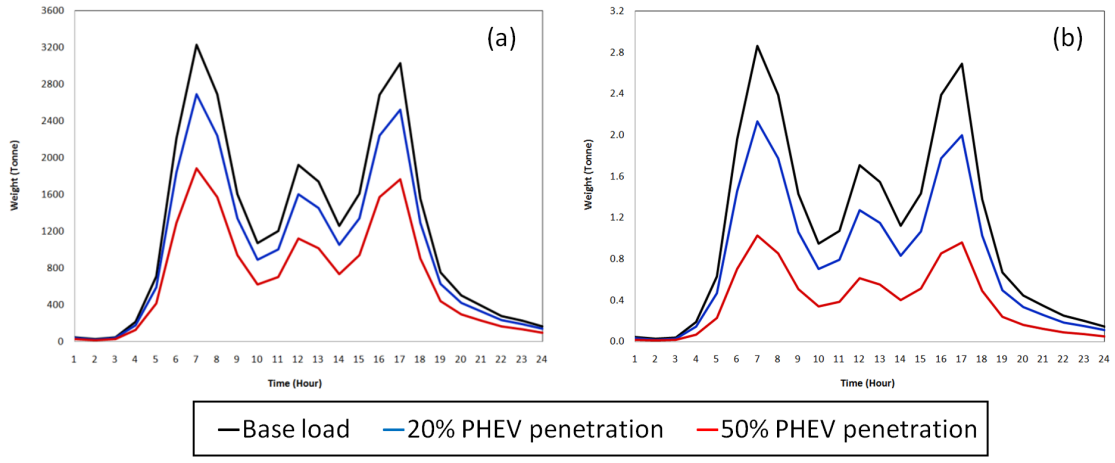

Fig. 4. Hourly emissions from commuter traffic with 20% and 50% penetration of PHEVs in the NYMA for: (a) CO_2, and (b) NO_x.

Table 2

Daily baseline emissions from commuters and emissions reduction from 20% penetration of PHEV in the NYMA.

	CO (ton day^{-1})	VOC (ton day^{-1})	NOx (ton day^{-1})	$PM_{2.5}$ (ton day^{-1})	PM_{10} (ton day^{-1})	CO_2 (ton day^{-1})
Baseline	609.8	24.5	25.9	6.6	13.7	29198.9
Emissions reduction (20% PHEV)	156.5	6.3	6.7	1.7	3.5	4858.6

2.7.2 Power Plant Emissions

It is expected that all types of the emissions from power plants will increase as a result of PHEV penetration with the most significant increase coming from CO_2. Moreover, marginal emissions are dependent only on the specific fuel type and emission characteristics of those marginally dispatched generators. Therefore, quantitative and qualitative differences in the marginal dispatch of generation modeled with and without network constraints will be reflected in the marginal emissions.

In the unregulated charging scenarios the additional increases occur from the peak demand hours of the day to early hours of the next morning as commuters come back home from work with PHEV batteries needing charge. During the regulated charging scenarios the emission increase will occur during the allotted charging times from late night to early morning before commuters leave for work.

Table 3 expresses the modeling results over four demand scenarios and at 0% and

20% PHEV penetration. Table 3 illustrates that unilaterally the emissions of all pollutants from power plants will increase due to the introduction of PHEVs, but the magnitude of the increases vary with the level of PHEV penetration, charging scenarios and seasons.

Table 3

Daily power plant emissions increase in the NPCC region for unregulated and regulated charging scenarios in the summer and winter.

		Unregulated Charging				Regulated Charging			
Season	PHEV Penetration	Electricity generation (GWh)	CO_2 (ton day^{-1})	NOx (ton day^{-1})	SO_2 (ton day^{-1})	Electricity generation (GWh)	CO_2 (ton day^{-1})	NOx (ton day^{-1})	SO_2 (ton day^{-1})
	0%	2,420.8	975,052	786.7	4,148.6	2,420.8	975,052	786.7	4,148.6
	20%	2,422.7	976,344	787.7	4,149.1	2,422.7	976,135	787.3	4,149.2
Summer	Δ	1.9	1,292	1.0	0.5	1.9	1,083	0.6	0.6
	0%	2,175.8	809,205	671.1	4,007.7	2,175.8	809,205	671.1	4,007.7
	20%	2,177.7	810,493	672.0	4,010.3	2,177.7	810,649	672.5	4,013.9
Winter	Δ	1.9	1,288	0.9	2.6	1.9	1,444	1.4	6.2

Since coal units are among the heaviest emitters of CO_2, NO_x, and SO_2, the significant marginal dispatch of coal in wintertime produces higher marginal SO_2 emissions than in the summertime. Moreover, more marginal power from coal in the winter regulated case produces more emissions across the board compared to unregulated charging in the winter as well as unregulated and regulated charging in the summer. Marginal CO_2 and NO_x emissions results for unregulated charging are similar betweem summer and winter seasons. This is due to coal units marginally dispatched in winter and peaking oil units marginally dispatched in the summer have similar CO_2 and NO_x emissions characteristics. Regulated charging in summer using natural gas

plants produces the least marginal emissions, because coal is not extensively used due to their commitment to high base loads and peaking oil units are not deployed for valley loads at night.

2.7.3 Net Emissions

Net emissions are calculated from the sum of emissions from tailpipe and smoke stacks. Table 4 tabulate the results that net CO_2 emissions decrease significantly, NO_X emissions decrease noticeably and SO_2 emissions increase slightly. The decrease in vehicle CO_2 and NO_X emissions clearly offset the increase resulting from power plants in the region. Figure 5 shows the hourly net CO_2 emissions with 20% and 50% penetration of PHEVs in the NYMA for unregulated and regulated charging.

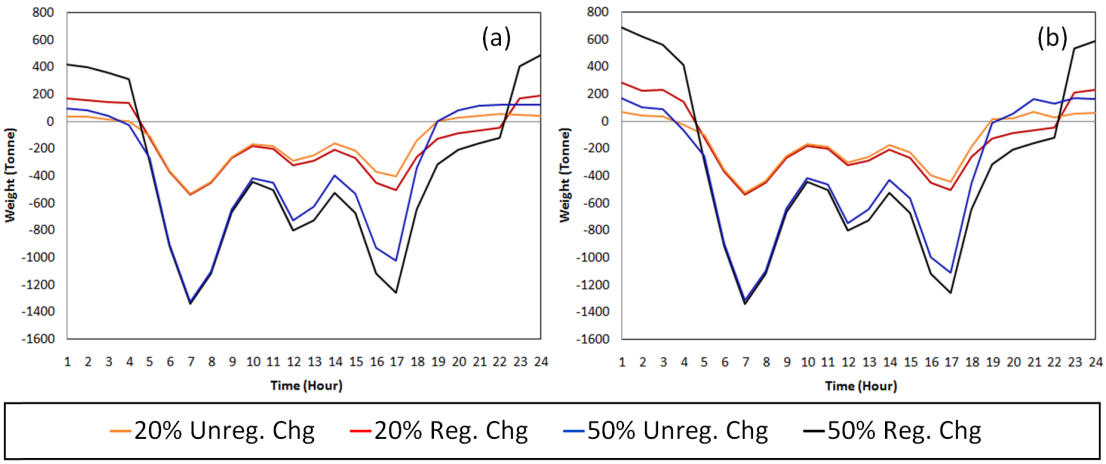

Fig. 5. Net hourly CO_2 emissions from the unregulated and regulated charging of PHEVs in the NYMA during: (a) summertime, and (b) wintertime.

Table 4

Daily net emissions in the NPCC region for both unregulated and regulated charging scenarios in the summer and winter.

Season	PHEV Penetration	Unregulated Charging		Regulated Charging	
		CO2 (ton day^{-1})	NOx (ton day^{-1})	CO2 (ton day^{-1})	NOx (ton day^{-1})
Summer	0%	1,004,251	812.6	1,004,251	812.6
	20%	1,000,684	806.9	1,000,475	806.5
	Δ	-3,567	-5.7	-3,776	-6.1
Winter	0%	838,404	697.1	838,404	697.1
	20%	834,833	691.2	834,989	691.8
	Δ	-3,571	-5.9	-3,415	-5.3

From early morning to late night, net emissions profile is largely dictated by vehicle activity. This again shows that vehicle emissions reduction is the dominant factor compared to power plant emissions during these hours. This is due to the fact that power plants are cleaner than vehicle engines in producing energy for transportation. The increase in net emissions from late night to early morning hours for unregulated and regulated charging cases show that at these times, power plant emissions increase is the dominant factor compared to vehicle emissions reductions. This is due to the fact that at these hours, there is little vehicle activity overall such that the percentage substitution of PHEV makes little difference in vehicle emissions reduction. Simultaneously however, the continual charge of PHEV batteries at home are still drawing large amount of power from the grid. Consequently, emissions from producing power for charging PHEVs are higher than the emissions reduction from PHEVs on the road, resulting in positive net emissions at the late night to early

morning hours. This net emissions increase is more noticeable in the regulated charging cases, because the same batteries charging energy requirements are allotted in a smaller time window in regulated charging. This increases the corresponding power requirement from the grid, and thereby increases emissions from the power sector while vehicle emissions reduction remains unchanged between unregulated and regulated charging.

Moreover, as vehicle emissions reduction remains constant in regulated and unregulated cases in both summer and winter seasons, trends in net emissions mimic the same trend from power plant emissions. Namely, regulated charging of PHEVs in the summer produces the most marginal net emissions reduction; unregulated charging in summer and winter produces similar marginal net emissions reduction; regulated charging in winter produces the least marginal net emissions reduction.

2.7.4 Summary of Results for 1%, 5% and 10% Penetrations of PHEVs

Daily energy demand for 1%, 5% and 10% penetrations of PHEVs are 0.1 GW h, 0.5 GW h and 1.0 GW h, respectively. The marginal generation for and net CO_2 and NO_x reductions from 1%, 5% and 10% penetrations of PHEVs are dominated by coal units in the winter and natural gas units in the summer. At 10% penetration, there is minimal increase of generation and emissions from oil units at summer peak demand. In general, net CO_2 and NO_x reductions from the three penetrations are approximately the corresponding fractions of the reductions from the 20% penetration. Overall, net

CO_2 and NO_x reductions in wintertime average about 5% less than those in summertime due to the use of coal versus the cleaner natural gas units. Finally, regulated charging marginally reduces more net emissions than unregulated charging in the summer and vice versa in the winter. This trend is consistent with that in higher PHEV penetrations and consistent with the use of different marginal fuels.

2.8 Effects of Network Constraints

As described at the beginning of this chapter, many existing PHEV assessments do not contain network transmission constraints. However, the power to charge PHEVs must be delivered by the grid, and therefore such power flows must adhere to transmission constraints. Using our reduced model of the NPCC grid, we show that engineering and operational constraints in a realistic US power grid, such as line impedance, line flow and bus voltage limits, significantly alter the generation dispatch from a pure economic dispatch without network constraints. Consequently, an economic dispatch model with grid constraints is a more realistic approach to analyze the energy and environmental impacts of PHEVs.

Figure 6 shows the difference in generation dispatch between economic dispatches with and without grid constraints using a 50% penetration of PHEVs with base load. Results are calculated from economic dispatches with network constraints less those without network constraints.

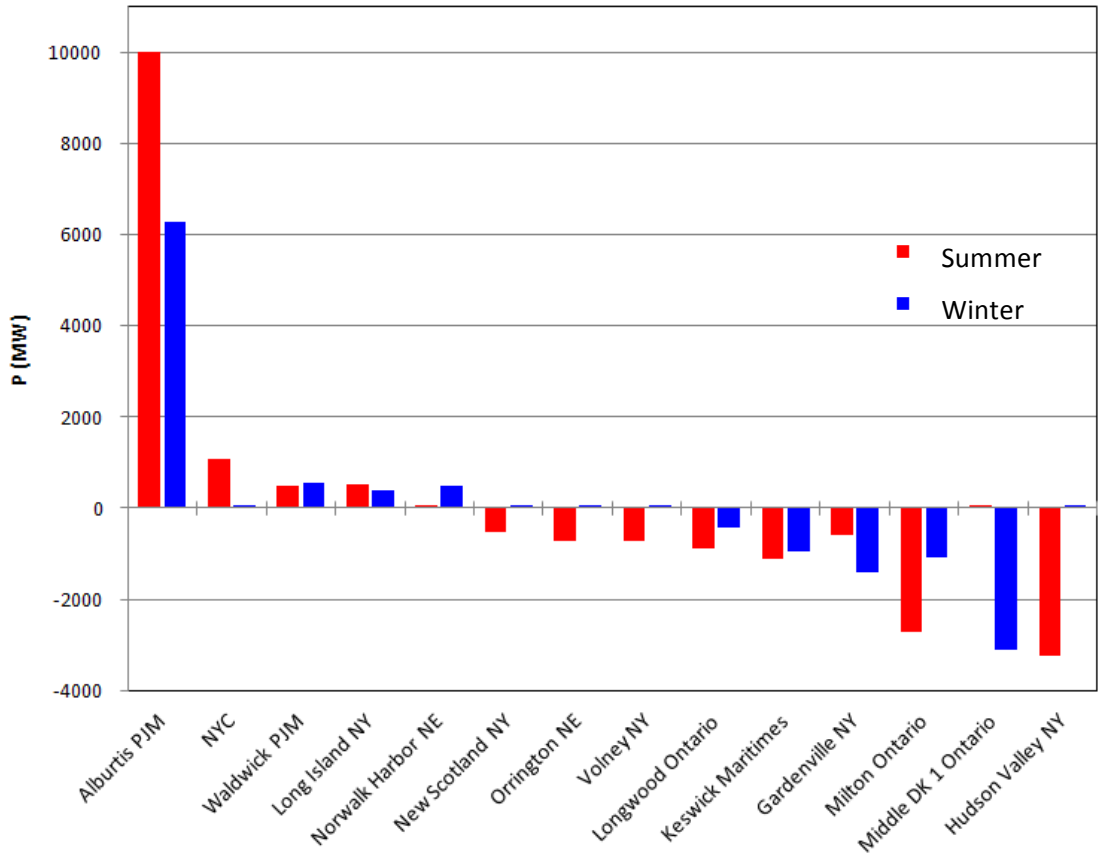

Fig. 6. Difference between economic dispatch of total generation with and without grid constraints with 50% penetration of PHEVs in the summer and winter.

The effects of network constraints are significant at daytime summer peak load and at nighttime winter valley loads as shown. Network impedance, not congestion, has the foremost influence on the generation dispatch pattern in our summer peak and winter valley load cases. This suggests that I^2R line loss minimization is an economic priority with network constraints. Moreover, the aggregation of the differences between grid and no-grid results over all the buses gives the total power losses of the network due to network impedance. (This is about 1 GW in our cases.) However, generation difference at individual buses can be 10 times the aggregate difference.

Particularly, the large difference in the generation at Alburtis (PJM, Bus 1) with and without network constraints suggests the importance of analysis using the grid. Figure 6 shows that reducing the overall impedance of the network dramatically decreases the dispatched generation at Alburtis, i.e. this generation with network impedance is much greater than that without. This result and direct topology inspection show the impedance of the topological region around Alburtis is smaller than other regions in the network. Thus, this bus is economically dispatched with less transmission losses to provide power to loads at other buses. On the other hand, when the impedance of the entire network is eliminated, the topological advantage of Alburtis is eliminated. This results in a reduction of power output from this bus and an increase of power output from other buses as shown.

These large generation differences at individual buses can cause significant differences in marginal fuel dispatch and emissions between economic generation dispatches with and without grid constraints. An example of such differences in marginal dispatch is obtained by comparing Figure 2a (with grid constraints) and Figure 7 (without grid constraints).

The difference between this marginal dispatch with grid constraints and a pure economic dispatch is significant. Pure economics without network constraints would only dispatch natural gas units at the three locations for 20% and 50% penetration of PHEVs as shown in Figure 7. Since these units at Millbury (New England) and Ramapo (Hudson Valley) are the cheapest, they are dispatched first to their capacities

with the rest of the marginal load served by the next cheapest units at Alburtis.

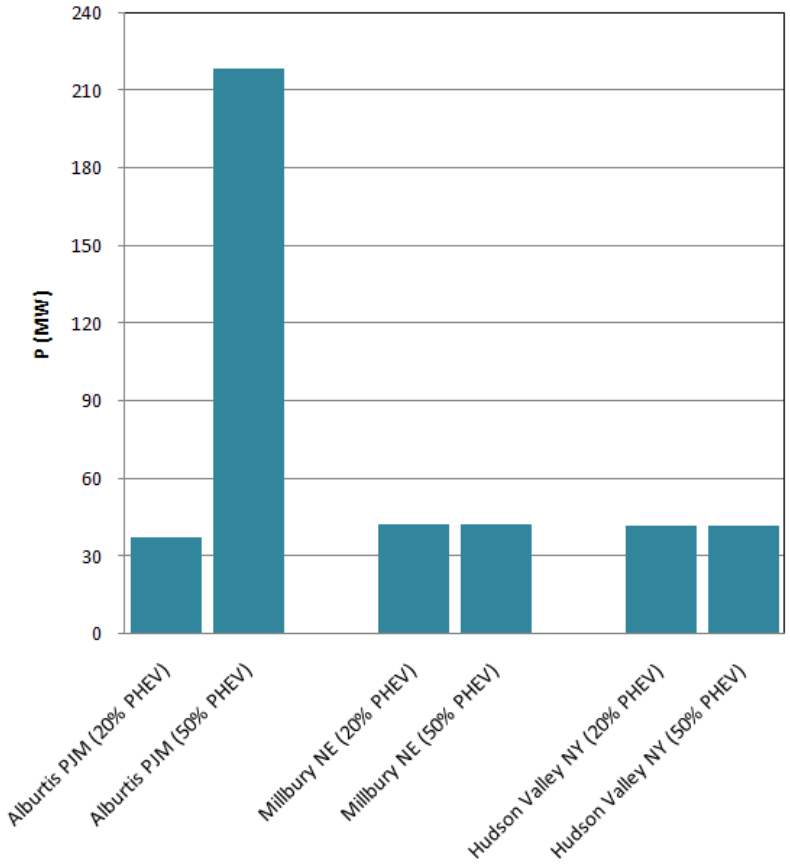

Fig. 7. Marginal economic dispatch at summer peak load for 20% and 50% penetrations of PHEVs using unregulated charging without grid constraints.

As our power system model realistically represents the physical NPCC grid, the difference between generation with and without network constraints in the model are manifested in the physical system. Compared to without grid constraints the marginal dispatch with grid constraints increases generation at certain buses and decreases generation at other buses (e.g. New Scotland in New York and Norwalk

Harbor in New England). These behaviors lead to uneconomic dispatches, which cannot not be observed in a dispatch model without grid constrains. In addition, there are multiple topological causes for the negative marginal dispatches depicted in Figure 7. For example, one cause is a thermal limit on a line from Waldwick in PJM to Ramapo in Hudson Valley. Moreover, the relaxation of grid constraints need not be topologically close to a bus for that bus to uneconomically dispatch significant generation. Consequently, the effects of grid constraints on economic dispatch are nonlinear and generally widespread when realistically assessing PHEVs' influence on regional power consumption and emissions.

2.9 Conclusions

This chapter demonstrates that network-constrained economic generation-dispatch models add significant realism in assessing the impact of PHEVs on regional power systems and the associated pollutant emissions. Using a model of the AC transmission network of the Northeast Power Coordinating Council region and a data-based transportation model of commuters in the New York Metropolitan Area, this chapter shows that (1) coal, natural gas and oil units are on the margin in the winter, and natural gas and oil units are on the margin in the summer, (2) commuter hourly driving behavior dominates changes in emissions from transportation and power production, (3) there is significant overall emissions reductions for CO_2 and NO_x, and a slight increase for SO_2, and (4) regulated charging from 11 PM to 5 AM produces less overall emissions than unregulated charging occurring whenever drivers arrive

home for the summer and vice versa for the winter.

Future work in the assessment of PHEVs is to incorporate unit commitment of generators into the network-constrained economic dispatch model such that generator start-up time is modeled. Moreover, as volatile renewable power sources such as wind and solar enter the generation mix, batteries of PHEVs have the potential to interact with the grid as distributed storage to help maintain network reliability and increase the capacity factors of these renewable power sources. Consequently, system planning models such as the one described in this chapter which incorporates network topology will be important in assessing the value and determining the operations of PHEVs as storage units.

ACKNOWLEDGEMENTS

We thank Timothy Mount, Robert Thomas, William Schulze, Ray Zimmerman, Douglas Mitarotonda and Daniel Shawhan for their insights and assistance. We also thank the Cornell Center for a Sustainable Future (CCSF) and Consortium for Electric Reliability Technology Solutions (CERTS) for the funding support.

REFERENCES

[1] Bradley T and Frank A. 2009. *Design, demonstration, and sustainability impact assessments for plug-in hybrid electric vehicles*. Renewable Sustainable Energy Review. Volume 13, Pages 115-128

[2] Markel T and Simpson A. 2006. *Plug-In Hybrid Electric Vehicle Energy Storage System Design.* Advanced Automotive Battery Conference. May 19th, 2006.

[3] Kintner-Meyer M, Schneider K and Pratt R. 2007. *Impact Assessment of Plug-In Hybrid Vehicles on Electric Utilities and Regional US Power Grids. Part I: Technical Analysis* Pacific Northwest National Laboratory

[4] Scott M J, Kintner-Meyer M, Elliot D B, and Warwick W M. 2007. *Impact Assessment of Plug-In Hybrid Vehicles on Electric Utilities and Regional US Power Grids. Part II: Economic Analysis* Pacific Northwest National Laboratory

[5] Electric Power Research Institute. 2007. *Environmental Assessment of Plug-In Hybrid Electric Vehicles, Vol. 1: Nationwide Greenhouse Gas Emissions*; 1015325; EPRI.

[6] Thompson T, Webber M, and Allen D T., 2009. *Air quality impacts of using overnight electricity generation to charge plug-in hybrid electric vehicles for daytime use*. Environmental Research Letters. Volume 4.

[7] Sioshansi, R.; Denholm, P. 2009. *Emissions Impacts and Benefits of Plug-In Hybrid Electric Vehicles and Vehicle-to-Grid Services.* Environmental Science and Technology, 43, 1199-1204.

[8] Hadley S W, Tsvetkova A., 2009. *Potential Impacts of Plug-In Hybrid Vehicles on Regional Power Generation.* The Electricity Journal. Volume 22. 56-68

[9] Hajimiragha A, Cañizares C, Fowler M, Elkamel, A, 2010. *Optimal Transition to Plug-In Hybrid Electric Vehicles in Ontario, Canada, Considering the Electricity-Grid Limitations.* IEEE Transactions On Industrial Electronics. Volume 57. 690-701

[10] Allen, Eric H., Jeffrey H. Lang, and Marija D. Ilic., 2008. *A Combined Equivalenced-Electric, Economic and Market Representation of the Northeast Power Coordinating Council U.S. Electric Power System*. IEEE Transactions on Power Systems. Volume 23. 896-907

[11] New York City Department of City Planning, Population Division. 2008. Journey to Work Tables <http://home2.nyc.gov/html/dcp/html/census/journey_tables.shtml>

[12] Parsons Brinckerhoff Quade and Douglas, Inc. 2000. *Regional Travel- Household Interview Survey, General Final Report.* <http://www.nymtc.org/project/surveys/files/fr00321.pdf>

[13] New York Metropolitan Transportation Council. 2005. *Congestion Management System Status Report*.

[14] US Department of Transportation, Research and Innovative Technology Administration. 2009. *National Transportation Statistics: Average Fuel Efficiency of U.S. Passenger Cars and Light Trucks.*

[15] New York Department of Transportation. 2008. MOBILE6.2 Emissions Factor Tables. 1999-2008. <https://www.nysdot.gov/portal/page/portal/divisions/engineering/environmental-analysis/mobil6/>

[16] R. D. Zimmerman, C. E. Murillo-Sánchez, and R. J. Thomas. *2009. MATPOWER's Extensible Optimal Power Flow Architecture*. *Power and Energy Society General Meeting, IEEE,* pp. 1-7, July 26-30 2009.

[17] U.S. Environmental Protection Agency. 2008. *Clean Air Markets: Data and Maps.* <http://camddataandmaps.epa.gov/gdm/index.cfm>.

[18] Independent Electricity System Operator. 2009. *Hourly Ontario Energy Price*. <http://ieso.ca/imoweb/marketdata/hoep.asp>

[19] New England Independent System Operator. 2009. *Hourly Zonal Information*. <http://iso-ne.com/markets/hstdata/znl_info/hourly/index.html>

[20] New York Independent System Operator. 2009. *Markets and Operations: Load Data*. <http://www.nyiso.com/public/market_data/load_data/load_forecast.jsp>

[21] New York Independent System Operator. 2009. *Markets and Operations: Pricing Data*. <http://www.nyiso.com/public/market_data/pricing_data/dam_lbmp_zonal.jsp>

[22] New York Independent System Operator. 2009. *Markets and Operations:* Day-Ahead Market LBMP – Zonal. <http://www.nyiso.com/public/market_data/pricing_data/dam_lbmp_zonal.jsp>

[23] PJM Interconnection. 2009. Day-Ahead LMP Data. <http://pjm.com/markets-and-operations/energy/day-ahead/lmpda.aspx>

[24] Green, K. 2003. *Modeling of Advanced Technology Vehicles*. U.S. Department of Transportation. Cambridge, MA.

CHAPTER 3

INTELLIGENT ELECTRIC VEHICLE CHARGING: RETHINKING THE VALLEY-FILL

3.1 Background

There is an increasing need for flexible loads that can respond to economic and reliability signals from energy providers to decrease energy cost and enhance the security of the grid [1, 2]. This dispatchable demand – much like generation – can be monitored and controlled by energy aggregators, such as ISOs/RTOs and utilities, to maintain generation and load balance via load scheduling, shifting, curtailing and provision of ancillary services [3, 4]. Load services can lower Locational Marginal Prices (LMPs), ease incorporation of intermittent renewable energy, and lower pollutant emissions from generators such as CO_2, NO_x, and SO_2 [2, 5]. Since a majority of the capital costs of acquiring flexible loads are covered by the customer for their primary functionalities (e.g., electric vehicles for transportation), energy aggregators will be tasked to provide the remaining monitor and control technology to network individual customers and energy providers.

The charging of lithium-ion batteries in Plug-in Electric Vehicles (PEVs) is one type of dispatchable load that has significant potential to provide many types of power system services without causing customer discomfort [3]. The control of PEV

charging will most likely involve discontinuous and/or variable charging of individual vehicles, which studies show does not cause battery degradation [6, 7]. As 85% of commuters in the U.S. drive 40 miles or less every day, the charging need for a typical PEV-40 (40-mile electric range) ranges from 10 kWh for a compact sedan to 18.4 kWh for a full-size SUV [8]. In this study, Level 1 chargers deliver 1.44 kW and Level 2 chargers deliver 7.68 kW in a typical household [9]. (Level 2 chargers with higher power ratings are not analyzed as it may cause current batteries and distribution transformers to overheat during vehicle charging.) Furthermore, PEVs will most likely be charged at owner's homes, at least in the short-term [10]. Consensus shows that unregulated charging of PEVs – allowing commuters to charge after work in the evening – will increase peak-load and LMP, while decreasing system reliability [10-12]. To prevent these undesirable consequences current literature suggests several regulated charging solutions, most notably the valley-fill scheme, where all charging takes place during the early morning, when system power demand is lowest [11, 13].

This study examines the maximum aggregated potential of PEV load to minimize a two-settlement wholesale energy market cost (system cost) and investigates the associated optimal scheduling of dispatchable PEV load in the New York Control Area (NYCA)—the power system in New York State. The New York Independent System Operator (NYISO) oversees NYCA along with parts of the Canadian system. NYCA interconnects PJM, New England, Ontario and Hydro Quebec. NYCA has a Total Resource Requirement of nearly 39,000 MW with 63% of capacity from gas and oil units, 14% from nuclear, 11% from hydro and 7% from coal.

This study considers zero capital, operation, and maintenance cost for PEV load services so as to determine the system value of controlling PEV charging.

3.2 Electric Vehicle Load and Traditional Charging Methods

Understanding the impact of electric vehicle charging on the power system requires characterizing both the number of vehicles and the time-dependant charging distribution. In this study, electric vehicle energy demand is characterized from US Census data, and two well known charging patterns – unregulated charging and valley-filling – are discussed. Table 1 presents a summary of all charging strategies outlined in the following sections (intelligent charging is discussed in Section 3.5).

Table 1

Summary of PEV charging methods.

Charging Method	Description
Unregulated	Charging begins immediately after a commuter returns home from work, incurring the highest cost.
Flat Valley-Fill	Charging is regulated to take place when system demand is lowest, incurring the lowest steady-state cost.
Smooth Valley-Fill	A valley-fill variation with minor smoothing at the endpoints of the valley to reduce ramping cost.
Intelligent	Charging can be dispatched whenever commuters are at home to minimize total system cost from steady-state and ramping operation.

3.2.1 Energy Requirement Modeling

Prior to investigating different PEV charging schedules, the total energy requirement of vehicle fleet must be determined. PEV charging in New York State is studied. The total number of vehicles within the state was approximated as the total number of

commuters who drive to their place of work: 4.6 million. This study obtained commuter data from the 2000 Census [14]. Once the number of vehicles is known, various PEV market penetration percentages are applied to obtain the number of PEVs on the road for a penetration level.

This study partitions the NYCA into 19 load centers detailed in the 36-bus Northeast Power Coordinating Council (NPCC) power system reduction model [15]. Population density data from the 2000 Census were used to apply "center city", "suburban", and "rural" labels to each of the 19 load centers in NYCA. To obtain the total PEV energy requirement in New York, the number of vehicles is multiplied by a distance driven daily, and any distance that is less than or equal to 40 miles is in turn translated to a PEV charge energy requirement. (Liquid fuel is assumed to power PEVs above the 40 miles mark.) Driving distances were computed using US Department of Energy data, specifying the average distance driven in "rural", "suburban", and "center city" regions. The average distances are 36.9 miles, 28.8 miles and 27.2 miles, respectively [16].

For each load center, a weighted average rate derived from 0.25 kWh mile^{-1} for compact sedans to 0.46 kWh mile^{-1} for SUVs is applied to convert miles driven to energy usage [8]. Equation 1 describes the required energy.

$$Daily\ PEV\ Energy = \sum_{i=1}^{19} M_{PEV} N_i D_i E_i \quad (1)$$

where M_{PEV} is the PEV market penetration and N_i, D_i, E_i are the number of commuting vehicles, average daily distance driven and the average electric energy used per mile at load center *i*, respectively. In terms of energy contribution, 5%, 10%, 20%, and 40% penetrations of PEVs charging between the valley-load hours of 3AM to 6AM is on average 2.6%, 5.3%, 10.6%, 21.1% of summertime electricity consumption during the same time frame.

3.2.2 Unregulated Charging Model

Unregulated charging refers to a method that charges the PEVs as soon as the commuter arrives home, and finishes charging when the battery becomes full or when the commuter leaves home. This type of charging scheme tends to exacerbate peak load and LMP.

The power consumption model for unregulated charging is largely the same as that in [12]. In summary, the charging scheme assumes that commuters start their commute from home with a fully charged battery. The time-varying electricity demand from PEVs is simulated using the number of commuters, PEV market penetrations, the times when commuters leave work, the speeds at which they travel, the daily commuting distances and the charger power ratings (Level 1 or Level 2). These input parameters were synthesized from the Regional Travel Household Interview Survey (RTHIS) and the 2000 Census Transportation Planning Package (CTPP).

In addition to these parameters, a traffic congestion factor known as Travel Time Index (TTI) of 1.15 is used in the Monte Carlo simulation of a thousand commuters to create a normalized commuter-at-home profile (CHP) and an unregulated charging profile [17-19]. The simulation provides a realistic sample of a variety of commuter transportation patterns that include different battery recharge requirements, home arrival and departure times. The CHP and unregulated charging profile is shown in Figure 1.

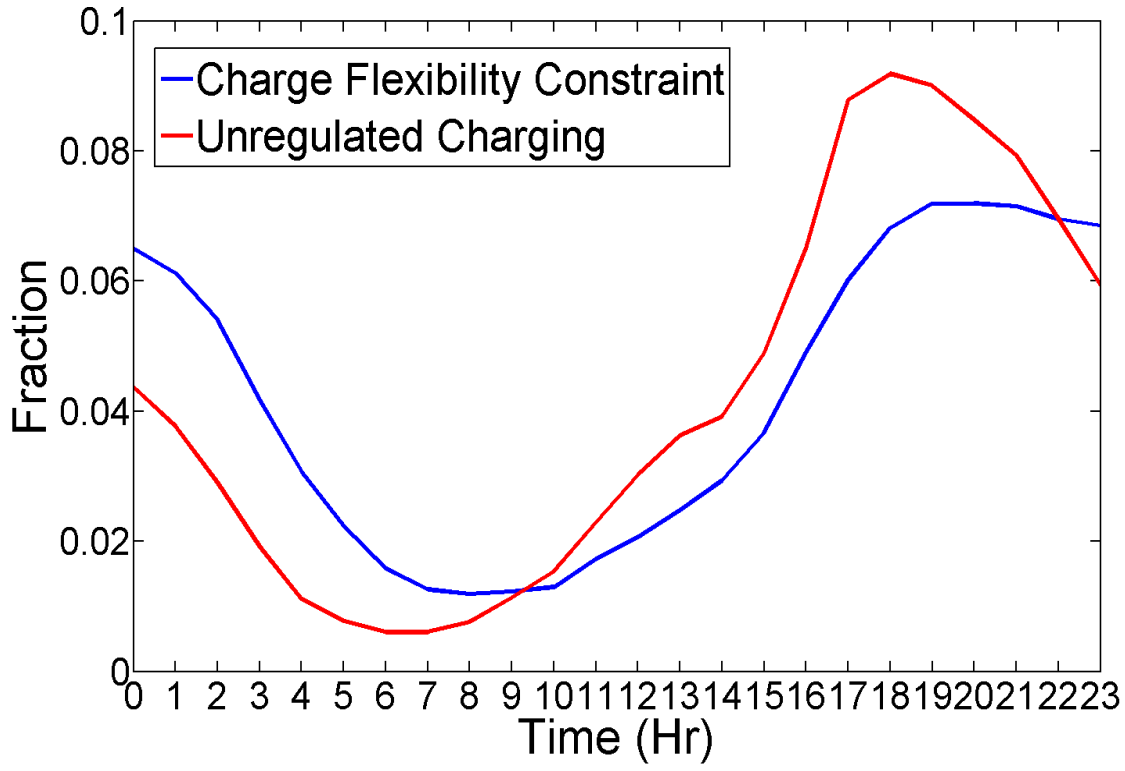

Fig. 1. Normalized Charging Flexibility Constraint (CFC) and unregulated PEV charging profile.

The normalized CHP has a sinusoidal shape whose valley is at 7:30 AM and peak at 7

PM, with peak approximately 7 times the valley. The normalized unregulated charging profile has a more skewed sinusoidal shape whose valley is at 6:30 AM and peak at 6 PM with peak about 15 times the valley. The unregulated charging profile is phased approximately 1-2 hours ahead of the CHP. This is because the CHP is the number of commuters at home, not the number of commuters arriving home. Consequently, many of the commuters that arrive home before 7 PM have finished charging their PEV batteries by 7 PM. A similar phenomenon occurs in the morning.

3.2.3 Valley-Fill Charging Model

Valley-filling is an approach that intuitively allocates all of PEVs' required charge at valley-load hours. This approach only charges PEVs at lowest steady-state loads and LMPs. The traditional valley-fill approach allocates PEV charge such that certain hours of the valley achieve a flat load. There are several variations on this basic approach, including minor smoothing for generator ramping reduction (see Section 3.3). Figure 2 contains examples of previously analyzed PEV charging schemes.

3.3 Wholesale Energy Market Model

The New York Independent System Operator (NYISO) operates on a two-settlement energy market: day-ahead and real-time. Traditionally, locational marginal prices (LMPs) and wholesale energy cost are determined from the unit commitment of generators in the day-ahead market (DAM) and economic dispatch in the real-time

market (RTM), while observing security constraints and emissions permits [20]. As generator offer curves, transmission network topology, network security constraints, and generator emission profiles are proprietary, this study develops an alternative statistical approach for assessing market cost for the entire NYCA using historical market and operation data. Consequently, the model approximates the LMP and system cost changes due to PEV penetrations in the NYCA without explicitly employing the techniques of unit commitment and economic dispatch. Principally, the model incorporates the entire generation fleet in the NYCA; therefore it does not couple PEV charging to a specific generator [4]. As a result, the dispatch of PEV charging provides direct benefit to the entire power system in NYCA.

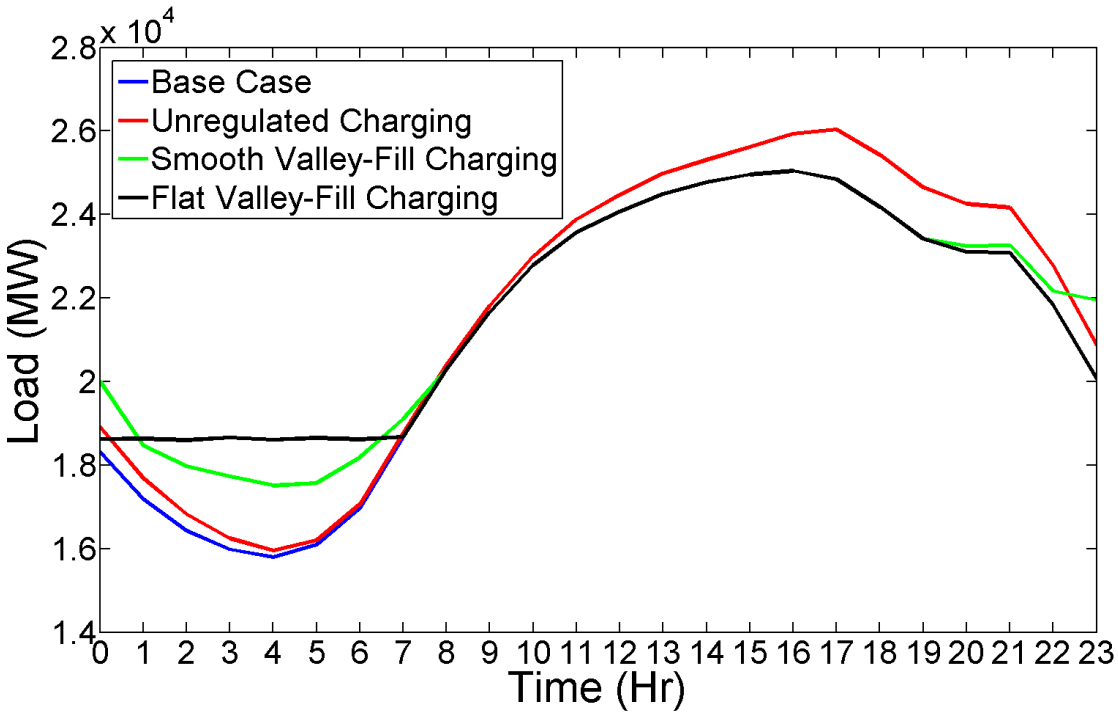

Fig. 2. Base case load profile with unregulated, smooth and flat valley-fill charging schemes for 40% PEV penetration.

This model expands the traditional steady-state dispatch model to explicitly include the system cost of ramping generators. The traditional steady-state cost model depends on the load at a dispatch time, and is constrained only by physical generator ramp rates without explicit cost assignment. However, it is evident that generators incur higher cost (maintenance and fuel consumption) when rapidly changing their set-points to match load changes [21]. This additional cost is the ramping cost. It is likely that this cost will become more significant as the power system incorporates a larger share of intermittent generation [22].

3.3.1 Power System Data

The NYISO provides an extensive archive of historical day-ahead and real-time load and LMP data. As the highest system loads occur in the summertime, this study considers only the summer months from June to August in order to characterize the maximum system benefit of intelligent PEV charging. The data used for this study consists of 21 days from the summer of 2006: June 19-25, July 9-15, and August 13-19. The year 2006 was chosen for its record-setting summer peak loads. These 21 days were also selected to provide a thorough characterization of the time-varying nature of summer loads and LMPs.

3.3.2 System Cost

The system cost for the energy market is formulated as the sum of the DAM cost and

cost of *dispatch adjustment* from the RTM, where cost is the product of LMP and load served by generators. This relationship is given in Equation 2.

Daily Total System Cost =

$$\sum_{t=0}^{T_1} LMP_{DAM,t}\left(P_{DAM,t}, |\Delta P_{DAM,t}|\right) * P_{DAM,t} + \sum_{t=0}^{T_2} LMP_{RTM,t}\left(P_{RTM,t}, |\Delta P_{RTM,t}|\right) * \left(P_{RTM,t} - P_{DAM,t}\right) \quad (2)$$

where the subscripts DAM and RTM refer to the day-ahead and real-time markets, respectively. LMP at time *t* is a function of steady-state load, P, and modulus of load difference, $|\Delta P|$ (assuming a symmetric ramping cost). T_1 is the 23rd hour in the DAM and T_2 is the 143rd ten-minute period in the RTM. The first summation in Equation 2 is DAM cost and the second summation is the cost of RTM adjustment to DAM.

3.3.3 LMP Model

This study incorporates a statistical LMP model for NYCA with PEV charge allocation affecting the LMP. The model uses base case LMPs from the 2006 summer to establish a 0% PEV penetration base case.

3.3.3.1 Cost Model: Inter-Day

To capture the LMP trend of the summer season from the 21 selected days and to

ensure accuracy from the use of Taylor Series expansion around the base case loads and LMPs, weighted average values of base case load, modulus of ramp and LMP were used to construct an approximate model for the daily system cost. This averaging method also preserves the sensitivity of system cost due to load changes while dampening the instability of real-time prices (see Section 3.3.3.2). Equation 3 shows the averaging process, while Equation 4 re-expresses Equation 2 in terms of averaged variables.

$$\sum_{t \in T} LMP_t(P_t, |\Delta P_t|) * P_t \approx \overline{LMP}(\bar{P}, \overline{|\Delta P|}) * \bar{P}_{sys} \quad (3)$$

where weighted averaging is indicated by the accent bar and $\bar{P}_{sys}$ is the equivalent average system load at time *t* (see Section 3.3.3.2).

Daily Total System Cost ≈

$$\overline{LMP}_{DAM}(\bar{P}_{DAM}, \overline{|\Delta P_{DAM}|}) * \bar{P}_{sys,DAM} + \overline{LMP}_{RTM}(\bar{P}_{RTM}, \overline{|\Delta P_{RTM}|}) * (\bar{P}_{sys,RTM} - \bar{P}_{sys,DAM}) \quad (4)$$

Taylor series expansion of the average LMP function around the base case results in Equation 5:

$$\overline{LMP}(\bar{P}, \overline{|\Delta P|}) \approx a_0 + a_1\bar{P} + a_2\bar{P}^2 + a_3\bar{P}\overline{|\Delta P|} + a_4\overline{|\Delta P|} + a_5\overline{|\Delta P|}^2 \quad (5)$$

where a_i is a constant.

Principle component analysis was performed to assess the magnitude of the terms in Equation 5, showing negligible $\overline{|\Delta P|}$ and $\overline{|\Delta P|}^2$ contribution. The final form of the average LMP equation is given in Equation 6:

$$\overline{LMP}\left(\bar{P}, \overline{|\Delta \mathrm{P}|}\right) \approx a_0 + a_1\bar{P} + a_2\bar{P}^2 + a_3\bar{P}\overline{|\Delta \mathrm{P}|} \tag{6}$$

Equation 6 statistically demonstrates that average NYCA LMP can be approximated by a quadratic function of average load, $\bar{P}$, with a ramping term, $\bar{P}\overline{|\Delta P|}$. The constants in this expression were determined from least-squares regression of NYISO DAM and RTM LMP and load data for the 21 summer days. Physically, Equation 6 shows that system ramping is more costly at peak-load than at valley-load due to the use of expensive peaking units.

3.3.3.2 Weighted Average Load: Intra-Day

Within a given day, the model must reflect the high cost of adding load at peak. Therefore, the average system load is a weighted average of three load regions: peak, shoulder and valley. Peak and valley-load hours account for approximately 12 hours in each day, so the sum of the peak-load weight (W_p) and the valley-load weight (W_v) adds up to ½. C_p and C_v are user-defined tuning factors that allow adjustment of the average LMP model to match market data. Thus,

$$C_pW_p + C_vW_v = \frac{1}{2} \tag{7}$$

Letting $R = \frac{W_p}{W_v}$ and $S = \frac{C_p}{C_v}$,

$$C_p W_p = \frac{RS}{2(1+RS)} \; and \; C_v W_v = \frac{1}{2(1+RS)} \tag{8}$$

In model implementation, *R* is calculated from the ratio of peak-load to valley-load and *S* is defined in the interval [*1/R* ≤ *S* ≤ *3/R*]. For example, a value of *S=1/R* results in $C_pW_p = C_vW_v = 1/4$: the non-weighted average load. A value of *S=1* was chosen for the average LMP model to approximate the NYCA load and LMP data. It is worth noting that *S* can be adjusted to better fit data from other control areas.

Finally, the weighted-average load is obtained from Equation 9:

$$\bar{P} = \sum_{i=1}^{I_1} C_p W_p \, P_{p,i} + \sum_{i=1}^{I_2} C_v W_v \, P_{v,i} + \sum_{i=1}^{12} \frac{1}{2} P_{s,i} \tag{9}$$

where *P* is load from data, *s* is shoulder-load region, and $I_1+I_2 = 12$. The equivalent system load, $\bar{P}_{sys}$, is a also function of both $\bar{P}$ and $\overline{|\Delta P|}$, as is in the case with LMP.

$$\bar{P}_{sys} = \bar{P}_{sys}(\bar{P}, \overline{|\Delta P|}) \tag{10}$$

Taylor series is employed to linearize $\bar{P}_{sys}$, resulting in Equation 11.

$$\bar{P}_{sys} \approx b_0 + b_1 \bar{P} + b_2 \overline{|\Delta P|} \tag{11}$$

The constants, b_i, are determined from fitting the ratio of system cost of unregulated PEV charge scheme to the base case such that it approximates the costs from the validation models in Section 3.3.3.3. For the NYCA, $b_0 \approx 0, b_1 \approx 1 \; and \; b_2 \approx 1$. Consequently the final expression for $\bar{P}_{sys}$ is given in Equation 12,

$$\bar{P}_{sys} \approx \bar{P} + \overline{|\Delta P|} \tag{12}$$

It is worth noting that the coefficients in Equations 6 and 11 can be tuned to analyze different scenarios of system ramping on wholesale energy cost, such as from incorporating volatile generation.

3.3.3.3 Model Verification and Validation

The average LMP model was checked for accuracy and stability across various load and PEV charging patterns. Specifically, four sample load curves (pictured in Figure 2) with 40% PEV penetration were tested: first is a base case without PEV charging, second is with a flat valley-fill charge, third is with a smoothed valley-fill charge (which adheres to the charging constraint), and last is with an unregulated PEV charge profile.

Two reference models were used to validate the performance of the average LMP model for these four load curves. The first reference model is a simple load-only regression model, where a quadratic curve is regressed to the base case load and LMP

data.

The second reference model uses MATPOWER, a security-constrained optimal power flow analysis tool, paired with the 36-bus reduced NPCC network, which includes New York, New England, and parts of Pennsylvania and Canada [15, 23]. MATPOWER was used to run economic dispatch of 693 generators in the reduced NPCC network for the base case as well as the unregulated charging case with PEV load scaled up from the NYCA base case to match the NPCC base case. Network constraints were disabled to produce purely economic dispatch prices for comparison with the average LMP with ramp model. The valley-fill case was not considered for economic dispatch, because MATPOWER currently uses a myopic optimization method that is not suited for non-linear ramp costs related to the valley-fill method.

Table 2 shows comparative results among the three LMP models average for the 21 summer days. The results are tabulated as ratios of different PEV charging scenarios and the base case. The smooth valley-fill and the flat valley-fill obtained close results, therefore only the smooth valley-fill results are shown. For the Simple Regression Model comparison the PEV market penetration is 40%; for the MATPOWER model the market penetration is 20%.

Table 2

Comparison of the average LMP model used to the Simple Regression Model and MATPOWER.

LMP Ratio	New York State		Northeast Power Coordinating Council	
	Simple Regression Model	Avg. LMP Model	MATPOWER	Avg. LMP Model
Unregulated/Base Case	1.071	1.051	1.029	1.022
Valley-Fill/Base Case	1.027	0.982	N/A	N/A
Unregulated/Valley-Fill	1.043	1.070	N/A	N/A

Table 2 validates the results of the average LMP model, showing variations ranging from 0.7% for the MATPOWER comparison, to 4.4% for the Simple Regression Model comparison. Interestingly, the average LMP model has a price ratio less than 1 for the valley-fill to base case comparison. This is due to additional load from PEV charging that smoothes the load curve reducing system ramping cost.

3.4 Charge Flexibility Constraint

The Charge Flexibility Constraint (CFC) is a function of commuter driving patterns and the charging infrastructure deployed throughout the system which limits the power withdraw. In this analysis, it is assumed that PEV charging only takes place at the vehicle owners' homes, resulting in the CHP (see Section 3.2.2). If charging is allowed to take place at other locations, such as at work, then a less restrictive profile describing vehicle idleness would be used instead.

The type of charging station available to an individual imposes an additional limitation on power consumption. There are two types of electric vehicle chargers considered in

this study: Level 1 chargers are standard 120V/12A outlets, capable of delivering a maximum of 1.44 kW, while Level 2 chargers considered in this study are rated at 240V/32A and can deliver 7.68 kW (see Introduction for rationale) [9].

The aggregate PEV charging constraint for a specified time period, expressed in kilowatts, is given by Equation 13:

$$CFC(t) \leq CHP(t) M_{PEV} N[1.44\alpha + 7.68(1-\alpha)] \quad (13)$$

where M_{PEV} is the market penetration of PEVs, N is the total number of vehicle owners, and α is the fraction of Level 1 vehicle chargers.

The CFC is independent of any wholesale market model, and is enforced for all PEV charging schemes. Figure 3 shows that at valley-load hours, the maximum charging power decreases sharply from 1 AM to 6 AM averaging close to 1 GW hour^{-1}. From 6 AM to 8 AM the CFC achieves its minimum at approximately 700 MW for a 70/30 Level 1/Level 2 charger mixture.

Figure 3 shows that a flat valley-fill charging scheme violates the CFC for a 70/30 charger mix. It is worth noting that the 70/30 ratio corresponds to an average 3.31 kW power draw for each vehicle, and most PEVs on the road today (Chevy Volt and Nissan Leaf) are limited by the onboard power converter to 3.3 kW. To accommodate the possibility of a flat valley-fill charging scheme, significant infrastructure investment must be made to attain a 30/70 charger mixture. The

system benefit of such an investment is further discussed in Section 3.6.4.

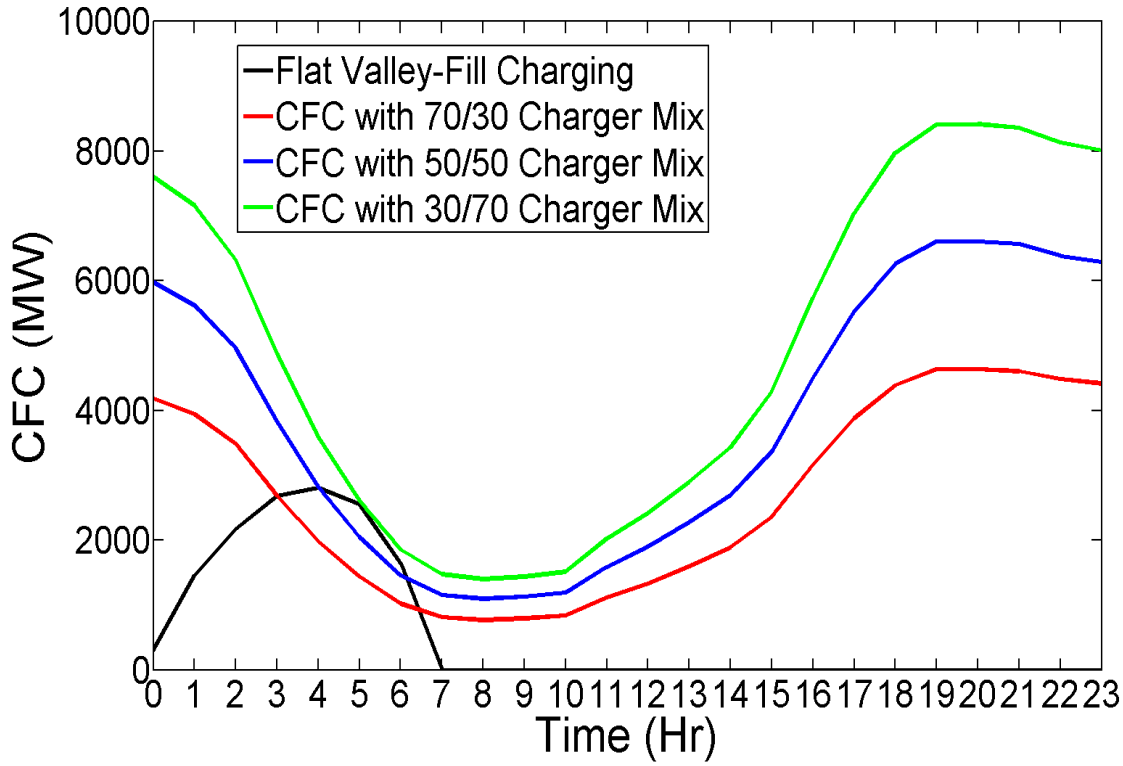

Fig. 3. Flat valley-fill PEV charging profile overlaid with Charge Flexibility Constraint (CFC) for 70/30, 50/50 and 30/70 (Level 1/Level 2) charging infrastructure.

3.5 Intelligent PEV Charging

Intelligent Charging allows an aggregator to allocate PEV charging such that overall system steady-state and ramping costs are minimized in the day-ahead and real-time wholesale energy markets. Intelligent charging also considers the realistic aggregate charging constraint imposed by the CFC. This charging scheme can occur at any time when commuters are at home, and is therefore not limited to valley-load hours. Mathematically, intelligent charging changes system load profiles and ramping

requirements such that both $\bar{P}$ and $\overline{|\Delta P|}$ change.

Total system cost was determined through a linked two-stage optimization process, which was solved for each of the 21 days using Simulated Annealing, a metaheuristic that has been successfully applied to many problems in power systems [24-26]. For each day, the optimization problem is formulated in Equations 14-18 for the DAM stage and Equations 19-21 for the RTM stage.

Day-Ahead Market Stage:

$$\min_{PEV_{DAM,t},\ PEV_{RTM,t}} \begin{cases} \overline{LMP}_{DAM}\left(\bar{P}_{DAM}, \overline{|\Delta P_{DAM}|}\right) * \bar{P}_{sys,DAM} \\ +E\left[\overline{LMP}_{RTM}\left(\bar{P}_{RTM}, \overline{|\Delta P_{RTM}|}\right) * (\bar{P}_{sys,RTM} - \bar{P}_{sys,DAM})\right] \end{cases} \quad (14)$$

s. t.

$$0 \le PEV_{DAM,t} \le CFC_t \qquad \forall t \in \{0 \dots T_1\} \quad (15)$$

$$0 \le PEV_{RTM,t} \le CFC_t \qquad \forall t \in \{0 \dots T_1\} \quad (16)$$

$$0 \le \sum_{t=0}^{T_1} PEV_{DAM,t} \le \sum_{i=1}^{19} M_{PEV} N_i D_i E_i \quad (17)$$

$$\sum_{t=0}^{T_1} PEV_{RTM,t} = \sum_{i=1}^{19} M_{PEV} N_i D_i E_i \quad (18)$$

Real-Time Market Stage:

$$\min_{PEV_{RTM,t}} \begin{cases} \overline{LMP}_{DAM}\left(\bar{P}_{DAM}, \overline{|\Delta P_{DAM}|}\right) * \bar{P}_{sys,DAM} \\ \quad + \overline{LMP}_{RTM}\left(\bar{P}_{RTM}, \overline{|\Delta P_{RTM}|}\right) * (\bar{P}_{sys,RTM} - \bar{P}_{sys,DAM}) \end{cases} \quad (19)$$

s. t.

$$0 \leq PEV_{RTM,t} \leq CFC_t \qquad \forall t \in \{0 \dots T_2\} \quad (20)$$

$$\sum_{t=0}^{T_2} PEV_{RTM,t} = \sum_{i=1}^{19} M_{PEV} N_i D_i E_i \quad (21)$$

where for each day, $PEV_{DAM,t}$ and $PEV_{RTM,t}$ are the PEV charging committed in the day-ahead market (DAM) and dispatched in the real-time market (RTM), respectively.

The DAM solver uses NYISO day-ahead load forecasts for the base load, and the unregulated charging case profile as the initial solution to minimize the energy market cost given a daily PEV energy requirement. The day-ahead solver has an expectation of the RTM LMP based on historical data to evaluate the cost effectiveness of *hourly* PEV charge allocation in the DAM. Moreover, the daily PEV energy requirement is an inequality constraint in the DAM (Equation 17), and an equality constraint in the expected RTM (Equation 18). This way PEVs are guaranteed charging without forcing day-ahead commitment. At this stage, the PEV charge allocation in the DAM is binding, and that in the expected RTM is not binding. The second RTM stage in the optimization algorithm solves for the actual real-time PEV allocation, *in 10-minute increments*, given the pre-determined day-ahead schedule in the first DAM stage. The second stage uses the same LMP model, but with coefficients regressed

for the real-time market. The PEV energy requirement is active in this RTM stage (Equation 21).

3.6 Results and Discussion

3.6.1 Load Profiles with Intelligently Charged PEVs

Figure 4 shows typical intelligent charging allocations for the 21 summer days tested. Results indicated that charging mostly occurs during 7 valley-load hours of 1 AM to 8AM. However, there is noticeable charging during peak hours (12pm to 9pm), specifically from 6 PM to 8:30 PM. Charging during shoulder-load hours is also observed.

3.6.2 Intelligent Charging vs. Valley-Filling

Fundamentally, the intelligent charging model optimizes the combined system benefit of charging at periods of low base load and charging to reduce system ramping. This principle is clearly demonstrated in Figure 4, where the base load ramps down and then up again by roughly 1 GW over 2.5 hours in the late evening, creating a second load peak. The cost of rapidly changing generator set points can be high—$50 to $400 per ramp operation depending on the generator type [27]. Consequently, the system can encourage PEV charging at this time to fill this second valley and smooth the overall load profile.

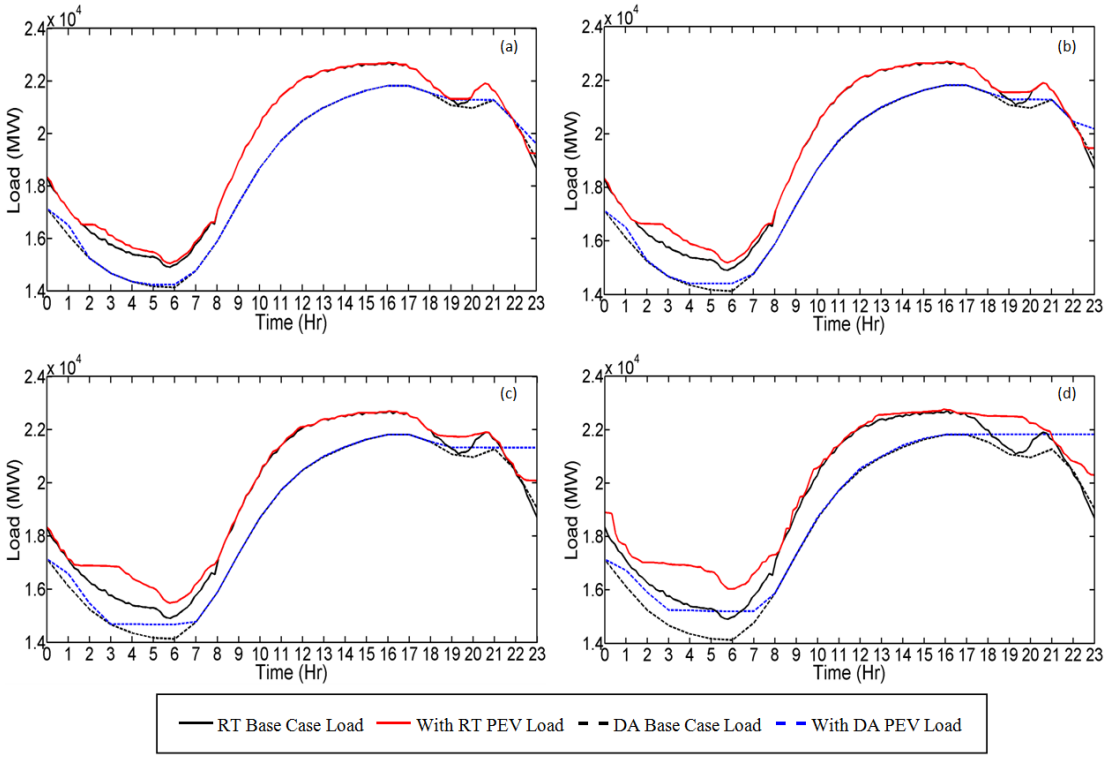

Fig. 4. Day-ahead (DA) and Real-time (RT) load profiles with intelligent PEV charging for July 9th with a 70/30 (Level 1/Level 2) charger mixture. PEV penetrations: (a) 5%, (b) 10%, (c) 20% and (d) 40%.

While smoothing takes place even at the lowest PEV penetrations, the true utility of this dispatchable load is evident only with a larger number of vehicles. At 20% PEV penetration, the second peak is effectively eliminated, and at 40% the peak is further smoothed to create the familiar concave load shape from 8 AM to 11 PM.

Specifically for July 9th, Table 3 tabulates the relative percentages of energy charged at valley-, shoulder-, and peak-load hours, where

$$PEV\ Charge\ Percentage = \frac{Amount\ of\ energy\ charged\ at\ period}{daily\ PEV\ energy\ requirement} * 100 \quad (21)$$

Table 3 illustrates that for July 9th, there is significant charging at peak-load hours averaging from 11.6% for 5% PEV penetration to 24.0% for 40% PEV penetration. Charging at shoulder is approximately equal to that at peak-load. Overall, charging at non-valley-load hours account for about *1/2* of the total daily charge. Peak-load charging percentage increases across the four PEV penetrations. The corresponding load profiles show that the peak-load is dramatically smoothed at 40% PEV penetration. Moreover, the valley-load dip at 6 AM remains with all four PEV penetrations. Subsequent analysis shows that this dip is due to a base case load dip and the 70/30 charging constraint.

Table 3

Charging at valley, shoulder, and peak hours for July 9th 2006.

July 9th (70/30 Charger Mix)	**Real-Time**		
PEV Penetration (%)	Valley Charge (%)	Peak Charge (%)	Shoulder Charge (%)
5	77.6	11.6	10.8
10	74.8	15.4	9.8
20	70.3	14.3	15.4
40	55.6	24.0	20.4

Given the 70/30 ratio of Level 1/Level 2 chargers, average charging percentages for all four PEV penetrations has similar average trends for the three months. Namely,

76.4% to 78.8% of charging is done at valley-load hours, 8.3% to 11.4% at peak-load hours and 11.3% to 12.9% at load shoulder-load hours.

Table 4

Average vehicle charging at valley, shoulder, and peak hours for June, July, and August 2006.

June Avg. (70/30 Charger Mix)	**Real-Time**		
PEV Penetration (%)	Valley Charge (%)	Peak Charge (%)	Shoulder Charge (%)
5	79.2	10.5	10.4
10	80.3	10.4	9.3
20	81.0	7.9	11.2
40	73.0	12.6	14.4
Average	78.4	10.3	11.3
July Avg. (70/30 Charger Mix)	**Real-Time**		
PEV Penetration (%)	Valley Charge (%)	Peak Charge (%)	Shoulder Charge (%)
5	77.9	9.8	12.3
10	82.2	7.8	10.0
20	81.7	5.5	12.8
40	73.5	9.9	16.6
Average	78.8	8.3	12.9
August Avg. (70/30 Charger Mix)	**Real-Time**		
PEV Penetration (%)	Valley Charge (%)	Peak Charge (%)	Shoulder Charge (%)
5	78.0	11.1	10.9
10	79.4	11.0	9.6
20	78.4	9.8	11.8
40	69.9	13.5	16.6
Average	76.4	11.4	12.2

Table 4 tabulates the average charging percentages for the month of June, July and August. On average, charging at valley-load hours is 3.5 times charging at non-

valley-load hours. For all three months there is decreased average marginal incentive to charge at valley-load hours at 40% PEV penetration compared to lesser penetrations. In an optimal charging scenario, there are competing incentives for scheduling at both valley and non-valley hours: during valley hours the steady-state cost of energy is low, however there is less benefit in terms of ramping reduction due to the $\bar{P}\overline{|\Delta P|}$ term in Equation 6; conversely at non-valley hours, there is a larger benefit to ramping reduction, but it is offset by higher steady-state cost.

While the exact charging percentages vary from day to day, the general trend for charging at valley- and shoulder-load hours for the four PEV penetrations is clear. At low to medium PEV penetrations (5% to 10%), the marginal benefit of increasing charge at valley-load hours to take advantage of low steady-state base case load is higher than the marginal benefit of charging at non-valley-load hours to lower system ramping cost. The marginal benefit of charging at valley and non-valley hours is balanced at a medium to high PEV penetrations (10% to 20%). At high PEV penetrations (20% to 40%) there is decreased marginal economic incentive to charge at valley-load hours as the valley becomes smooth. Conversely, there is increased marginal incentive to reduce high system ramping costs at non-valley-load hours. This motivation is illustrated in Figure 5.

Figure 5 illustrates that (with the exception of July 9th) there is a benefit to charging at valley-load hours for low to medium PEV penetrations. However at high PEV penetration, there is not a clear trend for charging at peak. A close inspection of the

load profiles shows that different days (e.g. July 14th and 15th) have drastically different base case peak-loads. July 14th is a day where load at peak follow a smooth sinusoidal profile, requiring little PEV charge allocation for system ramp smoothing. However, July 15th has significant peak-load "dips", requiring PEV allocation at peak-load hours to decrease system ramping cost. Consequently, different base case load shapes are the primary cause for the lack of a clear trend for high penetration PEV charge allocation at peak-load hours.

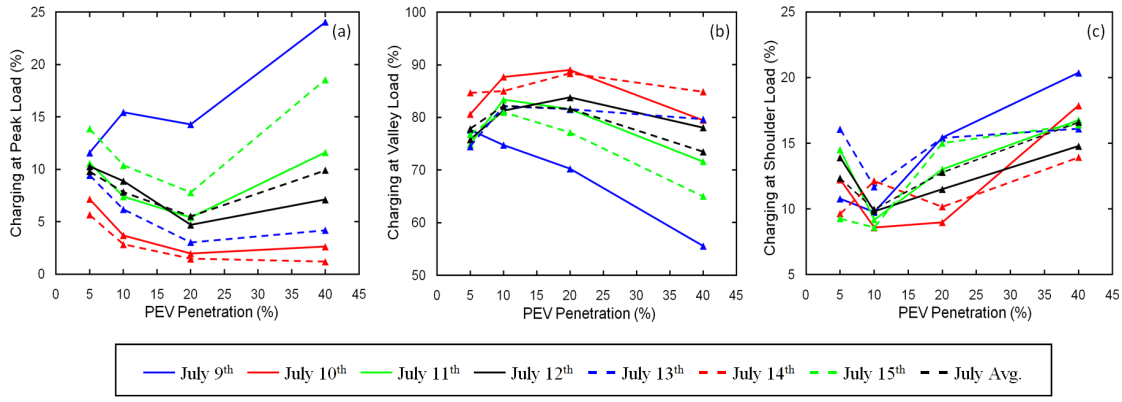

Fig. 5. Percentage of intelligent charging at: (a) peak-load hours, (b) valley-load hours, and (c) shoulder-load hours for July 9th to 15th.

The intelligent charging results from the 21 days are categorized as: maximum charging at peak-load hours, maximum charging at valley-load hours, and typical charging. In Figure 6, July 9th is one of the maximum peak charging scenarios. System cost reductions due to intelligent PEV charging and a flat valley-fill approach is based off unregulated charging, which will occur without retail electricity price penalties, grid reliability constraints or instituted policy.

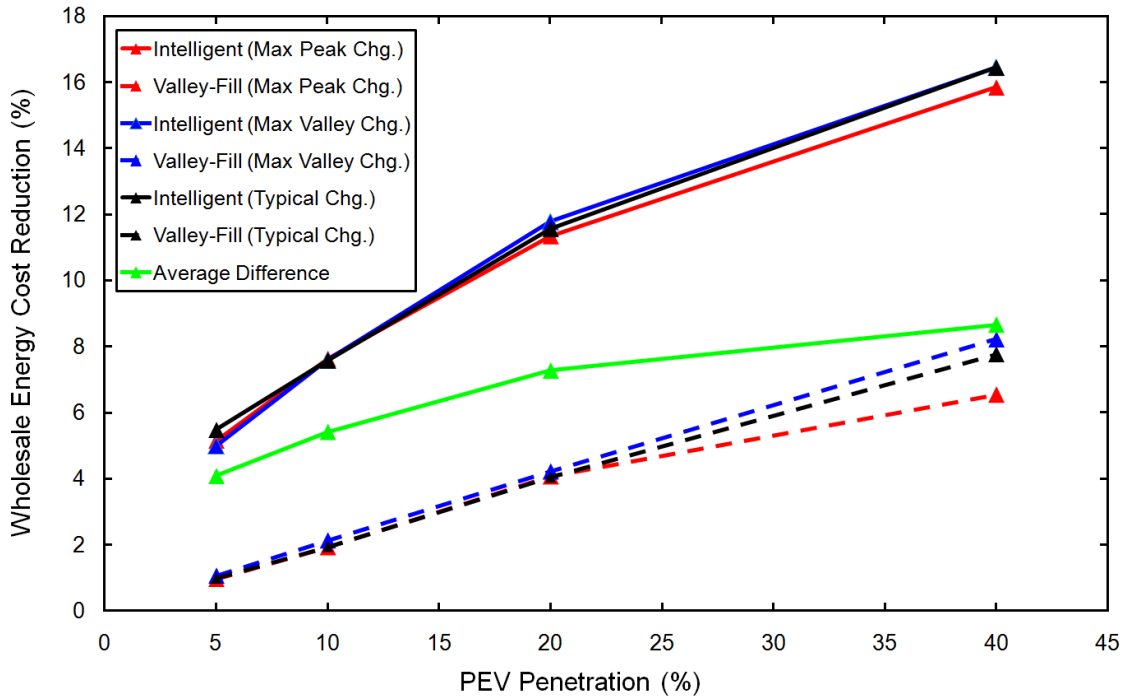

Fig. 6. Wholesale energy cost reductions due to intelligent and valley-fill PEV charging with 70/30 (Level 1/Level 2) charger mixture for three charging results: maximum charging at peak, at valley and typical charging.

Figure 6 demonstrates that an intelligently charged PEV fleet that is charged mostly at valley-load, with some charging at shoulder and peak-load, reduces system cost from 5% at 5% PEV penetration to 17% at 40% PEV penetration. In comparison, a flat valley-fill charging scheme reduces system cost 1% to 8%; 4% to 9% less than intelligent charging.

3.6.3 Impact of the Charge Flexibility Constraint

Independent of cost modeling, the Charge Flexibility Constraint (CFC) has a

significant impact on the dispatch of PEV charging demand, particularly in the morning load valley period. Installing 50% Level 2 chargers relaxes this constraint; however the system benefit of adding these high power charging stations diminished rapidly.

Figure 7 shows that charging at valley hours from 2 AM to 6 AM increases as more Level 2 chargers are used. This trend is demonstrated with Level 2 charger percentages from 30%, to 50% to 70%. The CFC for the 70/30 (Level 1/Level 2) charger mix prohibits any additional PEV charging between hours 2 AM to 6 AM. This constraint prohibits a flat valley-fill. The CFC is greatly alleviated with a 50/50 charger mix, and the valley-load becomes flatter. With a significant Level 2 charger investment resulting in a 30/70 charger mix, the charging constraint is mostly eliminated, except from 5 AM to 6 AM. This allocation reduces ramping cost at valley-load while taking advantage of the low steady-state load and price at those hours.

The slight valley-load dip from 2 AM to 5 AM is never completely eliminated. An inspection of the CFC indicates that the constraint is inactive between these hours. Instead the cause of such a slight dip is economic. Instead of completely smoothing valley-load, PEV is marginally allocated at the peak-load hours of 7 PM and 8 PM, and shoulder-load hours of 10:30 PM to 11 PM. This is because the marginal economic benefit of completely flattening valley-load is less than that for allocating the remaining PEV load at the indicated hours. Furthermore, at 4 AM to 5

AM the constraint is still active forcing the dip in load. Consequently, at 2 AM and 3 AM PEV charging is also slightly curtailed to allow for smoother ramping once the CFC becomes active.

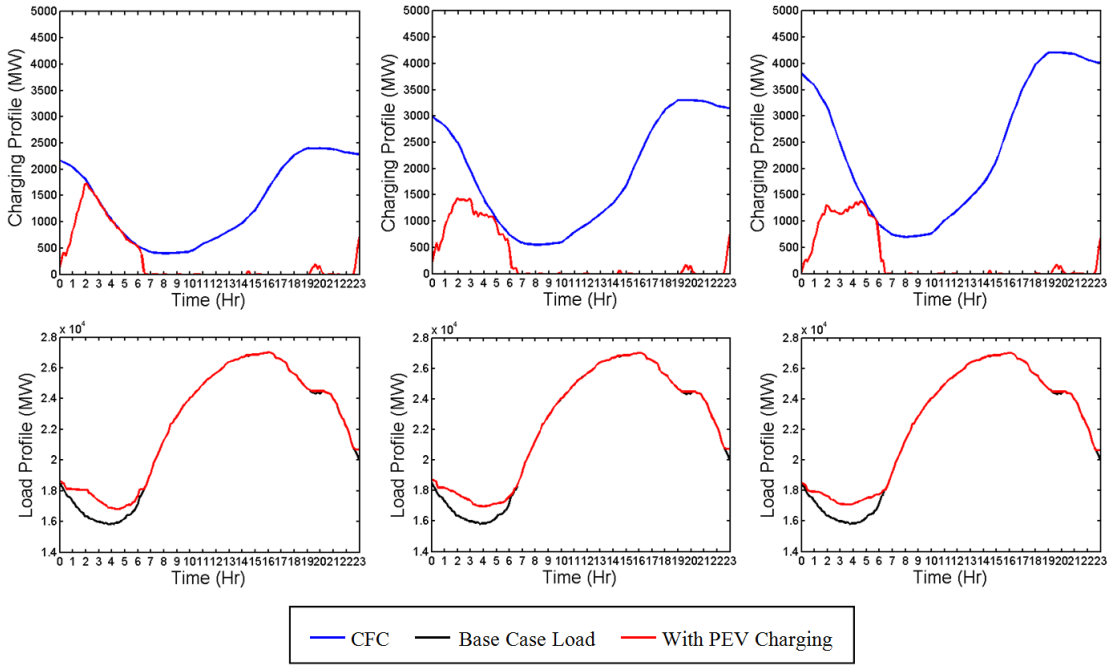

Fig. 7. Effect of the Charge Flexibility Constraint (CFC) on the intelligent charging of 20% PEVs with Level 1/Level 2 charger mixtures: (left) 70/30, (middle) 50/50 and (right) 30/70.

As the valley-load timing can significantly change the PEV allocation (particularly with large market penetrations) the importance of accurate load forecasting becomes clear. If forecast misses the timing of the valley-load, then there can be a noticeable error in the commitment of the generators and PEV allocation. Such circumstances would create additional system inefficiencies from over- or under-commitment. This

phenomenon is shown in Figure 8.

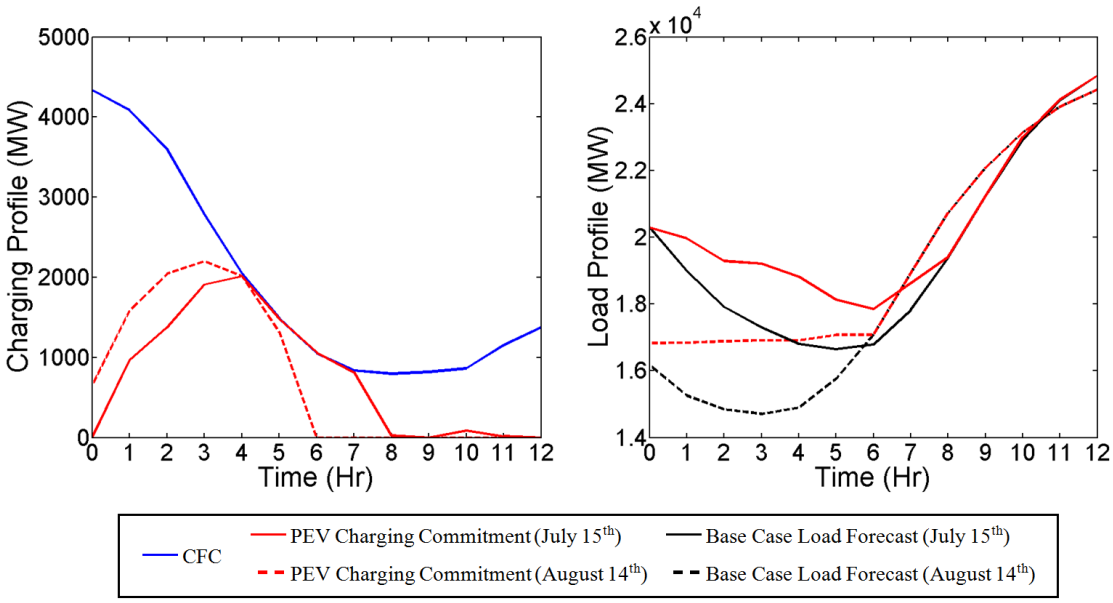

Fig. 8. Effect of base case load forecast and the Charge Flexibility Constraint (CFC) on day-ahead PEV charging commitment in the load-valley for July 15th and August 14th.

This charging constraint can place severe limitations on any valley-filling approach when the valley-load hours are centered on 5 AM. However, due to a sharp decrease in maximum charging from 1 AM to 6 AM, a valley-load shift of 1 to 3 hours to the left can significantly diminish the effect of the CFC.

It is worth noting that Figure 7 shows that there is a minute amount of PEV charging at the end hour. This is a solver limitation. Because this study only analyzed a daily load pattern rather than a longer time frame, the model attempts to smooth the ramping

down at the end hour without connecting to the next day. If the connection is made, then there will be a slightly smoother valley-load, and slightly less PEV allocation at the end hour.

3.6.4 Impacts of Adding Level 2 Chargers

The normalized unregulated charging profile in Figure 1 is constructed with a 70/30 charger mixture. With higher Level 2 charger penetration, the problem of PEV charging at peak load will be exacerbated, resulting in a quadratic increase in LMP and cubic increase in wholesale energy cost.

Figure 9 shows wholesale energy market cost reductions from intelligently charged PEVs with Level 2 charger penetrations at and above 30%, with the same three charging categories as in Figure 6. Figure 9 shows that at low to medium PEV penetrations (5%-10%) increasing the infrastructure investment from 30% to 50% Level 2 chargers reduces wholesale electricity cost by 0.40% on average. However, at medium to high PEV penetrations (20% to 40%), this investment only reduces cost by 0.25% on average. Further investment to increase the share of Level 2 chargers from 50% to 70% or from 50% to 100% would on average reduce system cost less than or equal to 0.11% or 0.15%, respectively.

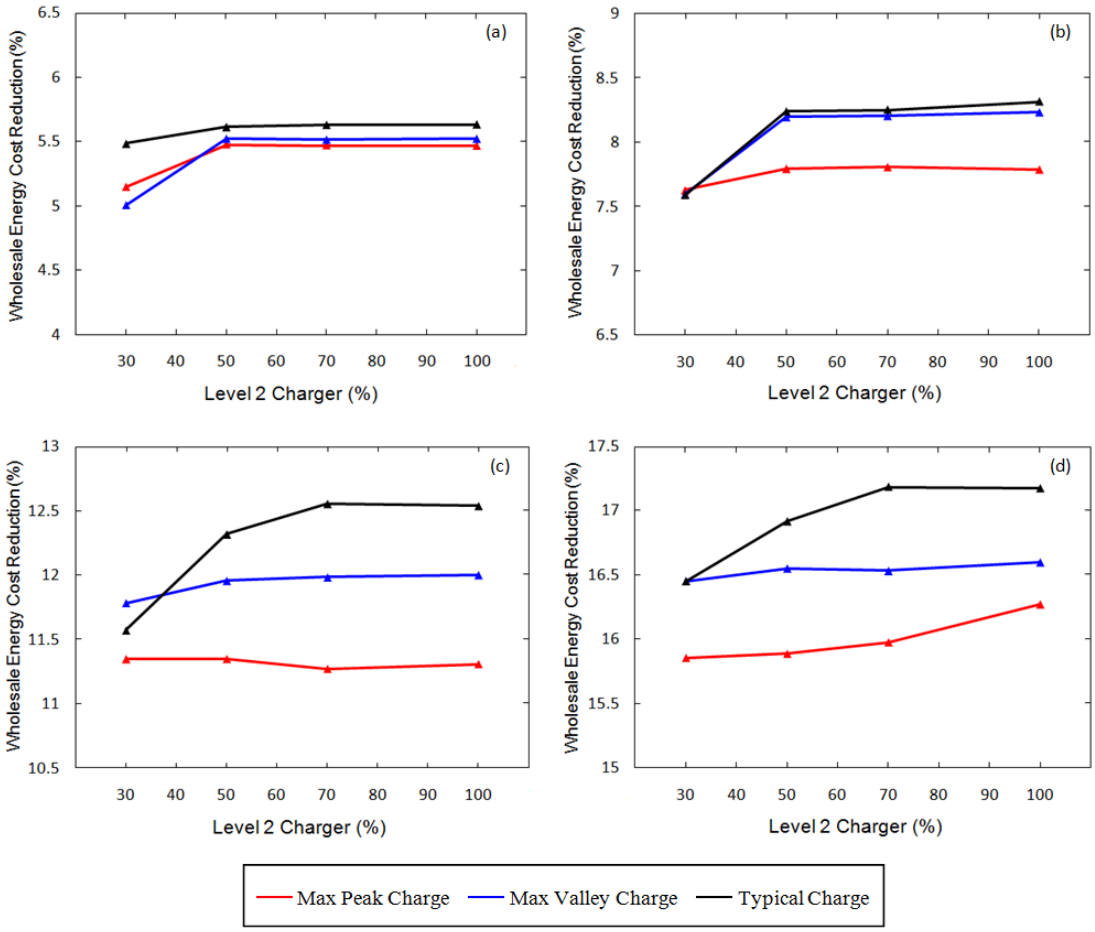

Fig. 9. Effect of Level 2 charger penetration on wholesale energy cost for three charging results: maximum charging at peak, at valley and typical charging. PEV penetrations: (a) 5%, (b) 10%, (c) 20% and (d) 40%.

Overall, the system benefit is significantly reduced for more than 50% penetration of Level 2 chargers due to the decreased effect of the CFC on PEV charging in the morning valley load hours. This reduction in benefit is exacerbated by a decrease in the percentage of valley charging for higher PEV penetrations as illustrated in Figure 5. Moreover, as more PEVs charge at peak- and shoulder-load hours, the difference between the optimal charge profile and the unregulated charge profile decreases.

From the perspective of only regulating PEV charging, the additional cost of investing in Level 2 chargers above the 50/50 mixture may outweigh the benefit in reducing system cost.

It is worth noting that in Figure 9 the reduction in system cost is relative to a fixed unregulated charging profile with a 70/30 charger mixture. This value, the lowest considered in this study, was selected to provide a benchmark for the system benefit of adding additional high power charging stations.

3.7 Conclusions

As Plug-in Electric Vehicle (PEV) ownership grows, controlling when these vehicles charge becomes an important issue for energy providers. Perhaps the most well-known regulated charging policy is the so-called valley-fill where vehicle charging takes place only in the early morning when system demand is lowest.

Motivated to improve upon the valley-filling method, this study considers PEV market penetrations of 5%, 10%, 20%, and 40% in New York State, participating in the New York Independent System Operator's day-ahead and real-time energy markets. For 21 days in June, July and August of 2006, vehicle scheduling decisions are made using a statistical Locational Marginal Price (LMP) and wholesale energy cost model that explicitly includes the dynamic cost of generator ramping in addition to the traditional steady-state operation model. This model creates a framework with two competing

cost objectives.

This study also proposes a Charge Flexibility Constraint (CFC) modeling commuter driving behavior and the investment in Level 1 (1.44 kW) and Level 2 (7.68 kW) charging infrastructure. The CFC, which is independent of market modeling, severely restricts PEV charging, particularly in the morning load valley hours. As a result, a complete valley-filling in the New York Control Area cannot be achieved for most charger mixtures. Using a Simulated Annealing optimization algorithm, the proposed intelligent PEV charging method, which minimizes cost from both steady-state and ramping operations, is shown to reduce wholesale energy cost 4% to 9% beyond that of the valley-fill scheme.

Adding more Level 2 chargers without regulating PEV charging will significantly increase LMP and wholesale energy cost due to increased unregulated charging at peak load. The proposed intelligent PEV charging method will lead to a noticeable reduction in system cost if the penetration of Level 2 chargers is increased from 70/30 to 50/50 (Level 1/Level 2) mixture. However, the system benefit is drastically decreased for higher penetrations of Level 2 chargers due to the diminished effect of CFC on PEV charging in the morning. This trend is exacerbated by a smaller percentage of charging at valley load hours for high PEV penetrations.

ACKNOWLEDGEMENTS

We would like to thank Tim Mount, Lindsay Anderson, Ray Zimmerman and Robert Thomas at Cornell University for their feedback. This paper was prepared with the support of the U.S. Department of Energy for "The Future Grid to Enable Sustainable Energy Systems," an initiative of the Power Systems Engineering Research Center which is an NSF Industry/University Cooperative Research Center.

REFERENCES

[1] M.H. Albadi, E.F. El-Saadany, A summary of demand response in electricity markets, Electric Power Systems Research, Volume 78, Issue 11, November 2008, Pages 1989-1996, ISSN 0378-7796, DOI: 10.1016/j.epsr.2008.04.002.

[2] Richard N. Boisvert, Peter A. Cappers, Bernie Neenan, The Benefits of Customer Participation in Wholesale Electricity Markets, The Electricity Journal, Volume 15, Issue 3, April 2002, Pages 41-51, ISSN 1040-6190, DOI: 10.1016/S1040-6190(02)00277-4.

[3] Brooks, A.; Lu, E.; Reicher, D.; Spirakis, C.; Weihl, B.; , "Demand Dispatch," *Power and Energy Magazine, IEEE* , vol.8, no.3, pp.20-29, May-June 2010, DOI: 10.1109/MPE.2010.936349

[4] Papavasiliou, A.; Oren, S.S.; "Coupling Wind Generators with Deferrable Loads," *Energy 2030 Conference, 2008. ENERGY 2008. IEEE* , vol., no., pp.1-7, 17-18 Nov. 2008, DOI: 10.1109/ENERGY.2008.4781058

[5] Keith, G., Biewald, B., White, D., "Modeling Demand Response and Air Emissions in New England". Synapse Energy Economics (prepared for US EPA), 2003.

[6] B. K. Purushothaman and U. Landau, J. Electrochem. *Rapid Charging of Lithium-Ion Batteries Using Pulsed Currents*. Soc. 153, A533 (2006), DOI:10.1149/1.2161580

[7] Jun Li, Edward Murphy, Jack Winnick, Paul A. Kohl, The effects of pulse charging on cycling characteristics of commercial lithium-ion batteries, Journal of Power Sources, Volume 102, Issues 1-2, 1 December 2001, Pages 302-309, ISSN 0378-7753, DOI: 10.1016/S0378-7753(01)00820-5

[8] Denholm, P., Short, W., 2006. *An Evaluation of Utility System Impacts and Benefits of Optimally Dispatched Plug-In Hybrid Electric Vehicles* [NREL].

[9] The Massachusetts Division of Energy Resources, *Installation Guide for Electric Vehicle Charging Equipment*, 2000.

[10] Mohseni, P.; Stevie, R.G.; , "Electric vehicles: Holy grail or Fool's gold," *Power & Energy Society General Meeting, 2009. PES '09. IEEE* , vol., no., pp.1-5, 26-30 July 2009, DOI: 10.1109/PES.2009.5275921

[11] Parks, K., Denholm, P., Markel T., 2007. *Costs and Emissions Associated with Plug-In Hybrid Electric Vehicle Charging in the Xcel Energy Colorado Service Territory* [NREL].

[12] Keenan Valentine, Jonathan Acquaviva, E.J. Foster, K. Max Zhang, Transmission network-based energy and environmental assessment of plug-in hybrid electric vehicles, Journal of Power Sources, Volume 196, Issue 6, 15 March 2011, Pages 3378-3386, ISSN 0378-7753, DOI: 10.1016/j.jpowsour.2010.11.110.

[13] Axsen, Jonn and Kenneth S. Kurani (2008) The Early U.S. Market for PHEVs: Anticipating Consumer Awareness, Recharge Potential, Design Priorities and Energy Impacts. Institute of Transportation Studies, University of California, Davis, Research Report UCD-ITS-RR-08-22

[14] US Census (2000), Summary File 3 <http://factfinder.census.gov/jsp/saff/SAFFInfo.jsp?_lang=en&_sse=on&_content=sp4_decennial_sf3.html&_title=Summary+File+3+%28SF+3%29>

[15] Allen, Eric H., Jeffrey H. Lang, and Marija D. Ilic., 2008. *A Combined Equivalenced-Electric, Economic and Market Representation of the Northeast Power Coordinating Council U.S. Electric Power System*. IEEE Transactions on Power Systems.

[16] U.S. Department of Energy, *Transportation Energy Data Book*, 29th Edition. <http://www-cta.ornl.gov/data/index.shtml>

[17] National Congestion tables, <http://mobility.tamu.edu/ums/congestion_data/tables/national/table_1.pdf>.

[18] New York City Department of City Planning, Population Division, Journey to Work Tables (2008). <http://home2.nyc.gov/html/dcp/html/census/journey tables.shtml>

[19] Parsons Brinckerhoff Quade Douglas Inc., General Final Report, 2000. <http://www.nymtc.org/project/surveys/files/fr00321.pdf>

[20] NYISO market information page <http://www.nyiso.com/public/about_nyiso/understanding_the_markets/energy_market/index.jsp>

[21] Makoto Tanaka, Real-time pricing with ramping costs: A new approach to managing a steep change in electricity demand, Energy Policy, Volume 34, Issue 18, December 2006, Pages 3634-3643, ISSN 0301-4215, DOI: 10.1016/j.enpol.2005.07.012.

[22] Mount, T.; Lamadrid, A.J.; , "Are existing ancillary service markets adequate with high penetrations of variable generation?," *Power and Energy Society General Meeting, 2010 IEEE* , vol., no., pp.1-9, 25-29 July 2010

[23] R. D. Zimmerman, C. E. Murillo-Sánchez, and R. J. Thomas, "MATPOWER's Extensible Optimal Power Flow Architecture," *Power and Energy Society General Meeting, 2009 IEEE*, pp. 1-7, July 26-30 2009.

[24] Deeb, N.; "Simulated annealing in power systems," *Systems, Man and Cybernetics, 1992., IEEE International Conference on* , vol., no., pp.1086-1089 vol.2, 18-21 Oct 1992, DOI: 10.1109/ICSMC.1992.271645

[25] Viana, A.; de Sousa, J.P.; Matos, M.; "Simulated annealing for the unit commitment problem," *Power Tech Proceedings, 2001 IEEE Porto*, vol.2, no., pp.4 pp. vol.2, 2001, DOI: 10.1109/PTC.2001.964747

[26] M. Basu, A simulated annealing-based goal-attainment method for economic emission load dispatch of fixed head hydrothermal power systems, International Journal of Electrical Power & Energy Systems, Volume 27, Issue 2, February 2005, Pages 147-153, ISSN 0142-0615, DOI: 10.1016/j.ijepes.2004.09.004.

[27] C.Wang; S. M. Shahidehpour, “Optimal generation scheduling with ramping costs,” *IEEE Trans. Power Syst.*, vol. 10, pp. 60–67, Feb. 1995.

CHAPTER 4

THE RELATIONSHIP BETWEEN WIND POWER, ELECTRIC VEHICLES AND CHARGER INFRASTRUCTURE IN A TWO-SETTLEMENT ENERGY MARKET

4.1 Background

As both renewable energy and PEV market penetrations increase, there is a growing intent of using the flexible charging of PEVs as a demand-side resource to improve the integration of intermittent generation resources into power systems [1, 2]. In terms of wind energy, areas of improvement include reducing wind curtailment and diminishing the effects of wind variability and unpredictability on generation-load balancing. Consequently, traditional wisdom suggests the coupled benefit of these two resources, i.e. wind and PEVs mutually benefit their individual integration into electricity markets and that they both benefit the markets as system-level resources.

There is a growing body of literature on the charging of an aggregated number of PEVs and the dispatch of regional wind generation. Several charging control mechanisms and aggregation methods have been investigated in direct coupling wind energy and PEVs [3-6], and many of them involve ancillary services enabled by vehicle-to-grid (V2G) technologies [7-9]. A single-settlement approach was adopted to model energy markets [10, 11], which reported decreases in wind power curtailment with flexibly charged PEVs. A yearly generation planning algorithm was applied to

assess the impact of PEVs on the mixture of Ireland's energy and capacity needs based on the island's existing units and potential new builds [12]. Another study optimized PEV charging and dispatch of renewable assets using a non-market approach based on thermal generator costs and emissions to report decreases in system costs and pollutant emissions [13].

This study adds to the body of literature on electric vehicles and wind integration by: (1) modeling the dispatch of PEVs and wind generators with various charging infrastructures in a two-settlement energy market—the common structure of U.S. energy markets, (2) examining the dispatch linkage between EVs and wind units with forecasted and realized wind profiles, and (3) revealing an economic substitution effect between EVs and wind power in minimizing wholesale energy cost.

This work expands the two-settlement market model previously developed by the authors. The market model incorporates the steady-state production cost and systemic ramping cost of the thermal generators. Flexible PEV charging and wind power dispatch subject to curtailment and must-take regulations are optimized in the market model where the objective is to minimize total wholesale market cost. Level 1/Level 2 charger infrastructures at 95/5, 85/15, 70/30, 50/50 and 30/70 mixtures are incorporated based on a commuter transportation model [14]. The study spans 21 days in June, July and August of 2006—a summer of record breaking peak loads—with 0%, 2%, 5%, 10%, 15% and 25% wind power penetrations and the same six market penetrations for PEVs for a total of 7,560 scenarios.

4.2 Modeling of a Two-Settlement Energy Market, Wind Power and PEVs

4.2.1 A Wholesale Energy Market Model, Net Load and Generator Cycling

This two-settlement market model is calibrated to the day-ahead and real-time markets administered by the New York Independent System Operator (NYISO). The New York bulk power system serves 19 million people and NYISO administers trades of power products worth $7 billion annually. In 2006, the average generation mixture was 30% natural gas, 30% nuclear, 18% conventional hydro, 15% coal, 5% petroleum and 2% renewables. This was a much cleaner and diverse mixture compared to the then national average of 49% coal, 21% natural gas, 19% nuclear, 7% conventional hydro, 2% petroleum and 2% renewables. As of 2013, the peak load in the NYCA was set in August of 2006 at approximately 34 GW. For the 3 summer weeks studied, the average load was 22 GW, average locational marginal price (LMP) was $71/MWh and highest LMPs were well over $500/MWh.

The day-ahead market (DAM) contracts generators and settles LMPs approximately 20 hours in advance of the actual system operation. On a 5-minute basis, the real-time market (RTM) adjusts generation and LMPs according to actual system conditions. The commitment cost from the DAM and adjustment cost from the RTM form the total wholesale energy market cost.

The proprietary and protected nature of generator and network data renders a unit

commitment and optimal power flow (OPF) based approach unlikely to yield accurate market outcomes with publically available information. Consequently, the authors developed a non-linear two-settlement model based on market fundamentals and historical market data. This model is calibrated to duplicate the prices and generation/load balance in NYISO's DAM and RTM. The model will determine a price response to a change in the system's net load in order to evaluate the impact of adding wind power and PEVs [15]. Net load, $P_{net,t}$, is the load to be met by conventional generators at time t. It is calculated by adding PEV load to and subtracting wind power from the base case load [16].

While a traditional energy market considers generator ramp limits, it does not explicitly incorporate cost of ramping, such as from additional variable O&M costs. As wind power is variable and unpredictable, the additional costs from increased cycling of thermal generators are most probable. Consequently, the market model in this study includes the cost of ramping generators by adding variables derived from changes in the net load. Specifically, the daily total wholesale energy market cost is defined by Equations 1 [15].

Daily Total Energy Cost =

$$\overline{LMP}_{DAM}\left(\bar{P}_{DAM}, \overline{|\Delta P_{DAM}|}\right) * \bar{P}_{sys,DAM} + \overline{LMP}_{RTM}\left(\bar{P}_{RTM}, \overline{|\Delta P_{RTM}|}\right) * (\bar{P}_{sys,RTM} - \bar{P}_{sys,DAM}) \quad (1)$$

The first term is the DAM cost and the second terms is the RTM's adjustment cost.

In DAM, wholesale cost is the product of a LMP function and derived system load. In RTM, the day-ahead system load is replaced by the difference between real-time load and day-ahead load [15].

Equation 2 explains the load-weighted LMP function is composed of steady-state load, $\bar{P}$, and modulus of system ramp, $\overline{|\Delta P|}$, defined as the absolute value of the difference between net load at two consecutive time periods.

$$\overline{LMP}\left(\bar{P}, \overline{|\Delta \mathrm{P}|}\right) \approx a_0 + a_1\bar{P} + a_2\bar{P}^2 + a_3\bar{P}\overline{|\Delta \mathrm{P}|} \tag{2}$$

Equation 2 statistically shows that NYISO's LMP is approximately second-order in net load (steady-state) with a mixed term of net load and ramp. Economically, Equation 2 shows system ramp costs are expectedly higher at peak-load than valley-load due to the high cost of peaking units [15].

4.2.2 Wind Power Inputs to the Market Model

Inaccurate forecast and variable production of wind power add to the cost of wind integration [17]. This study uses geographically and temporally varying land-based wind power data provided by the National Renewable Energy Laboratory (NREL) to build a large selection of wind scenarios based on production predictability and variability [18]. These scenarios include realized wind power in 10-minute increments and forecasted wind power with day-ahead and four-hour-ahead horizons

in hourly increments.

Wind power from 66 potential wind farms in New York State with a total capacity of 14,860 MW are used for 2%, 5% and 10% wind penetration scenarios [18]. A hundred-and-seventy potential wind farms with a total capacity of 20,580 MW are added to support 15% and 25% wind penetration scenarios [18]. Figure 1 shows the average realized wind power, four-hour-ahead and day-ahead wind power forecasts for the selected 21 summer days.

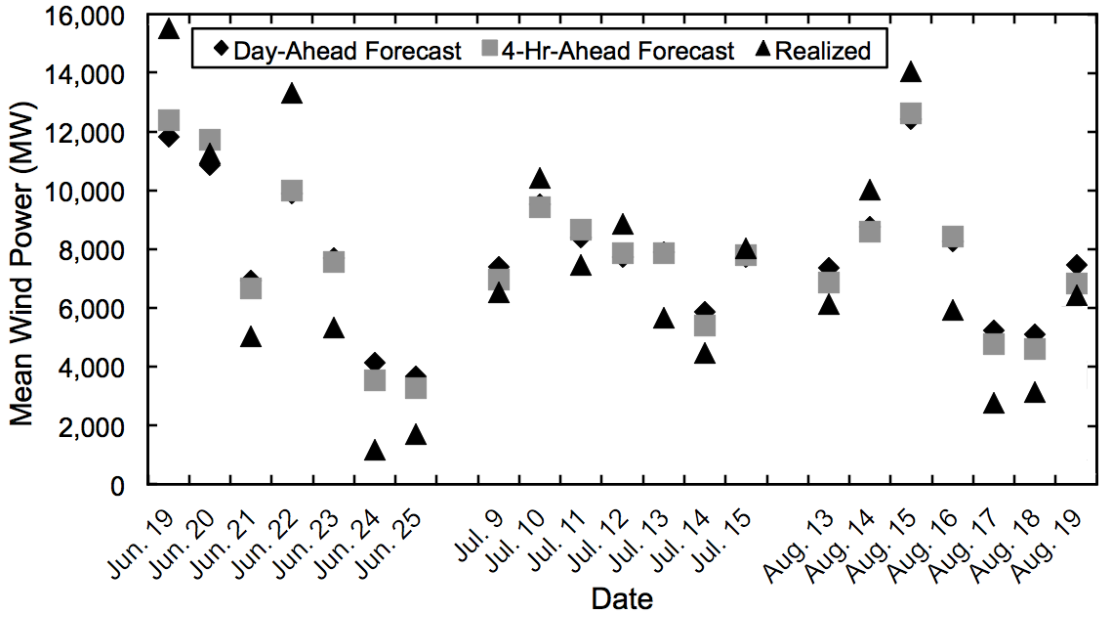

Fig. 1. Average of simulated wind power realizations and forecasts from four-hour-ahead and day-ahead horizons for 21 summer days in 2006. The scenarios show a wide range of under- and over-forecasts of wind power [18].

Figure 1 also shows that the average wind power realizations range from

approximately 1,200 MW to 15,600 MW. The narrative is for a highly variable wind resource across days. In addition, the average wind power supply varies from 3% to 45% of the total nameplate capacity. There is a small mean and spread of the difference between the averages of the forecasts (mean of 7%, standard deviation of 7%) and a large mean and spread for that between the averages of the forecast and realized wind power (mean of 47%, standard deviation of 60%). As a consequence of the different wind data sets, wind production inputs in the DAM use a day-ahead forecast. The RTM use a persistence scheme based on realized production for the hour-ahead, a four-hour-ahead forecast for hours two to four ahead, and a day-ahead forecast for hours five to twenty-four ahead.

There is also a variety of intraday production variability exemplified in Figure 2. The two time-series of normalized wind production on June 25th and August 18th showcase high production and high volatility in the morning and midday, respectively, while July 10th showcases relatively steady wind production.

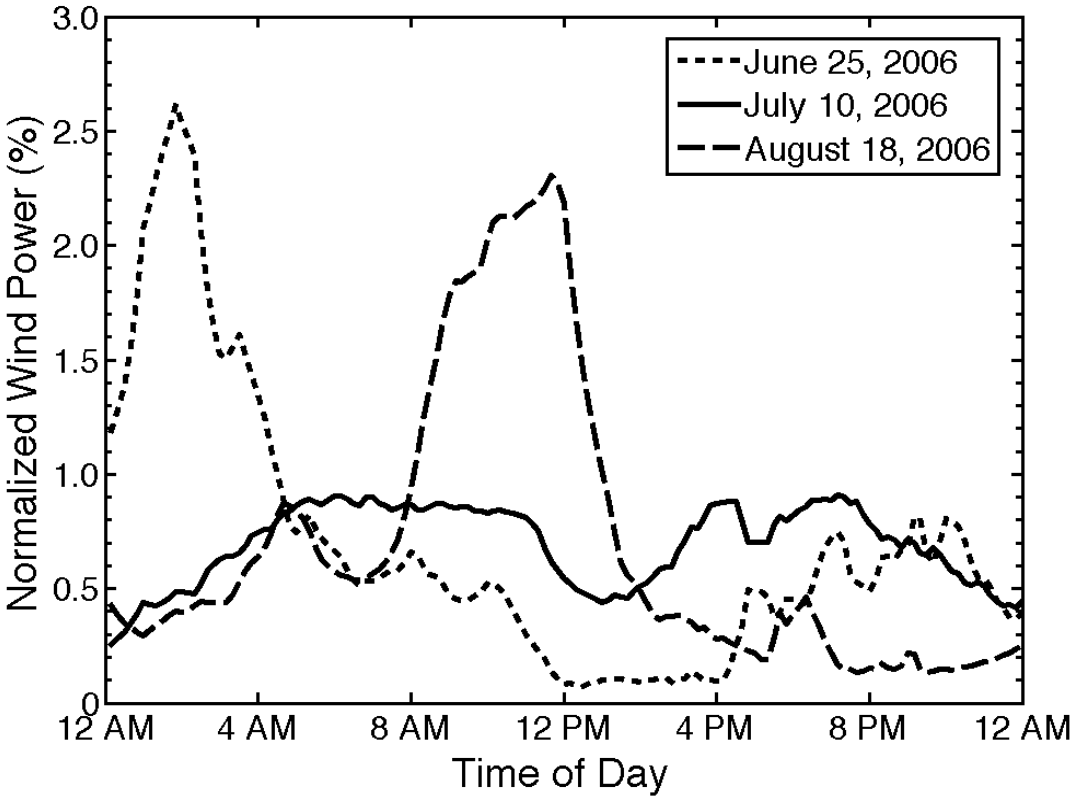

Fig. 2. Time-series of diverse intraday variability in normalized wind production in summer 2006. The spectrum of wind forecast accuracy and production variability in the case studies provides a comprehensive analysis on the relationships between wind, PEV and charger infrastructure in energy markets.

Sixteen types of wind power categories from four selection criteria are used in the 7,560 scenarios. The first three criteria assess wind resource and the fourth criterion is based on regulatory policy.

1. Under- or over-forecast (between day-ahead forecasted and realized wind power)
2. High or low predictability (between day-ahead forecasted and realized wind power)
3. High or low variability (within realized wind power)
4. Must-take or curtailable wind

A "must-take wind" policy is a requirement on the power system to absorb all available wind production. This type of policy enforces wind participation—overriding market-based dispatches, where cost of system ramps due to wind variability and forecast error can curtail some wind. A "curtailable wind" policy adheres to market-based dispatches, where wind can be curtailed to reduce total system cost. (See Section 4.2.1 for system cost explanation and Section 4.2.4 for details on dispatch formulation.)

4.2.3 The Charge Flexibility Constraint in the Market Model

The Charge Flexibility Constraint (CFC) and Level 1/Level 2 charging infrastructure are critical in deriving the optimal PEV charging profiles [15]. The CFC is a time-varying profile that provides an upper bound on the aggregated charging power for commuters to charge at home. The CFC is derived from the ratio of Level 1 and Level 2 charger infrastructure in the NYCA and a commuter transportation model built from several data sources [14]. The maximum charging available to commuters

places limits on the PEV's power withdraw from the grid. A Level 1 charger delivers 1.44 kW at 120V/12A and a Level 2 charger delivers 7.68 kW at 240V/32A. Analysis of PEV charging at the distribution system level is beyond the scope of this study. It is reported that charging above 7.68 kW may have adverse impacts on distribution feeders and is not studied here [19-21]. However, the concept of a CFC is expandable to incorporate distribution constraints as such limitations directly impact charging flexibility.

The data needed to build the transportation model include the 2000 US Census survey containing the 4.6 million commuters in New York State, categories of drivers in "center city", "suburban" and "rural", and the electricity used per mile for a range of vehicle types [22]. The transportation model also used the Regional Travel Household Interview Survey (RTHIS), the 2000 Census Transportation Planning Package (CTPP), and different Travel Time Indexes to formulate traffic and profiles of commuters at home [14].

4.2.4 Optimal PEV Charging and Wind Power Dispatch

Optimal PEV charging utilizes the concept of an aggregator that is able to actively manage all charging in its service territory. In this study, the task for an aggregator is to resolve the PEV charging profiles that minimize the daily wholesale energy market cost subject to the CFC. In addition to the reduced charging cost for PEV owners, aggregators and their customers may be rewarded for rendering services to the power

system. In contrast to optimal charging, unregulated charging schemes allow commuters to charge whenever they are home, which exacerbates load peaks. In contrast to aggregators acting as market representatives of the PEVs, grid-scale wind farms are bulk power suppliers directly dispatched by a system operator. In the case of a must-take wind policy, wind power is an exogenous input directly modifying the system load prior to optimizing PEV charging. Such a wind policy enforces the injection of any available wind power at the potential expense from increased system ramping and decreased economic optimality. On the other hand, a curtailable wind policy strives to lower system costs via treating wind supply as a flexible competitor to other types of generation. A curtailable wind scenario encompasses a must-take policy in the sense that zero curtailment is a specific solution. It is conceivable that wind unpredictability and variability can increase system cost at times—making wind curtailment a more optimal outcome than must-take wind. Curtailment approach binds wind dispatch between 0 MW and the maximum wind resource.

Algorithmically, a metaheuristic adapted from Simulated Annealing and Dynamically Dimensioned Search optimizes the market model via controlling PEV charging and/or wind dispatch depending on the wind injection policy. A metaheuristic solver is used due to the non-convexity of the objective function with the ramping variables. Both optimal PEV charging and curtailable wind power dispatch are determined from a coupled two-stage optimization over a 24-hour horizon with the DAM in hourly increments and the RTM in 10-minute increments. Equations 3 through 9 shows the DAM optimization and Equations 10 through 13 shows the RTM optimization.

Day-ahead market stage:

$$\min_{\substack{\mathrm{PEV}_{\mathrm{DAM},t},\mathrm{PEV}_{\mathrm{RTM},t} \\ \mathrm{Wind}_{\mathrm{DAM},t},\mathrm{Wind}_{\mathrm{RTM},t}}} \Big\{ \overline{\mathrm{LMP}}_{\mathrm{DAM}}(\bar{P}_{\mathrm{DAM}}, \overline{|\Delta P_{\mathrm{DAM}}|}) \times \bar{P}_{\mathrm{sys,DAM}} + E[\overline{\mathrm{LMP}}_{\mathrm{RTM}}(\bar{P}_{\mathrm{RTM}}, \overline{|\Delta P_{\mathrm{RTM}}|}) \times (\bar{P}_{\mathrm{sys,RTM}} - \bar{P}_{\mathrm{sys,DAM}})] \Big\} \tag{3}$$

s.t.

$$0 \le \mathrm{Wind}_{\mathrm{DAM},t} \le \mathrm{Wind}_{\mathrm{Max},t} \quad \forall t \in \{0, \ldots, T_1\} \tag{4}$$

$$0 \le \mathrm{Wind}_{\mathrm{RTM},t} \le \mathrm{Wind}_{\mathrm{Max},t} \quad \forall t \in \{0, \ldots, T_1\} \tag{5}$$

$$0 \le \mathrm{PEV}_{\mathrm{DAM},t} \le \mathrm{CFC}_t \quad \forall t \in \{0, \ldots, T_1\} \tag{6}$$

$$0 \le \mathrm{PEV}_{\mathrm{RTM},t} \le \mathrm{CFC}_t \quad \forall t \in (0, \ldots, T_1) \tag{7}$$

$$0 \le \sum_{t=0}^{T_1} \mathrm{PEV}_{\mathrm{DAM},t} \le \sum_{i=1}^{19} M_{\mathrm{PEV}} N_i D_i E_i \tag{8}$$

$$\sum_{t=0}^{T_1} \mathrm{PEV}_{\mathrm{RTM},t} = \sum_{i=1}^{19} M_{\mathrm{PEV}} N_i D_i E_i \tag{9}$$

Real-time market stage:

$$\min_{\mathrm{PEV}_{\mathrm{RTM},t},\mathrm{Wind}_{\mathrm{RTM},t}} \Big\{ \overline{\mathrm{LMP}}_{\mathrm{DAM}}(\bar{P}_{\mathrm{DAM}}, \overline{|\Delta P_{\mathrm{DAM}}|}) \times \bar{P}_{\mathrm{sys,DAM}} + [\overline{\mathrm{LMP}}_{\mathrm{RTM}}(\bar{P}_{\mathrm{RTM}}, \overline{|\Delta P_{\mathrm{RTM}}|}) \times (\bar{P}_{\mathrm{sys,RTM}} - \bar{P}_{\mathrm{sys,DAM}})] \Big\} \tag{10}$$

s.t.

$$0 \le \mathrm{Wind}_{\mathrm{RTM},t} \le \mathrm{Wind}_{\mathrm{Max},t} \quad \forall t \in \{0, \ldots, T_2\} \tag{11}$$

$$0 \le \mathrm{PEV}_{\mathrm{RTM},t} \le \mathrm{CFC}_t \quad \forall t \in \{0, \ldots, T_2\} \tag{12}$$

$$\sum_{t=0}^{T_2} \mathrm{PEV}_{\mathrm{RTM},t} = \sum_{i=1}^{19} M_{\mathrm{PEV}} N_i D_i E_i \tag{13}$$

The DAM and RTM optimizations are for PEV charging and wind power dispatch under a curtailable policy. The market optimizations under a must-take policy would have equivalent constraints for wind (Equations 4, 5 and 11). The objective is to minimize the wholesale energy market cost which is a function of both load and ramping (See Section 4.2.1). One model of the system cost is used for both the DAM and RTM. However, coefficients are separately regressed for each market [15]. PEV charging and wind dispatch are the decision variables. Algorithmically, changing decision variables changes the daily steady-state load, $\bar{P}$, and system ramp, $\overline{|\Delta P|}$, and thereby changes the cost function. LMP is the locational marginal price. M_{PEV}, N_i, D_i and E_i are respectively the PEV market penetration, number of commuting vehicles, average distance driven in a day and the average electricity used per unit distance at load center i (Nineteen load centers are considered in NYISO) [15].

In the DAM, all variables are based on day-ahead forecasts with an expectation of RTM cost. Wind dispatch can take on any value between 0 MW and the maximum wind power supply at time t. Regional PEV charging at time t takes on any value between 0 MW and the maximum power withdraw prescribed by the Charge Flexibility Constraint (CFC). The PEV energy constraints (Equations 8 and 9) guarantees PEVs are fully charged before commuters leave home without forcing full day-ahead commitment. This enables arbitrage opportunity between DAM and RTM. The hourly DAM solution of PEV charging and wind dispatch becomes an

input in the RTM stage.

In the RTM stage, PEV and wind are optimized on a 10-minute basis. Via Equation 10, this stage adjusts the DAM cost to arrive at the daily wholesale energy market cost in a two-settlement structure. The decision variables are similarly constrained while the PEV energy is an equality constraint (Equation 13) as this study requires fully charged PEVs.

4.3 Results and Discussion

4.3.1 Time-Series Wind and PEV Dispatch

Figure 3 reveals the time-varying power dispatch relationships between wind power, optimal PEV charging, CFC and base case load. Figures 3a, 3b and 3c showcase the original loads and net loads (with 10% wind, 15% PEV and 95/5 Level 1/Level 2 charging) for July 15th and August 13th. System cost is minimized via a combination of lowering and flattening the net load as shown in the three graphs. Figure 3f displays the Charge Flexibility Constraint, whose limit on PEVs' maximum aggregate power withdraw is clearly present.

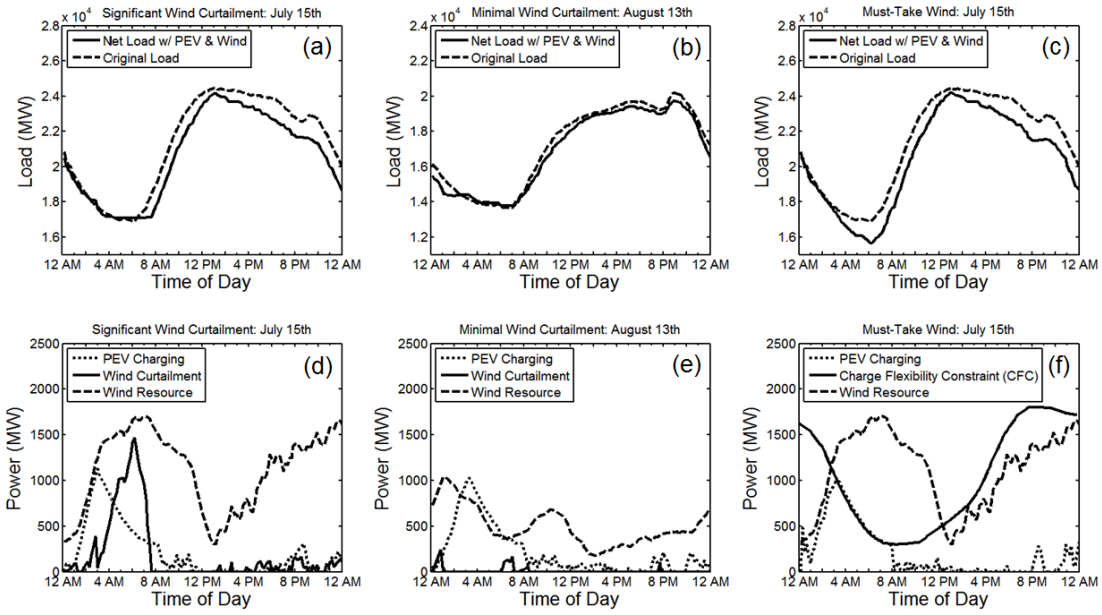

Fig. 3. Optimal PEV charging and wind power dispatch under curtailable and must-take policies to minimize wholesale energy market cost. Principle time-based influences are revealed between wind power, PEV charging and net load from a dispatch perspective. Figures (a) and (d), (b) and (e), (c) and (f) showcase typical results with significant wind curtailment, minimal wind curtailment and must-take wind, respectively.

July 15th is a typical example with excess wind power supply in the early morning where a "curtail if economic" policy is followed. Excess wind is defined as the wind generation under a must-take policy that increases system cost. Furthermore, PEVs are optimally charged in the early morning to take advantage of low prices and also to reduce generator cycling (minor amount of charging and curtailment at 8 PM to reduce ramping of peaking units). In contrast to the morning, the large availability of wind power in the afternoon and nighttime is almost completely utilized to reduce peak load

as seen in Figure 3a. Thus, wind curtailment and PEV charging are observed to occur at the same time as they are both strategies facilitated by system operators to reduce thermal generator cycling in energy markets with excess wind.

In contrast, August 13th is a typical case with a relatively flat and low load valley and low wind power supply in the early morning where "curtail if economic" policy is adopted. In Figure 3e, PEV largely charges in the early morning when it is the cheapest to purchase electricity. However, there is only minor amount of wind curtailed at the same hours, because the net load with optimal PEV charging is already relatively flat at that time period. Therefore, PEV charging is not correlated in time with wind curtailment for energy markets with minimal excess wind power.

It is also observed that PEV charging is not correlated in time with wind dispatch under a must-take policy over the horizon of a day. Furthermore, PEV charging is not correlated in time with wind power variability over the horizon of a day. These two conclusions are seen in Figure 3e and 3f. The cause is the same for both conclusions—original load, not wind power, is the primary contributor to a net load profile before optimizing PEV charging, shown in Figure 3b and 3c. On July 15th for example, the percentage difference between the average original load and the average net load less PEV charging is -5.2%. The difference between the standard deviations of the two loads is 8.7%. As the original and net loads are largely sinusoidal and PEVs must charge in a 24-hour horizon to fulfill the driving needs of the commuter, aggregators managing the PEVs will charge most vehicles during a load valley for the

low prices, and charge the remaining PEVs to reduce any uneconomic ramping of thermal generators. On the other hand, the time-series profile for must-take wind power is dependent on the physical wind resource and its capture by the wind farms. Consequently, the PEV charging and wind resource in the morning of July 15th in Figure 3f is coincidental. This happenstance disappears in the afternoon and nighttime. This reasoning is valid up to a moderate amount of wind power penetration. However, when net load is dominated by wind power via extreme wind penetrations, it is likely that PEV charging will correlate in time with wind variability and wind resource.

4.3.2 Wind Curtailment and PEVs

Figure 4 reveals the relationship between reductions in wind energy curtailment and PEV penetration, where energy is the sum of dispatched power over a 24-hour horizon. Results are averaged and classified into four categories based on wind uncertainty and variability. Uncertainty refers to the difference between the mean forecast and mean realization, where over-forecast is with mean forecast larger than mean realization and under-forecast is the opposite. Figure 4 presents wind uncertainty in three categories: significant over-forecast, significant under-forecast and minimal. Wind variability is shown in two categories: significant and minimal. The six combined categories are reduced to four due to the marginal effects of variability. The category with minimal uncertainty and variability provides a base case for comparison.

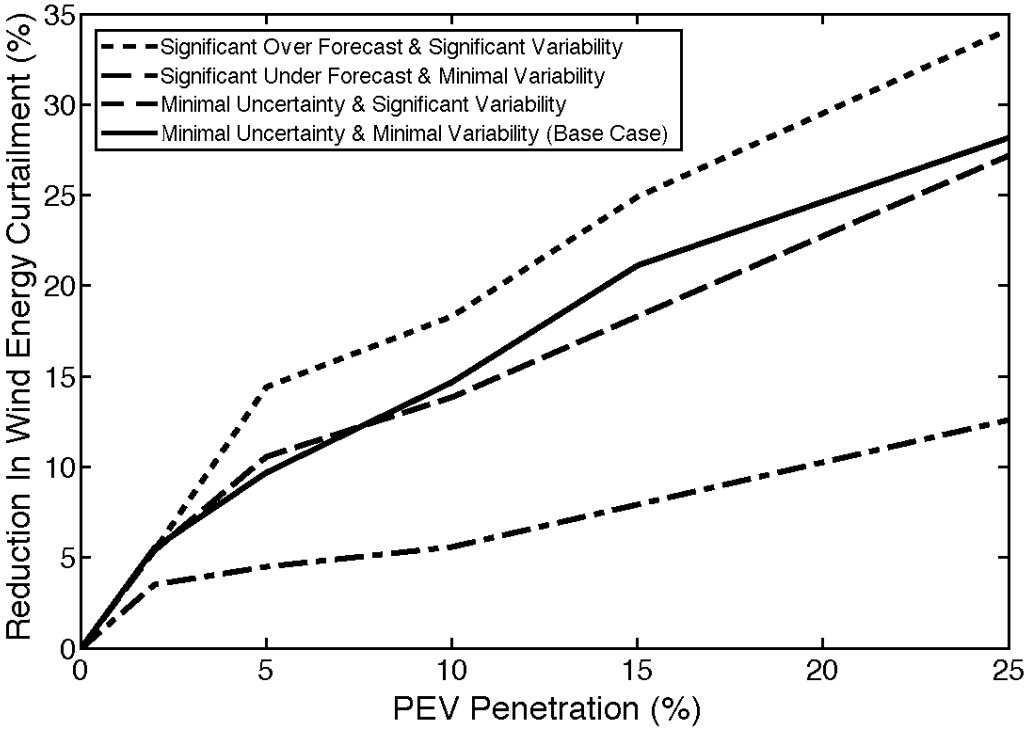

Fig. 4. PEV penetration and reduction in wind curtailment are positively correlated under various categories of wind power uncertainty and variability.

Energy-wise, results show increased PEV penetration reduces daily wind curtailment. Since wind bids into the market lower than generation that burns fuel, it is contracted at higher levels to balance the added PEV load. On average, curtailed energy is reduced 1% for every 1% increase in PEV penetration. Curtailment reduction results are very close between the two cases with minimal forecast uncertainty but vastly different variability. This shows wind variability have only a minimally effect on the relationship between PEV penetration and curtailed wind energy. This result compliments the observation in Section 4.3.1 on the lack of time-wise correlation between PEV charging and wind power variability. The reason is the same: wind power variability is a minor contributor to net load variability when compared to

original load, based on the penetration cases studied.

Figure 4 also shows that wind uncertainty affects the magnitude of the positive relationship between PEV penetration and reduction in curtailed wind energy. Specifically, over-forecast amplifies and under-forecast diminishes this relationship. The principle cause of this conclusion lies in that the best available forecast is still different than realized wind power. Over-forecast presents the inaccurate information that there is more wind generation than in reality. Therefore, the magnitude of a wind curtailment based on the over-forecast is lessened when it is compared to realized wind. The opposite is true for under-forecasted wind. For example, a 100 MWh curtailment decision made with a 1,000 MWh forecast injects 900 MWh of wind energy into the market. If the realized wind resource is 950 MWh, the resultant wind curtailment is 50 MWh or 5%. However, if the realized wind is 1,050 MWh, the resultant wind curtailment is 150 MWh or 14%. For the scenarios examined, wind power over-forecast shows an average increase of 1.4% in wind curtailment reduction for every 1% increase in PEV penetration while that for under-forecast is at 0.5% with the base case at 1.1%.

4.3.3 Energy Market Cost Reductions

Figure 5 reveals the influence of PEV charging, wind dispatch, and Level 1/Level 2 charging mixture on wholesale energy costs. (Reductions are calculated from the base case without PEVs and wind.) It is clear that for the penetrations studied,

optimal PEV charging, increased Level 2 charging and higher wind penetration (both curtailable and must-take) all reduce wholesale energy costs.

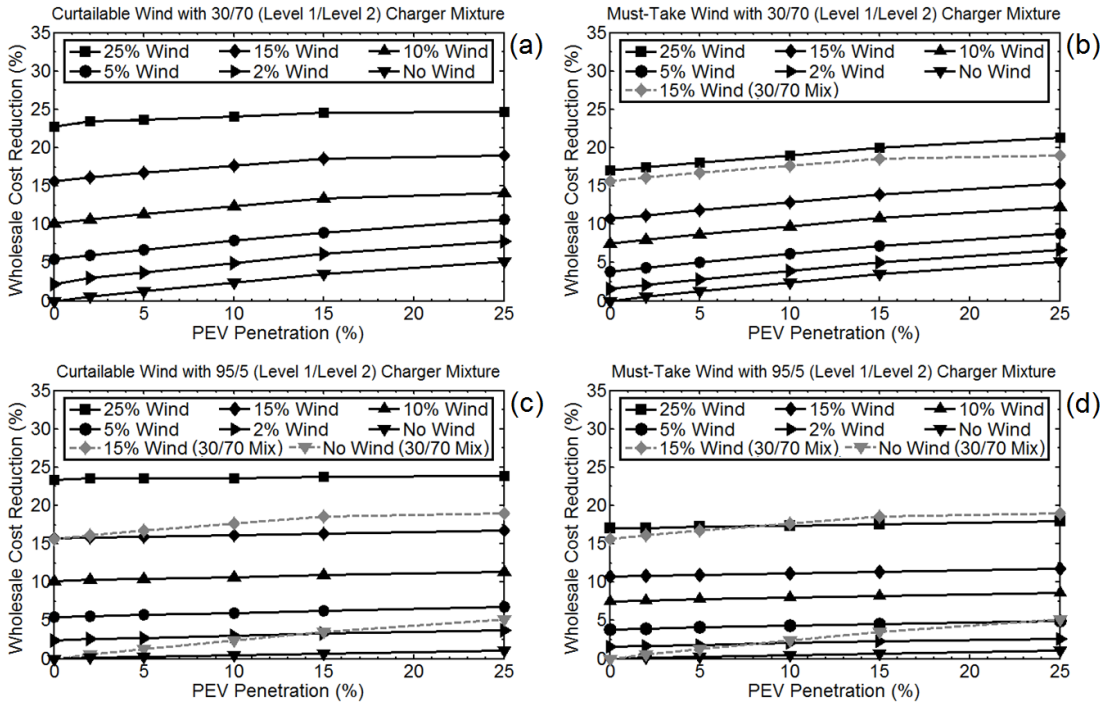

Fig. 5. Reductions in wholesale energy costs are derived from PEV penetrations with optimal charging, wind power penetrations under curtailable and must-take policies and various mixtures of Level 1/Level 2 charger infrastructures. System cost reductions range from approximately 1% to 25% depending on resource penetration. Results reveal adverse coupling or competition between wind power and PEVs as system-level resources in reducing energy cost.

Even though PEV penetration increases net load, optimal charging is observed to reduce energy cost via a flattened load profile and decreased ramping of the system. On the other hand, must-take wind reduces energy cost by lowering the overall net

load while potentially increasing system ramping. Curtailable wind performs better than must-take wind by allowing the market to economically reject any amount of wind that creates a cost increase from cycling generators over the savings from reducing the net load. Lastly, aggregators that use more Level 2 chargers have more dispatchable power from PEVs to reduce market costs. However, as the PEV penetration increases beyond the scope of this study at 25%, it is likely that the increased cost to charge PEVs will outweigh any savings from a smoothed system load—netting an overall cost increase for PEV participation.

Economic coupling among PEVs, wind power and charger mixtures can be defined from their cost-based interactions. In this study, two resources are considered economically coupled when one influences the other's effect on energy market costs. The degree to which they are coupled is based on the magnitude of such influence. Quantitatively for this study, decoupling occurs when a wholesale cost reduction from a nonzero PEV penetration and a nonzero wind power penetration is equal to the sum of the cost reduction from the same PEV penetration and zero wind power penetration, and the cost reduction from the same wind power penetration and zero PEV penetration. Adverse coupling occurs when the cost reduction is less than the sum. Conversely, favorable coupling occurs when the cost reduction is more than the sum.

Figure 5a and c illustrate: (1) optimally dispatched wind power and charged PEVs are adversely coupled for all mixtures of Level 1 and Level 2 charging, and (2) higher mixtures of Level 2 charging increases the degree of adverse coupling. Figure 5b

and 5d reveal: (1) must-take wind power and optimally charged PEVs are decoupled.

Dispatchable wind and high ratio of Level 2 PEV charging lower energy market cost more than any other scenario category. This is due to their unsurpassed flexibility in dispatch compared to the more constrained scenarios of a must-take wind policy or low penetrations of Level 2 charging. Ironically, it is this high resource flexibility that forces wind and PEV to compete for the same opportunities in reducing system ramping through optimal curtailment and charging. Consequently, as low penetrations of Level 2 charging reduce resource flexibility, system cost reductions are lower, but the adverse coupling between wind and PEVs is weaker. Must-take wind and PEVs are largely decoupled as resource flexibility only exists with PEV charging with wind power as an exogenous outcome.

Lastly, superimposing Figure 5a onto b, c and d shows various combinations of optimal PEV charging, wind dispatch and Level 1/Level 2 charging infrastructures may be economically equivalent—potentially making the three resources mutual substitutes in the wholesale energy market. This is due to flexible resources participating in the same platform create competition and substitution. There are other factors outside the scope of this study to consider when fully evaluating this observation, e.g. long term variability of wind resources versus commuter driving patterns, transmission congestion and implementation costs. Nevertheless, it is more likely for the resource substitutions to vary from system to system than for there to be no substitutions that achieve economic equivalency.

4.3.4 Study Limitations

The limitations in this study should be investigated to tailor the results to specific systems. For example, scenario selections can be expanded to include not only load and wind power supply in the summer, but also in other seasons and years. Nonzero wind production costs and penalties accrued from actual versus contracted production will diminish the idealized market for wind integration studied here. Transmission reliability considerations, such as line flow limits and reserve allocation, can constrain system operation and market equilibrium [23, 24]. Distribution system constraints can exacerbate the Charge Flexibility Constraint. The severity of the CFC can be lessened by charging at places other than home, e.g. at work and parking lots. Lastly, transportation inputs can include commercial and fleet vehicles with characteristically different driving patterns compared to residential commuters.

4.4 Conclusions

This study assesses the relationship between electric vehicle charging and wind power dispatch in two-settlement electric energy markets. Based on modeled results for NYISO and by incorporating transportation constraints, Level 1/Level 2 charger infrastructure and wind power forecasts and realizations, the following conclusions are presented.

From the dispatch perspective:

- Optimal PEV charging occurs at the same time as wind curtailment for an energy market with excess wind power.
- Optimal PEV charging is not generally correlated with must-take wind power (wind resource) or with wind power variability.

From the wind curtailment perspective:

- An increase in optimally-charged PEVs reduces curtailment in wind energy.
- Uncertainty in wind power forecast affects the magnitude of the base case relationship between PEV charging and wind energy utilization. In particular, over-forecast amplifies and under-forecast diminishes this relationship.
- Variability in wind power does not significantly affect the base case relationship.

From the energy cost perspective:

- High PEV, curtailable wind power and Level 2 charger penetrations have the lowest wholesale market costs.
- PEVs and curtailable wind power are adversely coupled.
- PEVs and must-take wind power are decoupled.
- Levels of PEV penetration, wind power integration and Level 2 charging may be economically equivalent in the wholesale energy market.

These conclusions are accompanied by the understanding that there are limitations with the model (See Section 4.3.4). Future work to generalize the model to multiple markets and to allow for additional inputs can further support or add layers of complexity on top of current findings.

ACKNOWLEDGEMENTS

This study is supported by the U.S. Department of Energy under "The Future Grid to Enable Sustainable Energy Systems" initiative through the Power Systems Engineering Research Center and by the Consortium for Electric Reliability Technology Solutions (CERTS).

REFERENCES

[1] Denholm, P., Kuss, M., & Margolis, R. M. (2013). Co-benefits of large scale plug-in hybrid electric vehicle and solar PV deployment. *Journal of Power Sources*, *236*, 350-356.

[2] Galus, M. D., Vayá, M. G., Krause, T., & Andersson, G. (2013). The role of electric vehicles in smart grids. *Wiley Interdisciplinary Reviews: Energy and Environment*, *2*(4), 384-400.

[3] Li, Z., Sun, H., Guo, Q., Wang, Y., Zhang, B., 2011. Study on wind-EV complementation in transmission grid side. IEEE Power and Energy Society General Meeting.

[4] Andersson, S.L., Elofsson, A.K., Galus, M.D., Goransson, L., Karlsson, S., Johnsson, F., Andersson, G., 2010. Plug-in hybrid electric vehicles as regulating power providers: case studies of Sweden and Germany. Energy Policy 38 (6), 2751-2762.

[5] Luo, X., Xia, S., & Chan, K. W. (2014). A decentralized charging control strategy for plug-in electric vehicles to mitigate wind farm intermittency and enhance frequency regulation. *Journal of Power Sources*, *248*, 604-614.

[6] Ekman, C., 2011. On the synergy between large electric vehicle fleet and high wind penetration-an analysis of the Danish case. Renewable Energy 36 (2), 546-553.

[7] Kempton, W., Dhanju, A., 2006. Electric vehicles with V2G. Windtech International 2 (2), 18-21.

[8] White, C. D., & Zhang, K. M. (2011). Using vehicle-to-grid technology for frequency regulation nd peak-load reduction. *Journal of Power Sources*,*196*(8), 3972-3980.

[9] Peterson, Scott B., J. F. Whitacre, and Jay Apt. "The economics of using plug-in hybrid electric vehicle battery packs for grid storage." *Journal of Power Sources* 195.8 (2010): 2377-2384.

[10] Lund, H., Kempton, W., 2008. Integration of renewable energy into the transport and electricity sectors through V2G. Energy Policy 26 (9), 3578–3587.

[11] Goransson, L., Karlsson, S., Johnsson, F., 2010. Integration of plug-in hybrid electric vehicles in a regional wind-thermal power system. Energy Policy 38 (10), 5482-5492.

[12] A. Shortt, M. O'Malley, 2009. Impact of optimal charging of electric vehicles on future generation portfolios. IEEE PES/IAS Conference on Sustainable Alternative Energy (SAE) 2009

[13] Saber, A., Venayagamoorthy, G., 2011. Plug-in vehicles and renewable energy sources for cost and emission reductions. IEEE Transactions on Industrial Electronics 58 (4), 1229-1238.

[14] Valentine, K. Foster, E., Acquaviva, J., Zhang, K.M., 2011a. Transmission network-based energy and environmental assessment of plug-in hybrid electric vehicles. Journal of Power Sources 196 (6), 3378-3386.

[15] Valentine, K., Temple, W., Zhang, K.M., 2011b. Intelligent electric vehicle charging: rethinking the valley-fill. Journal of Power Sources 196 (24), 10717-10726.

[16] Zavadil, R., Piwko, R., Jordan, G., Hinkle, G., Miller, N., 2010. New England wind integration study.

[17] Tuohy, A., Meibom, P., Denny, E., O'Malley, M., 2009. Unit commitment for systems with significant installed wind penetration. IEEE Transactions on Power Systems 24 (2), 592-601

[18] National Renewable Energy Laboratory, 2010. Eastern wind integration and transmission study.

[19] Webster, R., 1999. Can the electricity distribution network cope with an influx of electric vehicles? Journal of Power Sources 80 (1-2), 217-225.

[20] Shao, S., Pipattanasomporn, M., Rahman, S., 2009. Challenges of PHEV penetration to the residential distribution network. IEEE Power and Energy Society General Meeting. Calgary, Canada.

[21] Clement, K., Haesen, E., Driesen, J., 2009. Coordinated charging of multiple plug-in hybrid electric vehicles in residential distribution grids. IEEE PES Power Systems Conference and Exposition. Seattle, Washington.

[22] Kintner-Meyer, M., Schneider, K., Pratt, R., 2007. Impact assessment of plug-in hybrid vehicles on electric utilities and regional US power grids. part 1: technical analysis. Pacific Northwest National Laboratory.

[23] Lamadrid A., Mount, T., Thomas, R., 2011. Geographical averaging and ancillary services for stochastic power generation. International Journal of Innovations in Energy Systems and Power 6 (1), 13-21.

[24] Chen, J., Mount, T.D., Thorp, J.S., Thomas, R.J., 2005. Location-based scheduling and pricing for energy and reserves: a responsive reserve market proposal. Decision Support Systems 40 (3-4), 563-577.

CHAPTER 5

IMPROVING COMPLIANCE RATE, CUSTOMER DISPATCH AND STORAGE VALUE IN DEMAND RESPONSE: AN AGGREGATOR'S PERSPECTIVE

5.1 Background

Demand response (DR) aims to bring demand elasticity to the electricity sector. Current markets are dominated by supply-side flexibility. In nonmarket territories, load-serving entities (LSEs) are obligated to serve demand. In both types of systems, generators of various types, e.g. fossil fuel, nuclear, hydro and renewable, seek to supply a nearly inelastic load. Wholesale electricity prices, known as location marginal prices (*LMP*s), and in particular real-time LMPs, are volatile due to several factors: (1) demand inelasticity, (2) scarcity of supply at peak loads, (3) lack of electricity storage, and (4) network congestion. Price volatility is often exacerbated by outages of key generators and transmission lines—creating peak LMPs 10 to 50 times the average.

Most residential, many commercial customers do not see these price volatilities. In fact, the majority only see a constant retail price or some form of simple tiered pricing structure. This disconnect between true cost of electricity and what customers pay at a sufficiently fine time interval creates significant economic inefficiencies called deadweight losses [1]. These losses fundamentally describe the discrepancy between

the value of electricity consumed and its cost of production. This leads to adverse consequences of over- and under-consumption and cross-subsidies, e.g. under-consumption at low *LMP*s subsidizes the cost of over-consumption at high *LMP*s. Consequently, demand elasticity is crucial to removing the price disconnect and lowering price volatility.

This study focuses on the currently dominant form of DR—supply-side DR based on probabilistic customer participation. There are generally two categories of demand elasticity currently in practice or trial phase: (1) supply-side or reward-based DR, and (2) demand-side or savings-based DR. Supply-side DR is often facilitated by an aggregator, such as EnerNOC, and relies on probabilistic customer participation or direct load control. It competes with generators at sufficiently high *LMP*s. In contrast, demand-side DR exposes retail customers to time-varying rates that track *LMP*s, e.g. real-time pricing (RTP) and time-of-use (TOU) rates. Demand-side DR does not require a third-party representation or control.

Economically, supply-side DR appears to have two problems: (1) double payments in the form of DR rewards and avoided costs of consumption, and (2) unverifiable nature of customers' baseline or intended energy consumption levels. One solution to these problems is the notion that customers pay to own their demand before selling portions of it back as avoided generation [1]. This concept of demand subscription takes advantage of an arbitrage opportunity between wholesale and retail price during DR. A fair cost structure for ex-ante demand ownership, such as demand subscription,

eliminates double payments as compensation is the buy-and-sell price difference. In terms of energy, the amount of demand each customer buys reveals the baseline consumption. Section 4 contains details on how this study uses the concept of demand subscription.

Being in existence for only a few years, the dominant supply-side DR programs in wholesale markets have not performed consistently. For example, DR programs in PJM cost more than $300 million during the first 6 months of 2014, mostly in the form of capacity, while its observed compliance rate is only 28%. In stark contrast, PJM's equivalent availability factor (EAF) for generators is 80% overall, 85% for combustion turbines (CTs) and 82% for combined cycles (CCs)—the types of units that DR competes with—for the same 6 months [2]. In 2013, DR's observed compliance rate is 82% while the EAF for generators is 84% overall, 90% for CTs and 86% for CCs in PJM [3]. The extreme difference between DR's compliance rates at 28% and 82% is due in part to the voluntary nature of the 2014 DR events while those in 2013 were mandatory. It is tempting to institute all DR events as mandatory. However, such mandates can decrease DR program participation due to customer fatigue and insufficient financial compensation (See Section 2.1). Cappers et al. also noted the low participation rates of the DR in energy markets in NYISO and ISONE using the Subscribed Performance Index (SPI) [4].

Overall, much of the academic literature leaves DR reliability out of the scope of study. Rahimi et al., Greening et al. and Siano discussed programs and frameworks

under which DR would be a valuable resource to electricity markets [5-7]. Pudjianto et al. used a virtual power plant (VPP) to explain the aggregator concept and to dispatch distributed energy resources [8]. Conejo et al. and Rastegar et al. focused on how prices affect DR, but neglected DR reliability itself [9,10]. Valero et al. used self-organizing maps to deterministically classify and aggregate customers' DR potential [11]. Medina et al. incorporated distribution network operations to deterministically dispatch DR [12]. Ruiz et al. used linear programming to simulate directly control of AC units EnergyPlus in order to maximize load reduction for a VPP [13]. Jonghe et al. incorporated deterministic DR and wind energy into determining system-level generation mixtures [14]. Aalami et al. extended deterministic demand response models to include penalty for customer noncompliance when called upon [15].

However, there is an emerging interest to understand and improve DR compliance. Kim et al. discussed the reliability challenges stemmed from the common failures of demand response from the perspectives of consumer, producer and structural barriers [16]. Kwag et al. and Joung et al. incorporated customer compliance uncertainty into ISOs' DR dispatch models with a goal of decreasing load curtailments and loss of load probabilities [17,18]. Zheng et al. sized storage using arbitrage-based cost-benefit analysis to aid the business case for probabilistic residential DR [19]. Taylor et al. used a restless bandit framework to introduce the classic paradigm of exploration-exploitation to the dispatch of well-known customers versus new customers for DR [20].

In industry practice, new curtailment service providers (CSPs) would indeed employ a learning process of trial-and-error to dispatch new customers. However, established CSPs classify customers to form core asset groups and riskier groups with live-event dispatch focused on core customers. Moreover, instead of learning customer compliance during ISOs' DR events, CSPs would perform offline tests to gauge riskier customers' compliance characteristics. Such offline learning largely circumvent the exploration-exploitation problem by separating exploration from exploitation. Consequently, exploration—hence compliance rates—defines the live-event dispatch.

This paper studies demand response, aggregators and storage use with a focus on customer dispatch probabilities, i.e. aggregators' DR compliance rates. The value of this work is in (1) the treatment of DR as random variables, (2) the focus on improving DR compliance rates for aggregators, (3) the use of compliance rates to optimally dispatch customers in DR events, (4) a case study using air conditioning loads in the TRNSYS simulator, and (5) the proposition of storage use in DR and energy price arbitrage. The organization of this paper is also in this order.

5.2 Demand Response Uncertainties and Quantification

5.2.1 Sources of DR Uncertainty and Noncompliance

Loads are separated into two categories: (1) flexible and (2) nonflexible. Flexible

loads have the potential to be aggregated and offered into the energy market to reduce net load. Nonflexible load are typically loads not subject to modification by noncustomers. In the category of flexible loads, there are causes of reduction uncertainty, i.e. difference between scheduled and actual reduction. Below are some major causes expressed by aggregators:

1. Uncertain base load (forecast error)
2. Customer behavior (e.g. overrides, fatigue, insufficient advanced notice, lack of training)
3. Uncertain mixture of electrical devices: some devices are highly flexible (e.g. EV charging) and some are minimally flexible (e.g. street lights) [21,22]
4. Varying technical load reduction capability of devices (e.g. a window AC unit versus central AC)
5. Compensating resources that changes net load, e.g. energy storage
6. Insufficient financial compensation, e.g. declining DR payments

Monitor and/or control systems targeting customers' power consumption can reduce the potency of these drivers of DR uncertainties and noncompliance. Certainly, existing aggregators have their hardware and software installed at customer sites and operated from their control centers.

Efficient control and market prices may not be enough to fully incentivize DR [23]. Discrete-and-active purchase, lottery-like DR payments and other approaches that

couple financial incentives with human behavior may help to further develop DR [24, 25].

5.2.2 Single-Class Dispatch Probability

An aggregator's payoff for participating in DR can simply be reward minus penalty, where total reward is reward price multiplied by load reduction and total penalty is penalty price multiplied by missing load reduction. Consequently, highest revenue per load reduction called translates to maximized dispatch probability (*DP*), a nonnegative non-dimensionalized form of load reduction, i.e. compliance rate. Collectively, an aggregator has a portfolio of assets from customers to storage and backup generators. Building on *DP*, this study also describes an aggregator's composite dispatch probability, *CDP*—the collective compliance rate that discounts a CSP's total DR obligation. It is worthy to note that storage can directly arbitrage in an energy market in addition to firm DR obligations (See Section 2.4).

The significance and utility of *DP* and *CDP* are twofold: (1) to quantify the probabilistic difference between DR obligation and DR delivered, and (2) to optimize the dispatch of DR assets in any aggregator's portfolio. For example, a *CDP* with a maximized mean optimizes DR reward and noncompliance penalty to achieve maximum expected revenue for the aggregator.

Figure 1 is a diagram illustrating: (1) the flow of an aggregator's DR and storage

arbitrage actions (grey arrows), and (2) the influence of compliance rates denoted by *DP* for asset classes and *CDP* for the aggregator (black arrows).

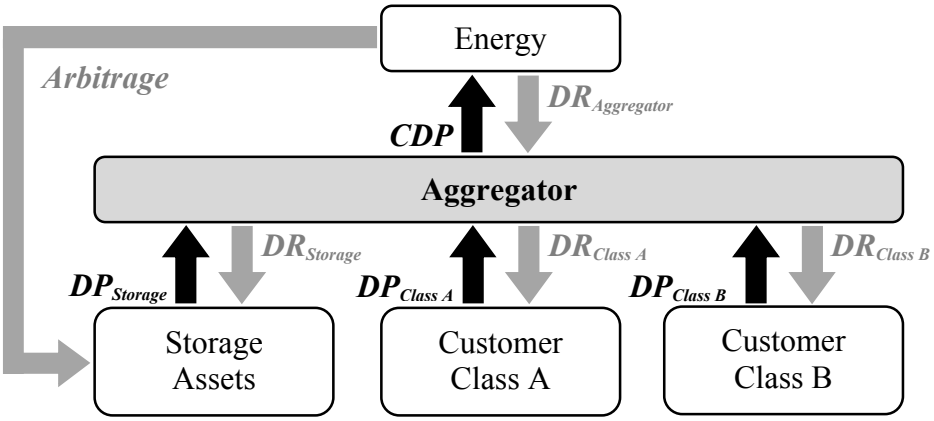

Figure 1. Diagram illustrating: (1) the flow of an aggregator's DR and storage arbitrage actions (grey arrows), and (2) the influence of compliance rates denoted by *DP* for asset classes and *CDP* for the aggregator (black arrows).

There is a direct feedback loop between an aggregator's actions and compliance rates. Specifically, an aggregator schedules load reductions, $DR_{Aggregator}$, in an energy market. The CSP then partitions its total load reduction obligation to its assets via $DR_{Customer\ Class}$ and/or $DR_{Storage}$. The corresponding *DP* discount produces actual DR per asset. The resulting total actual load reduction is equivalent to the aggregator's compliance rate, *CDP*, discounting $DR_{Aggregator}$. Moreover, *DP* and *CDP* are functions of the intrinsic DR capacities of the underlying assets and extrinsic DR signals (See below and Section 2.3).

DP for a DR-eligible load class is defined by Equation 1.

$$DP_{class} = \frac{Inferred\ Load\ Reduction_{class}}{Called\ Load\ Reduction_{class}} \quad (1)$$

$$= \frac{LR_{inferred,class}}{LR_{called,class}} = \frac{Load_{forecast,class} - Load_{measured,post\ DR,class}}{LR_{called,class}}$$

$$= \frac{Load_{forecast,class} - (Load_{actual,class} - LR_{actual,class})}{LR_{called,class}}$$

All load classes mentioned in this study are assumed DR-eligible unless otherwise stated. Inferred load reduction for a load class, $LR_{inferred,class}$, is the amount of load reduction estimated by a noncustomer, e.g. aggregator, RTO/ISO or utility, for only the customers know their true intended load. Load reduction requirement, $LR_{called,class}$, is the amount of DR called for by the RTO/ISO or an entity administering the DR event. Consequently, this reduction is the DR signal that aggregators receive to decrease net load. $Load_{forecast,class}$ is the baseline load forecast for a particular load class and $Load_{measured,post\ DR,class}$ is the resultant load measured after DR for a load class. $Load_{actual,class}$ is the actual baseline load equal to the sum of every customer's intended electricity consumption before DR in a load class. This is not a measurable quantity. $LR_{actual,class}$ is the actual load reduction from the baseline of $Load_{actual,class}$.

Load forecast error for a load class is defined as,

$$e_{load\ forecast,class} = \frac{Load_{forecast,class} - Load_{actual,class}}{LR_{actual,class}} \quad (2)$$

Load forecast error can be caused by modeling error on the part of the aggregator or system operator. In stark contrast to modeling errors, if customers are not obligated to pay to own their demand before selling back as avoided generation, they can intentionally manipulate their baseline loads to increase their dispatch probability. This is possible due to the information asymmetry that exists between the customer, aggregator and system operator/auditor, i.e. customers always know their true pre-DR power usage better. Regardless of the cause of forecast error,

$$DP_{class} = min\left\{1, \frac{LR_{actual,class}}{LR_{called,class}}\left(1 + e_{load\ forecast,class}\right)\right\} \quad (3)$$

where $0 \leq LR_{actual,class} \leq LR_{called,class}$. Graphically, the relationship between *DP* and LR_{called} is illustrated in Figure 2 (with $e_{load\ forecast} = 0$).

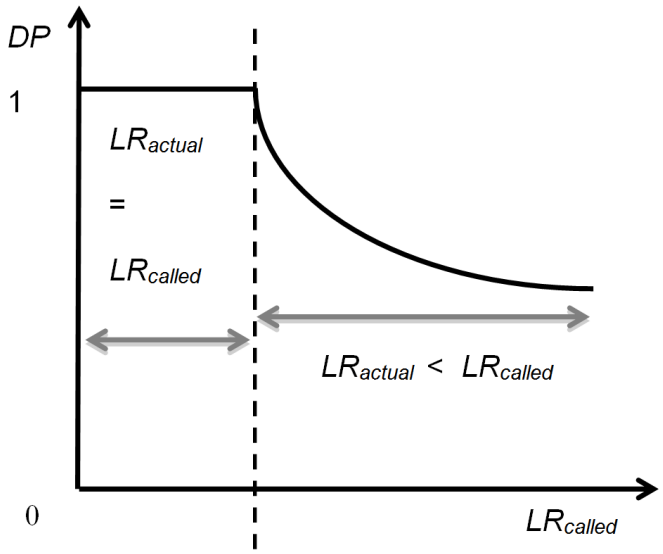

Figure 2. Dispatch probability versus called load reduction.

Aggregator-controlled storage increases net reducible load, not necessarily actual load

reduced, because storage can be discharged for purposes other than DR. An example is storage directly participating in the energy market as a generator. When storage is actually used in DR, it effectively increases actual load reduction via decreased remaining load served by the utility or system-operated generation fleet. Therefore, storage dispatch can increase mean of *DP* and decrease variance of *DP*. Figure 3 graphically illustrates the relationships between mean of *DP*, LR_{called}, storage dispatch and LR_{actual}. The figure extends the *DP* concept conveyed in Figure 2.

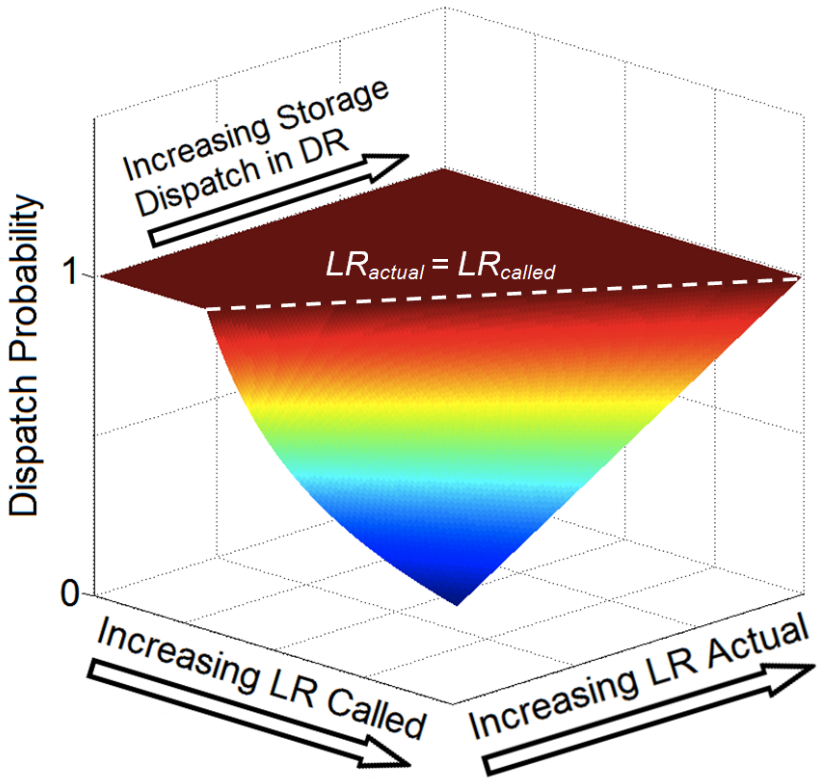

Figure 3. Storage dispatch in demand response can increase actual load reduction and dispatch probability. Increasing load reduction called can decrease dispatch probability.

5.2.3 Composite Dispatch Probability

A single *DP* can describe a homogenous DR-eligible load class, e.g. residential customers with 20% to 25% of controllable loads. However, a nonnegative *CDP* is necessary when an aggregator has multiple DR-eligible load classes and a storage asset. Residential, commercial, industrial loads and storage are used as examples. (Note: difference between actual and forecasted load for non-DR-eligible loads is not part of *CDP* formulation.)

Equation 1 decomposes to Equation 4,

$$CDP = \frac{(\sum_{i \in class} LR_{inferred,i}) + Storage\ Dispatch_{inferred,DR}}{LR_{called,total\ load}} \quad (4)$$

$$= \frac{LR_{inferred,res} + LR_{inferred,com} + LR_{inferred,ind} + Storage\ Dispatch_{inferred,DR}}{LR_{called,total\ load}}$$

With $w_{class} = \frac{LR_{called,class}}{LR_{called,total\ load}}$ and $w_{stor} = \frac{Storage\ Dispatch_{called,DR}}{LR_{called,total\ load}}$, Equation 4 becomes

$$CDP = \sum w_i DP_i, \forall i \in load\ classes\ and\ storage \quad (5)$$

$$= w_{res} DP_{res} + w_{com} DP_{com} + w_{ind} DP_{ind} + w_{stor} DP_{stor}$$

Implicit in Equation 5 are $LR_{actual,class} \leq LR_{called,class}$ and $Storage\ Dispatch_{actual,DR} \leq Storage\ Dispatch_{called,DR}$. The weighting factor, *w*, is the proportion of demand response requirement partitioned for corresponding DR-eligible load classes or storage.

Equation 5 partitions an aggregator's *CDP* into its component customer load classes and storage asset. Consequently, Equation 5 enables the optimal allocation of load reduction requirement to the different customer classes and the optimal dispatch of storage via maximizing *CDP*'s mean, minimizing *CDP*'s variance or another objective involving *CDP*. Equation 6 describes two constraints on the partitioned assets of load classes and storage.

$$\begin{cases} \sum w_i = 1 \\ w_i \geq 0 \end{cases} \forall\, i \in partitioned\ assets \tag{6}$$

5.2.4 Dispatch Probability of Storage

Aggregator-scale storage is a different kind of asset than contracts with customers to reduce load. Storage at this scale is often on the order of a few hundred kWs to MWs and an aggregator can technically controlled it. Without the uncertainties plaguing the load reduction capabilities of customers, storage can firm DR obligations to RTO/ISOs and can separately arbitrage between low and high prices in the energy market. Storage's flexible use is further quantified in Section 4.

Equations 7 through 9 define the dispatch probability of storage in DR.

$$DP_{storage} = \frac{Storage\ Dispatch_{inferred,DR}}{Storage\ Dispatch_{called,DR}} \tag{7}$$

$$= \frac{SOC_{forecast} - (SOC_{actual} - SD_{actual,DR})}{SD_{called,DR}}$$

$$DP_{storage} = min\left\{1, \frac{SD_{actual,DR}}{SD_{called,DR}}\left(1 + e_{SOC\ forecast}\right)\right\} \quad (8)$$

$$e_{SOC\ forecast} = \frac{SOC_{forecast} - SOC_{actual}}{SD_{actual,DR}} \quad (9)$$

State of charge (SOC) of a battery system is the measurable total amount of energy remaining in the batteries at a specified time. Forecast SOC is the day-ahead prediction of realized SOC, SOC_{actual}. There are two additional constraints on storage, specifically,

$$\begin{cases} \sum_{t\in T} SD_{called,DR,t} = SOC_{forecast}\ (1 - LF) \\ \sum_{t\in \tau} SD_{actual,DR,t} = SOC_{actual}\ (1 - LF) \end{cases} \quad (10)$$

where loss factor (*LF)* is the percentage of charged energy lost over the planning horizon *T* and dispatch horizon *τ*.

Unlike customer demand response, storage called for demand response purpose, $SD_{called,DR}$, is an aggregator-controlled asset. Thus, $SD_{called,DR} = SD_{actual,DR}$ in most circumstances. Moreover, $SOC_{forecast} = SOC_{actual}$ and $T = \tau$ under the same reasoning. Consequently in most situations,

$$DP_{storage} = 1 \quad (11)$$

$$\sum_{t\in T} SD_{DR,t} = SOC\ (1 - LF) \quad (12)$$

5.2.5 Three Categories of Aggregators Based on CDP and Load Manipulation

Due to information asymmetry, customers know their value of power consumption better than any other party. Aggregators and utilities that have customers' historical load data and real-time monitoring capability can develop good load baselines. Others relying on second-hand or reported information are the least able to quantify baseline loads. From the non-customer perspective, the term, $1 + e_{forecast}$, is indistinguishable in DP (See Equation 3). Manipulating baseline loads can increase $e_{forecast}$, and thus can artificially increase *DP*s and *CDP*s up to 1.

There are three categories of aggregators based on reliability and integrity.

1. A highly reliable and honest aggregator would:
    - Have more customer classes with high dispatch probabilities
    - Partition load reductions to customers with highest dispatch probabilities
    - Dispatch storage to maximize payoff; potentially increase *CDP* (See Section 4)
    - Honestly report customers' baseline loads and *CDPs* to RTO/ISOs and auditors
    - Appropriately incentivize customers to report their true baseline loads
2. A less reliable and honest aggregator would:
    - Have more customer classes with low dispatch probabilities
    - Ineffectively partition load reduction to customers

- Ineffectively dispatch storage or not have storage
- Honestly report customers' baseline loads and *CDPs*
- Appropriately incentivize customers to report their true baseline loads

3. A dishonest aggregator would:
    - Intentionally manipulate baseline loads, load forecasts or reporting of data to artificially increase *CDP*
    - Employ questionable methods and practices to inflate *CDP*

5.3 Optimal Demand Response Partitioning

The set of weights, $\{w_{class}\}$, an aggregator administers to its DR-eligible load classes defines a partitioning of RTO/ISO's DR dispatch specified to the aggregator. Therefore, operations involving $\{w_{class}\}$ seek to control *CDP*.

5.3.1 Maximizing mean of CDP

Equations 13 and 6 define the maximization. Storage related results are in Section 4.

$$max_{w_i}\ mean\ (CDP) \tag{13}$$

$$\text{s.t.} \quad \begin{cases} \sum w_i = 1 \\ w_i \geq 0 \end{cases}$$

$$\forall i \in load\ classes$$

Maximum flexible load (*MFL*) for a load class is the expected maximum load reduction deliverable in a DR event under the administration of an aggregator. *MFL* depends on a combination of technical, economic and social factors, such as devices' energy reduction capability and customers' willingness to comply with load reductions (See Section 2.1). Moreover, $MFL_{class} \geq LR_{actual,class}$. Note that a nonzero forecast error implicitly inflates or deflates *MFL* and is not explicitly expressed. Modifying Equation 5,

$$CDP = \sum min\left\{w_i, \frac{MFL_i}{LR_{called,total\ load}}\right\}, \forall i \in all\ load\ classes \tag{14}$$

There exists a threshold of load reduction requirement, LR_{th}, for every set of $\{w\}$, that separates the means of *CDP* equal to 1 from those less than 1. Mathematically,

$$CDP_{\mu} = \begin{cases} 1, & LR_{called,total\ load} \leq LR_{th} \\ \left(\sum_{j\in J} w_J\right) + \left(\sum_{k\in K} \frac{MFL_{k,\mu}}{LR_{th}}\right) < 1, & LR_{called,total\ load} > LR_{th} \end{cases} \tag{15}$$

μ denotes mean at each LR_{called}, J is the set of load classes with $w_{j\in J} \leq \frac{MFL_{j\in J}}{LR_{th}}$, and K is the set of load classes with $\frac{MFL_{k\in K}}{LR_{th}} < w_{k\in K}$. Thus, the maximization problem is equivalent to finding LR_{th} in order to evaluate w_{class}. Given Equation 14, at $LR_{called,total\ load} = LR_{th}$,

$$w_i = \frac{MFL_i}{LR_{th}}, \forall i \in all\ load\ classes \quad (16)$$

Thus,

$$\sum w_i = \frac{\sum MFL_i}{LR_{th}} = 1 \quad (17)$$

$$LR_{th} = \sum MFL_i \quad (18)$$

$$w_i = \frac{MFL_i}{\sum MFL_i}, \forall i \in all\ load\ classes \quad (19)$$

where $MFL_i = 0$ for a nonparticipating, DR-eligible, aggregated load class.

Equation 19 stipulates that as MFL_{class} increases, more of the load reduction is proportionally partitioned to that class. Conversely, as MFLs increase in other load classes, less of the load reduction is partitioned to that class in an inversely proportional manner.

A useful corollary is that $max\ \{mean\ (CDP)\} \geq mean\ (DP_{class})$. This implies the maximized mean of an aggregator's *CDP* can never decrease with additional customer classes. However financially, cost of acquiring additional customers may outweigh the benefits of a non-decreasing average.

5.3.2 Minimizing variance of CDP

Grid operators are naturally risk-averse and therefore prefer a high degree of reliability when it comes to aggregators participating in wholesale power markets.

Furthermore, capacity markets in the United States are designed in a way that rewards participants offering reliable capacity during peak load. Therefore, a *CDP* with minimized variance is desirable. Equations 20 and 6 define the minimization given DP_{class} is a truncated normal distribution with mean μ_{class} and variance σ^2_{class}. The optimal partitioning is demonstrated using 3 examples of DR-eligible load classes: residential, commercial and industrial.

$$min_{w_{res},w_{com},w_{ind}}\ var\ (CDP) \tag{20}$$

$$\text{s.t.} \quad \begin{cases} \sum w_{class} = 1 \\ w_{class} \geq 0 \end{cases} \forall\ class \in \{res, com, ind\}$$

Minimizing a sum of truncated and normally distributed DP_{class} is beyond the scope of this study. *CDP* and DP_{class} are therefore treated as normal distributions in this section. Indeed, *CDP* and *DP* are nearly normally distributed given $w_i\ LR_{called} \gg MFL_i, \forall i \in load\ class$.

$$var\ (CDP) = w^2_{res}\sigma^2_{res} + w^2_{com}\sigma^2_{com} + (1 - w_{res} - w_{com})^2\sigma^2_{ind} \tag{21}$$

The solution is,

$$w_{res} = \frac{\sigma^2_{com}\sigma^2_{ind}}{\Sigma^2},\ w_{com} = \frac{\sigma^2_{res}\sigma^2_{ind}}{\Sigma^2},\ w_{ind} = \frac{\sigma^2_{res}\sigma^2_{com}}{\Sigma^2} \tag{22}$$

where $\Sigma^2 = \sigma^2_{res}\sigma^2_{com} + \sigma^2_{res}\sigma^2_{ind} + \sigma^2_{com}\sigma^2_{ind}$.

As σ^2_{res} increases, less of the total called load reduction is partitioned to the

residential load class in an inversely proportional manner. Conversely, if either σ_{com}^2 or σ_{ind}^2 increases, more of the total load reduction is proportionally partitioned to the residential class. This reasoning also applies to the commercial and industrial load classes.

A corollary is that $min\{var\ (CDP)\} \leq var\ (DP_{class})$. This implies the minimized variance of an aggregator's *CDP* can never increase with additional load classes. Again, the financial cost of acquiring additional customers may outweigh the benefits of a non-increasing *var* (*CDP*).

5.3.3 Ranges of Equivalence (*ROE*) *and the Critical Load Reduction Requirement* (*CLR*)

The partition formulas for optimal *CDP*s (Equations 19 and 22) are useful in a system where an aggregator is rewarded for performance and penalized for nonperformance. On the surface, it seems that the different ways of partitioning would lead to *CDP*s having different averages. While this is true for a certain range of LR_{called}, it is discovered that different *CDP*s have the same maximized average when the corresponding LR_{called} is within two special ranges, denoted by *ROE*. Quantitatively, the *ROE* are <0, CLR^-> and <CLR^+, *Total System Load*>, assuming zero storage dispatch in DR.

There are three important consequences of this equivalence in CDP_μ-CDP_{var} space.

First, the mean of any *CDP* within *ROE* is *insensitive* to errors in customer dispatch. This is very advantageous when accurate customer dispatch is not achieved, measured and/or verified. Second, given any LR_{called} within *ROE*, an optimal partition of customers' load reductions is the set, $\{w_{op}\}$, that also minimizes the variance of *CDP* as maximized mean is guaranteed. Third, given any LR_{called} outside of *ROE*, an optimal *CDP* lies on a Pareto Efficient Frontier (PEF) connecting $CDP_{\mu,op}$ and $CDP_{var,op}$. A PEF exists due to simultaneous profitability and reliability objectives involving CDP_{μ} and CDP_{var}. The subscripts, μ, *var*, *arb* and *op* stand for mean, variance, arbitrary and optimal at each LR_{called}, respectively. Derivations of CLR^{+}, CLR^{-} are detailed here.

When $LR_{called} \geq CLR^{+}$, $CDP_{\mu,arb} = CDP_{\mu,op}$. Using

$w_{class}DP_{class} \leq min\left\{w_{class}, \frac{MFL_{class}}{LR_{called}}\right\}$,

$CDP_{\mu,arb} \leq \sum_{i \in class} min\left\{w_{i,arb}, \frac{MFL_{i,arb}}{LR_{called}}\right\}$ and

$CDP_{\mu,op} \leq \sum_{j \in class} min\left\{w_{j,op}, \frac{MFL_{j,op}}{LR_{called}}\right\}$. As $MFL_{class,arb} = MFL_{class,op}$,

$CDP_{\mu,arb} = CDP_{\mu,op}$ when $max\left\{\frac{MFL_{i,arb}}{LR_{called}}\right\} < w_{i,arb}, \forall\, i \in class$ and

$max\left\{\frac{MFL_{j,op}}{LR_{called}}\right\} < w_{j,op}, \forall\, j \in class$. Thus,

$LR_{called} > max\left\{max\left\{\frac{MFL_{i,arb}}{w_{i,arb}}\right\}, max\left\{\frac{MFL_{j,op}}{w_{j,op}}\right\}\right\}, \forall\, i,j \in class$. Since $w_{j,op} = \frac{MFL_{j,op}}{\sum MFL_{j,op}}$, $LR_{th} = max\left\{\frac{MFL_{j,op}}{w_{j,op}}\right\}$. It can be shown that $max\left\{\frac{MFL_{i,arb}}{w_{i,arb}}\right\} \geq LR_{th}$.

Consequently,

$$CLR^{+} > max\left\{\frac{MFL_{i,arb}}{w_{i,arb}}\right\}, \forall\, i \in load\ class. \tag{23}$$

When $LR_{called} \leq CLR^{-}$, $CDP_{\mu,arb} = CDP_{\mu,op}$. Using $w_{i,arb} < min\left\{\frac{MFL_{i,arb}}{LR_{called}}\right\}, \sum w_i = 1$ and following a similar reasoning as above,

$$CLR^{-} < min\left\{\frac{MFL_{i,arb}}{w_{i,arb}}\right\}, \forall\, i \in load\ class. \tag{24}$$

There is one characteristic distinction between CLR^{-} and CLR^{+}: CLR^{-} is guaranteed to exist while CLR^{+} approaches positive infinity when $w_{i,arb} = 0$. Furthermore, it can be shown $CLR^{-} \leq LR_{th} \leq CLR^{+}$, i.e. the load reduction threshold is outside *ROE*.

Figure 4 conceptualizes the paths of convergence for any *CDP* to achieve optimality in CDP_{μ}-CDP_{var} space for any LR_{called} inside of *ROE* and outside of *ROE*.

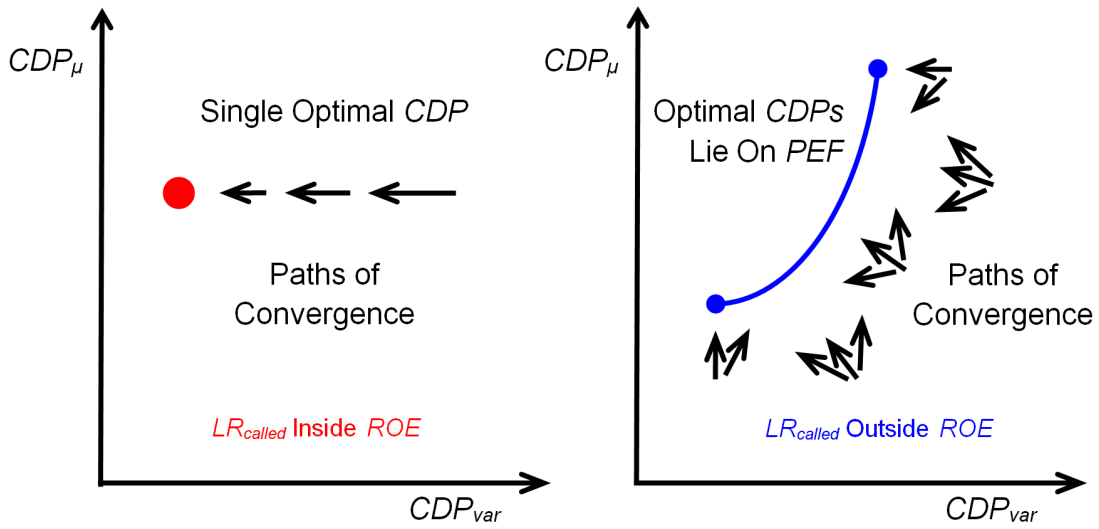

Figure 4. In CDP_μ-CDP_{var} space, optimal *CDPs* are bifurcated by a load reduction requirement, LR_{called}, being either inside or outside the Ranges of Equivalence (*ROE*). Within *ROE*, an optimal *CDP* has a maximized mean and a minimized variance. Outside of *ROE*, an optimal *CDP* lies on a Pareto Efficient Frontier (*PEF*) that connects a *CDP* with maximized mean and another with minimized variance. Any *CDP* would follow a path of convergence to reach an optimal *CDP*.

5.3.4 A Case Study of MFL and CDP By Modifying Temperature Settings of Air Conditioners

TRNSYS (A Transient Systems Simulation Program) is used to simulate a typical restaurant's summer cooling needs in New York City. Simulations used a built-in weather profile of NYC and TRNSYS's typical restaurant model to compute cooling loads [26]. The built-in restaurant model contains 3 zones: kitchen, dinning room and storage. Heat transfer coefficients of the restaurant vary with weather, e.g. wind

speed. Internal airflows depend on occupancy and fluidynamic coupling between the 3 zones. Internal heat generation changes with occupancy and energy-consuming devices, e.g. stoves. The kitchen is equipped with an air conditioner with a temperature setting at 20 ^{o}C. Simulations run from June to August at an hourly resolution. The resultant *MCL* occurs during first week of July.

The maximum cooling load (*MCL*) is the largest hourly cooling power used to maintain a structure's maximum temperature setting (*TS*) during summertime. This discrete TRNSYS output is then regressed via Equation 25 against *TS* for purpose of interpolation.

$$MCL_{TS} = \begin{cases} m(BP_x - TS) + BP_y, & TS < BP_x \\ a(b - TS)^c + d, & TS \geq BP_x \end{cases} \quad (25)$$

where (BP_x, BP_y) is the breakpoint that separates the linear and power regressions, and $\{a, b, c, d, m\}$ are regression constants. The *MCL*s are then used to derive the restaurant's MFL_{AC} via Equation 26. Optimal *CDPs* based on MFL_{AC} are subsequently computed and the *ROE* are revealed. Figure 5 shows *MCL* versus *TS* in a downward trend with regressed results closely adhering to TRNSYS simulated outputs. While settings in the 20s ^{o}C range are used in practice, all settings ≥ 20 ^{o}C are graphed for completeness.

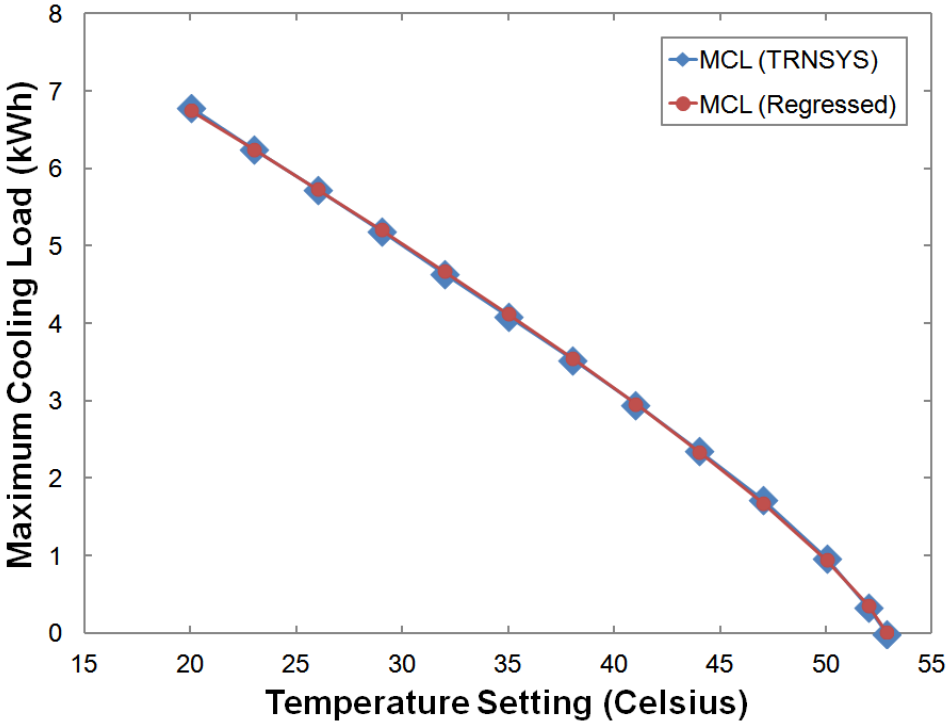

Figure 5. TRNSYS simulation of the maximum cooling loads (*MCL*s) of a restaurant in New York City. *MCLs* are used to compute maximum flexible loads and dispatch probabilities.

For a single time period with $TS_0 < TS$, MFL_{AC} is bounded in the following manner.

$$MCL_{TS_0} - MCL_{TS} \leq MFL_{AC}\left(C_{th}, MCL_{TS_0}, MCL_{TS}\right) \leq MCL_{TS_0} \tag{26}$$

TS_0 is the baseline temperature setting at 20 °C, C_{th} is the building's thermal capacitance and MFL_{AC} is a function *conservatively evaluated at the lower bound in this study*. This estimates the maximum flexible load as the instantaneous difference between *MCL*s at two temperature settings while conservatively ignoring the

amplifying effect of a structure's thermal capacitance. Indeed, $MFL_{AC} \approx MCL_{TS_0} - MCL_{TS}$ for a small restaurant with a low C_{th}. Conversely, $MFL_{AC} \approx MCL_{TS_0}$ for a very high C_{th}.

Figure 6a graphs two *CDP*s and their means resulted from aggregating 3 identical Restaurants, A, B and C, whose temperature settings increased by 1 °C, 3 °C and 5 °C, respectively. The single *DP* of Restaurant B is also graphed in Figure 6b. These restaurants serve as examples of load classes' varying abilities to engage in DR. A standard deviation (SD) of 10 is applied to each restaurant's individual *DP*. Air conditioning load is assumed to be 40% of a class's total load.

Two *CDP*s correspond to aggregating 3 restaurants' DR capabilities via *MFL*s: (1) *CDP* with a maximized mean, $CDP_{\mu,max}$, and (2) *CDP* with a minimized variance, $CDP_{var,min}$. The single *DP* of Restaurant B is shown to accentuate the improvements in *CDP*s of well-aggregated load classes. For example, 100% in average dispatch probability is maintained for up to 3% DR for the maximized mean case, while it is only maintained for up to 1% for the minimized variance and Restaurant B only cases. On the other hand, minimized variance case maintains the most consistent *CDP* and has less than half of the variance of the Restaurant B only case.

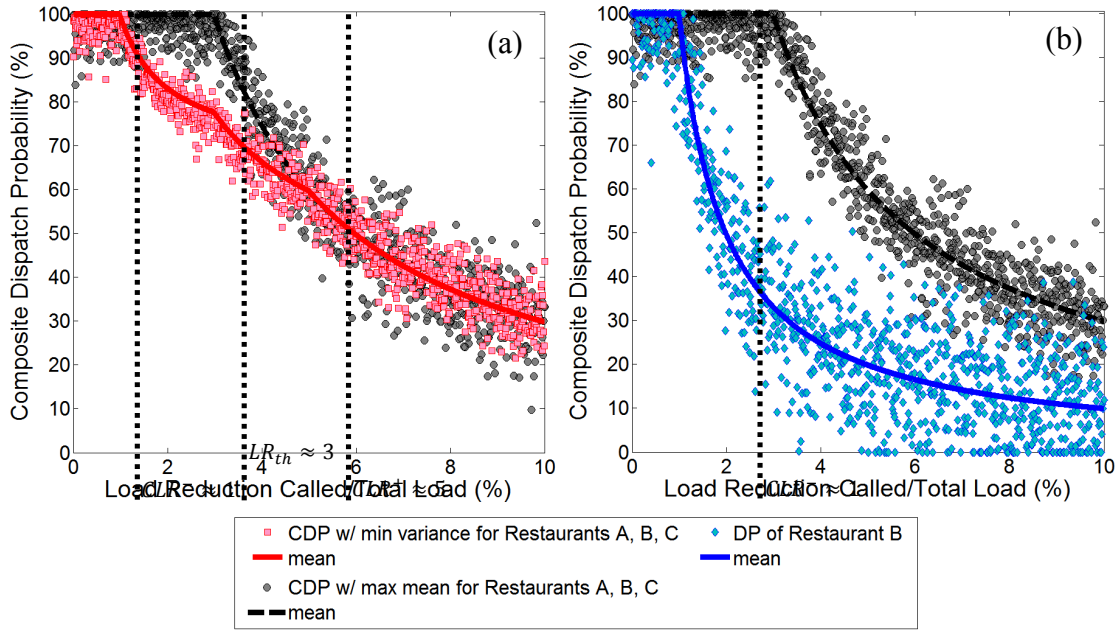

Figure 6. Composite Dispatch Probabilities (*CDP*s) show varying abilities of different aggregations of Restaurant A, B and C to provide demand response. 5a shows (1) a *CDP* with minimized variance, (2) a *CDP* with maximized mean and (3) *CDP* with minimized variance achieves maximum mean after a 5% DR requirement. 5b overlays Restaurant B's single *DP* to illustrate compliance rates without aggregation. Optimal aggregations provide higher quality DR.

Figure 6a reveals the nondimensionalized *ROE* for $CDP_{var,min}$ are approximately <0, 1> and <5, 100> with $CLR^- \approx 1$ and $CLR^+ \approx 5$. In Figure 6b, *ROE* for $DP_{Restaurant\ B}$ exists only in <0, 1> with $CLR^- \approx 1$ by coincidence while $CLR^+ \to \infty$. Within *ROE,* Figure 6a demonstrates that $CDP_{var,min}$ is the optimal solution with both minimized variance and maximized mean. Outside of *ROE*, $LR_{threshold} \approx 3$ and a *CDP* can have either the smallest variance or largest mean or neither but not both. It is clear that optimal aggregations of customer classes produce *CDPs* that either

increases average DR and/or decreases its variability—leading to higher quality DR.

5.4 Storage Participation in DR and Energy Markets

Storage is a versatile asset that can serve multiple purposes. Its deployment will dramatically increase in the next decade particularly given its grid value and current trajectory of cost reductions. Popular proposals for storage utility include renewable energy value maximization, energy price arbitrage, grid congestion relief and frequency regulation. These uses compete with other supply- and network-side resources, e.g. thermal generation, pumped-hydro and transmission improvements.

Since 2008, DR providers in PJM obtain >80% of their revenue from the RTO's capacity market and the rest mostly from its energy market [2]. Storage dispatch firms an aggregator's DR obligations via increased mean and decrease variance of its corresponding *CDP* or other improvements in *CDP*. From a demand-side perspective, storage in DR competes directly with an aggregator's option to acquire and aggregate new customers as both storage and customers alter *CDP*. Any remaining portion of or all of storage's charge would be used for price arbitrage directly in an energy market as a supply-side resource. Considering the increased range of value propositions, storage is closer to reaching its potential as a competitive resource.

An aggregator's decision to utilize storage is intended to maximize its payoff. In

practice, storage would charge at night paying low *LMP*s and discharge at peak hours receiving high DR payoffs and/or peak *LMP*s. There can also be a small amount of charging during certain hours to smooth "double peaks" in net load [21]. In this study, a single MW of storage power cannot be double counted as both DR and injection in an energy market. Storage directly impacts an aggregator's payoff function as shown in Equations 27 to 33 with representative residential, commercial and industrial aggregated load classes. Descriptively, the expected payoff is equal to revenue from energy arbitrage plus reward from DR compliance minus penalty from DR noncompliance.

$$\max_{stor_{eng},\{w\}} E\left\{\sum_{t\in T}\left[LMP_t stor_{eng,t} + P_{DR,t}LR_{actual,t} - P_{DR,nc,t}(LR_{called,t} - LR_{actual,t})\right]\right\} \quad (27)$$

s.t. $$LR_{actual,t} = LR_{called,t}CDP \quad (28)$$

$$LR_{actual,t} \leq stor_{DR,t} + \sum_{i\in class} MFL_i \quad (29)$$

$$\sum_{t\in T}(stor_{eng,t} + stor_{DR,t}) = SOC(1 - LF) \quad (30)$$

$$0 \leq stor_{DR,t} \quad (31)$$

$$w_{stor} + w_{res} + w_{com} + w_{ind} = 1 \quad (32)$$

$$0 \leq w_{stor}\,,\ w_{res}\,,\ w_{com}\,,\ w_{ind} \leq 1 \quad (33)$$

$stor_{eng}$ and $stor_{DR}$ are respectively the storage dispatch into an energy market and a demand response event, *t* is time and *T* is the dispatch horizon, e.g. 24 hours. P_{DR} is net reward price for DR compliance and $P_{DR,nc}$ is penalty price for DR

noncompliance.

P_{DR} is the DR reward price minus the price an aggregator pays to acquire the ownership of reduced load. It is important to include the cost of ownership so as to not double count the revenue from DR and savings from reduced load. For example, P_{DR} should include wholesale capacity and energy price as its reward components. The acquisition cost component should include price paid to the entity originally obligated to serve load, e.g. retail rate paid to a Load Serving Entity (LSE) [1]. However, an aggregator's private costs of conducting business, such as customer acquisition cost, are independent of the economics of DR at a system's level. The example of retail price paid to LSE is part of the system-level economics of DR, and therefore included in P_{DR}. Mathematically, an example of P_{DR} is,

$$P_{DR} = P_{capacity} + LMP - P_{retail} \tag{34}$$

Instead of presenting a multi-period solution, the single-hour solution more clearly reveals the influence of prices and loads on storage dispatch and aggregator payoffs. The purpose here is to gain insight on governing relationships rather than be mired in extraneous mathematical details. Ultimately, the multi-period solution layers an algorithm that sorts time-based payoffs on top of the single-period solution. With $stor_{DR} = w_{stor} LR_{called}$ and $LR_{actual,class} = min\{w_{class} LR_{called}, MFL_{class}\}$, the payoff maximization for a single peak hour is rewritten in Equations 35 to 37.

$$\max_{\{w_i\}} E\left\{\begin{matrix} LMP[SOC(1-LF) - w_{stor}LR_{called}] - P_{DR,nc}LR_{called} \\ +(P_{DR}+P_{DR,nc})\begin{bmatrix} min\{w_{res}LR_{called}, MFL_{res}\} + min\{w_{com}LR_{called}, MFL_{com}\} \\ + min\{(1-w_{res}-w_{com}-w_{stor})LR_{called}, MFL_{ind}\} + w_{stor}LR_{called}\end{bmatrix}\end{matrix}\right\} \quad (35)$$

s.t. $$0 \le SOC(1-LF) - w_{stor}LR_{called} \quad (36)$$

$$0 \le w_{stor},\ w_{res},\ w_{com} \le 1 \quad (37)$$

Analytically solving the maximization problem with $MFL \sim N(\mu,\sigma^2)$ requires operations on truncated normal distributions. Such mathematical complexity dilutes analyses on the relationships that govern storage dispatch. Hereinafter, *MFL*s realize ex ante to a live DR event, such as through offline dispatch tests. Consequently, Equation 35 becomes deterministic during a live DR event and an aggregator's payoff is analyzed via random sampling of *MFL*s. The optimal storage dispatch in DR, shown in Equation 38, reveals bifurcating conditions.

$$w_{stor} = \begin{cases} 0, & LR_{called} \le \sum_{i\in class} MFL_i \\ 0, & LMP > P_{DR} + P_{DR,nc} \\ \dfrac{min\{SOC(1-LF), LR_{called} - \sum_{i\in class} MFL_i\}}{LR_{called}}, & \begin{cases} LR_{called} > \sum_{i\in class} MFL_i & (A) \\ LMP \le P_{DR} + P_{DR,nc} & (B) \end{cases} \end{cases} \quad (38)$$

The solution involves a sum of DR's net reward and penalty prices, and thus may seem surprising given the aim of payoff maximization. However, the result is correct as DR payoff involves reception of compliance reward and the simultaneous avoidance of noncompliance penalty. Colloquially, this "kills two birds with one stone". On the other hand, $w_{stor} = 0$ implies that storage is arbitraged fully in an energy market at an hour with high *LMP*. This occurs when arbitrage generates more

revenue than firming DR. Hence, arbitrage and DR are competing objectives for storage. However, this paradigm of competition does not prohibit a storage unit's simultaneous participation in DR and arbitrage. Indeed, given ample stored energy and adherence to Conditions A and B, storage would both conduct arbitrage and firm DR.

Figure 7 shows the influence of storage capacity, DR noncompliance penalty and uncertainty in *MFL* (as characterized by standard deviation, SD) on an aggregator's maximized payoffs in a peak hour. The aggregator has the option to participate in a live DR event and/or in energy arbitrage via storage. For this case study, the aggregator has a collection of customers categorized into 3 classes, A, B and C. Based on the example restaurants in Section 3.4, Class A, B and C have average *MFL*s of 16.64 MWhs, 50.22 MWhs and 84.24 MWhs, respectively, for a total *MFL* of 151.10 MWhs. The peak LMP is \$100/MWh and DR reward price is \$85/MWh. Sixteen scenarios are created based on: (1) four storage capacities of 0%, 50%, 100% and 150% of average total *MFL*, (2) two DR noncompliance penalty prices of \$0/MWh and \$25/MWh (nearly 30% of LMP), and (3) two SDs of each *MFL* at 10% and 50% of their respective means.

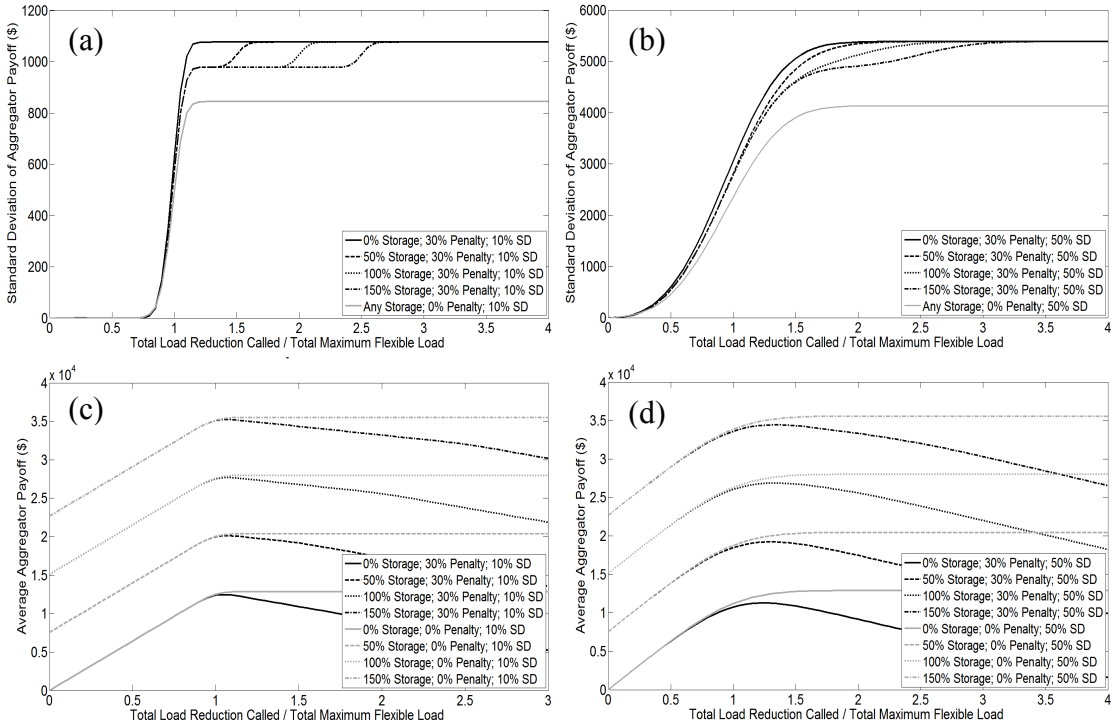

Figure 7. Effect of storage capacity and DR noncompliance penalty on an aggregator's maximized payoffs a peak hour with a live DR event. The aggregator has the option to participate in the DR event and/or in energy arbitrage via storage. Graphs reflect higher storage capacities and lower penalties increase average payoffs (c, d) and decrease standard deviations of payoffs (a, b).

The storage case study shows the following results for an aggregator's maximized payoffs during the peak hour:

1. Higher storage capacities and lower DR noncompliance penalties increase average payoffs (Figure 7c and 7d).

- Each 50%-*MFL* increment of storage capacity increases payoffs by approximately \$7500, an equivalent value when fully discharged in arbitrage.
- Both penalty cases show payoff increases at a rate of about \$85/MWh when $0 \leq \frac{LR_{called}}{mean\,(\sum_{i \in class} MFL_i)} \leq 1$. Zero penalty cases maintain highest payoffs while 30%-LMP penalty cases produce steady declines in payoff at a rate of about \$25/MWh when $\frac{LR_{called}}{(mean\ \sum MFL)} \gg 1$. The payoff vertices occur when $\frac{LR_{called}}{mean\,(\sum MFL)} \approx 1$ as DR rewards are maximized before any penalties.
- *MFL* uncertainties characterized by 10% and 50% SDs do not affect average payoffs when $LR_{called} \ll mean\,(\sum MFL)$. Payoffs with 50% SD are lower than those with 10% SD when $LR_{called} \approx mean\,(\sum MFL)$ as wLR_{called} replaces distributions of higher *MFL*s. Payoffs with 50% SD are slightly higher than those with 10% SD when $LR_{called} \gg mean\,(\sum MFL)$ as negative distributions of *MFLs* are replaced by zero.

2. Higher storage capacities and lower DR noncompliance penalties decrease payoffs' variability (Figure 7a and 7b), given $P_{DR,nc} < P_{DR} < LMP < P_{DR} + P_{DR,nc}$.

- $N(SD)^2 \approx \left(P_{DR} + P_{DR,nc}\right)^2 \sum_N [\sum MFL - mean\ (\sum MFL)]^2$ describes SDs for all scenarios with $\frac{LR_{called}}{(mean\ \sum MFL)} \gg 1 + \frac{Storage\ Capacity}{mean\ (\sum MFL)}$, where *N* is the number of *MFL* samples -1.
- $N(SD)^2 \approx LMP^2 \sum [\sum MFL - mean\ (\sum MFL)]^2$ describes SDs for scenarios with storage, penalties and bounded by $1 < \frac{LR_{called}}{(mean\ \sum MFL)} < 1 + \frac{Storage\ Capacity}{mean\ (\sum MFL)}$.
- $SD \approx 0$ describes SDs for all scenarios constrained by $\frac{LR_{called}}{(mean\ \sum MFL)} \ll 1$.
- At any positive LR_{called}, scenarios without noncompliance penalties achieve the lowest SDs that are invariant across storage capacities. According to Equation 38, this invariance is due to maximized payoffs require storage to participate only in energy arbitrage and thus its dispatch is insulated from fluctuations in *MFL*s.
- Scenarios with storage and a 30% penalty noticeably reduce payoff volatility. This is because $LMP < P_{DR} + P_{DR,nc}$ in the above SD equations.

In addition to times of high *LMP*s, there are instances of the other extreme—negative *LMP*s—when DR can also profit. These counterintuitive prices occur when the market disincentivizes additional energy supply due to operating factors, such as network congestion, and economic factors, such as the avoided costs of cycling

generators. ERCOT for instance has had negative *LMP*s due to overproduction from wind farms subsidized by a production tax credit. In these situations, demand from customers and charging storage is entitled to payments for consuming power. Thus, DR in the direction of increasing demand would profit and help restore positive *LMP*s. The DR revenue mechanism under negative prices would be the same as that under positive prices—optimize load and storage dispatch using the *CDP* and payoff framework established in this study. *CDP*s and payoffs would be derived from the probabilities that customer classes consume more power and that storage assets charge.

5.5 Study Limitations

Results on storage rely on the assumption that noncompliance penalties do not noticeably change the underlying *MFL*s during a live DR event. This can be achieved by aggregators absorbing any penalties without immediately passing on this cost to customers. An example of this strategy can be the aggregator passes on penalties in the form of low contract payments for low performance customers in next year's contracts. However, payoffs within $LR_{called} > mean\,(\sum MFL)$ would increase or decrease in response to cases where *MFL*s do increase or decrease as functions of noncompliance penalties.

This study focused on aggregators' payoffs in the form of revenues. Actual profits would also depend on its private costs of doing business in addition to the system-

level cost of owning demand as exemplified by Equation 34. Such private business costs would therefore include private dispatch costs, such as customer compensation, O&M costs for backup generators and storage units. Consequently, an aggregator's optimal profit models would likely combine the revenue elements in this study with the cost elements in economic dispatch models. For example, if owning and operating storage assets is the cheapest in a profit model, then storage dispatch would be prioritized above load dispatch.

5.6 Conclusion

This study explores the uncertainties in and improvements to demand aggregation for the purpose of demand response, including the use of storage assets. Demand dispatch probability, i.e. DR compliance rate, is derived from an aggregator's payoff function and is defined for a single, homogenous, DR-eligible load class. Composite dispatch probabilities partition an aggregator's overall dispatch probabilities into individual dispatch probabilities of client load classes and its storage assets via a set of DR allocation weights, $\{w\}$. Consequently, *CDP*s enable the optimal allocations of DR to various contracted and controlled assets via fine-tuning $\{w\}$. Optimal *CDP*s are derived for two cases: maximized mean and minimized variance. The Ranges of Equivalence is discovered to guarantee a *CDP*'s maximized mean for any set of allocation weights when total DR requirement is within *ROE*.

Using TRNSYS, a case study illustrates air conditioners' DR capabilities by

increasing the temperature settings of 3 example restaurants in New York City by 1 °C, 3 °C and 5 °C. Optimal aggregations demonstrate higher and/or more consistent DR compliance.

Finally, value of storage in DR and energy arbitrage is described by an aggregator's expected maximum payoff function. Results show single-hour storage dispatch depends on price and flexible load requirements. Specifically, storage value in DR requires: (1) *LMP*s less than or equal to DR reward price *plus* noncompliance penalty price, and (2) total called load reduction larger than sum of maximum flexible loads of load assets. Finally, more storage dispatch and less noncompliance penalty increase payoff expectation and decrease payoff volatility.

ACKNOWLEDGEMENTS

This study is supported by the U.S. Department of Energy under "The Future Grid to Enable Sustainable Energy Systems" initiative through the Power Systems Engineering Research Center and by the Consortium for Electric Reliability Technology Solutions (CERTS).

REFERENCES

[1] Chao, H., 2010. Price-responsive demand management for a smart grid world. The Electricity Journal 23 (1), 7-20.

[2] Monitoring Analytics, LLC, 2014. Quarterly State of the Market Report for PJM: January through June.

[3] Monitoring Analytics, LLC, 2013. State of the Market Report for PJM.

[4] Cappers, P., Goldman, C., Kathan, D., 2010. Demand response in U.S. electricity markets: empirical evidence. Energy 35, 1526-1535.

[5] Rahimi, F., Ipakchi, A., 2010. Demand response as a market resource under the smart grid paradigm. IEEE Transactions on Smart Grid 1 (1), 82-88.

[6] Greening, L., 2010. Demand response resources: who is responsible for implementation in a deregulated market? Energy 35, 1518-1525.

[7] Siano, P., 2014. Demand response and smart grids-a survey. Renewable and Sustainable Energy Reviews 30, 461-478.

[8] Pudjianto, D., Ramsay, C., Strbac, G., 2007. Virtual power plant and system integration of distributed energy resources. IET Renewable Power Generation 1 (1), 10-16.

[9] Conejo, A., Morales, J., Baringo, L., 2010. Real-time demand response model. IEEE Transactions On Smart Grid 1 (3), 236-242.

[10] Rastegar, M., Firuzabad, M., Aminifar, F., 2012. Load commitment in a smart home. Applied Energy 96, 45-54.

[11] Valero, S., Ortiz, M., Senabre, C., Alvarez, C., Franco, F., Gabaldon, A., 2007.

Methods for customer and demand response policies selection in new electricity markets. IET Generation, Transmission and Distribution 1 (1), 104-110.

[12] Medina, J., Muller, N., Roytelman, I., 2010. Demand response and distribution grid operations: opportunities and challenges. IEEE Transactions on Smart Grid 1 (2), 193-198.

[13] Ruiz, N., Cobelo, I., Oyarzabal, J., 2009. A direct load control model for virtual power plant management. IEEE Transactions on Power Systems 24 (2), 959-966.

[14] Jonghe, C., Hobbs, B., Belmans, R., 2012. Optimal generation mix with short-term demand response and wind penetration. IEEE Transactions On Power Systems 27 (2), 830-839.

[15] Aalami, H., Moghaddam, M., Yousefi, G., 2010. Demand response modeling considering interruptible/curtailable loads and capacity market programs. Applied Energy 87, 243-250.

[16] Kim, J., Shcherbakova, A., 2011. Common failures of demand response. Energy 36, 873-880.

[17] Kwag, H., Kim, J., 2014. Reliability modeling of demand response considering uncertainty of customer behavior. Applied Energy 122, 24-33.

[18] Joung, M., Kim, J., 2013. Assessing demand response and smart metering impacts on long-term electricity market prices and system reliability. Applied Energy 101, 441-448.

[19] Zheng, M., Meinrenken, C., Lackner, K., 2014. Agent-based model for electricity consumption and storage to evaluate economic viability of tariff arbitrage for residential sector demand response. Applied Energy 126, 297-306.

[20] Taylor, J., Mathieu, J., 2014. Index policies for demand response. IEEE Transactions on Power Systems 29 (3), 1287-1295.

[21] Valentine, K., Temple, W., Zhang, K.M., 2011. Intelligent electric vehicle charging: rethinking the valley-fill. Journal of Power Sources 196 (24), 10717-10726.

[22] Valentine, K., Foster, E., Acquaviva, J., Zhang, K.M., 2011. Transmission network-based energy and environmental assessment of plug-in hybrid electric vehicles. Journal of Power Sources 196 (6), 3378-3386.

[23] Subramanian, A., Garcia, M., Garcia, A., Callaway, D., Poolla, K., Varaiya, P., 2012. Real-time scheduling of deferrable electric loads. American Control Conference, Montreal, QC, 3643-3650.

[24] Kim, J., Shcherbakova, A., 2011. Common failures of demand response. Energy 36 (2), 873-880.

[25] Schwartz, G., Tembine, H., Amin, S., Sastry, S., 2014. Demand response scheme based on lottery-like rebates. 19th World Congress of the International Federation of Automatic Control. Cape Town, South Africa.

[26] Transsolar. http://www.transsolar.com/__software/download/de/trnflow_demo_readme_de.pdf

CHAPTER 6

OUTLINE OF CONCLUSIONS AND CONTRIBUTIONS

- Network-constrained economic generation-dispatch models add significant realism in assessing the impact of PHEVs on regional power systems and the associated pollutant emissions.

- Using a model of the AC transmission network of the Northeast Power Coordinating Council region and a data-based transportation model of commuters in the New York Metropolitan Area, results show that (1) coal, natural gas and oil units are on the margin in the winter, and natural gas and oil units are on the margin in the summer, (2) commuter hourly driving behavior dominates changes in emissions from transportation and power production, (3) there is significant overall emissions reductions for CO_2 and NO_x, and a slight increase for SO_2, and (4) regulated charging from 11 PM to 5 AM produces less overall emissions than unregulated charging occurring whenever drivers arrive home for the summer and vice versa for the winter.

- Motivated to improve upon the EVs' "valley-filling" charge method, this dissertation considers PEV market penetrations of 5%, 10%, 20%, and 40% in New York State, participating in the New York Independent System Operator's day-ahead and real-time energy markets. For 21 days in June, July and August

of 2006, vehicle-scheduling decisions are made using a statistical Locational Marginal Price (LMP) and wholesale energy cost model that explicitly includes the dynamic cost of generator ramping in addition to the traditional steady-state operation model. This model creates a framework with two competing cost objectives.

- A Charge Flexibility Constraint (CFC) is proposed to model commuter driving behavior and the investment in Level 1 (1.44 kW) and Level 2 (7.68 kW) charging infrastructure. The CFC, which is independent of market modeling, severely restricts PEV charging, particularly in the morning load valley hours. As a result, a complete valley-filling in the New York Control Area cannot be achieved for most charger mixtures. Using a Simulated Annealing optimization algorithm, the proposed intelligent PEV charging method, which minimizes cost from both steady-state and ramping operations, is shown to reduce wholesale energy cost 4% to 9% beyond that of the valley-fill scheme.

- Adding more Level 2 chargers without regulating PEV charging will significantly increase LMP and wholesale energy cost due to increased unregulated charging at peak load. The proposed intelligent PEV charging method will lead to a noticeable reduction in system cost if the penetration of Level 2 chargers is increased from 70/30 to 50/50 (Level 1/Level 2) mixture. However, the system benefit is drastically decreased for higher penetrations of Level 2 chargers due to

the diminished effect of CFC on PEV charging in the morning. This trend is exacerbated by a smaller percentage of charging at valley load hours for high PEV penetrations.

- This dissertation also assesses the relationship between electric vehicle charging and wind power dispatch in two-settlement electric energy markets. Work is based on modeled results for NYISO and by incorporating transportation constraints, Level 1/Level 2 charger infrastructure and wind power forecasts and realizations.

- From the dispatch perspective:
    - Optimal PEV charging occurs at the same time as wind curtailment for an energy market with excess wind power.
    - Optimal PEV charging is not generally correlated with must-take wind power (wind resource) or with wind power variability.

- From the wind curtailment perspective:
    - An increase in optimally-charged PEVs reduces curtailment in wind energy.
    - Uncertainty in wind power forecast affects the magnitude of the base case relationship between PEV charging and wind energy utilization. In

particular, over-forecast amplifies and under-forecast diminishes this relationship.

  - Variability in wind power does not significantly affect the base case relationship.

- From the energy cost perspective:
  - High PEV, curtailable wind power and Level 2 charger penetrations have the lowest wholesale market costs.
  - PEVs and curtailable wind power are adversely coupled.
  - PEVs and must-take wind power are decoupled.
  - Levels of PEV penetration, wind power integration and Level 2 charging may be economically equivalent in the wholesale energy market.

- This work also explores the uncertainties in and improvements to demand aggregation for the purpose of demand response, including the use of storage assets. Demand dispatch probability, i.e. DR compliance rate, is derived from an aggregator's payoff function and is defined for a single, homogenous, DR-eligible load class.

- Composite dispatch probabilities partition an aggregator's overall dispatch probabilities into individual dispatch probabilities of client load classes and its storage assets via a set of DR allocation weights, {w}. Consequently, CDPs

enable the optimal allocations of DR to various contracted and controlled assets via fine-tuning {w}.

- Optimal CDPs are derived for two cases: maximized mean and minimized variance. The Ranges of Equivalence is discovered to guarantee a CDP's maximized mean for any set of allocation weights when total DR requirement is within ROE.

- Using TRNSYS, a case study illustrates air conditioners' DR capabilities by increasing the temperature settings of 3 example restaurants in New York City by 1 °C, 3 °C and 5 °C. Optimal aggregations demonstrate higher and/or more consistent DR compliance.

- Value of storage in DR and energy arbitrage is described by an aggregator's expected maximum payoff function. Results show single-hour storage dispatch depends on price and flexible load requirements. Specifically, storage value in DR requires: (1) LMPs less than or equal to DR reward price plus noncompliance penalty price, and (2) total called load reduction larger than sum of maximum flexible loads of load assets.

- Finally, more storage dispatch and less noncompliance penalty increase payoff expectation and decrease payoff volatility.